

Copyright
by
Soraya Hengsawas
2016

The Dissertation Committee for Soraya Hengsawas Certifies that this is the approved version of the following dissertation:

Importance of Stability of Pharmaceutical Formulations

Committee:

Robert O. Williams III, Supervisor

Zhengrong Cui

Christopher R. Frei

Feng Zhang

James W. McGinity

Importance of Stability of Pharmaceutical Formulations

by

Soraya Hengsawas, B. Pharm., M. Pharm.

Dissertation

Presented to the Faculty of the Graduate School of

The University of Texas at Austin

in Partial Fulfillment

of the Requirements

for the Degree of

DOCTOR OF PHILOSOPHY

THE UNIVERSITY OF TEXAS AT AUSTIN

December 2016

Dedication

To my parents, with love

Acknowledgements

Words are inadequate to express my sincere appreciation for numerous people who have contributed towards and helped me throughout this journey of my Ph.D. study. Without their supports, I could not have accomplished this big chapter of my life. I really appreciate it.

First and foremost, I wish to express my deepest gratitude to my advisor, Dr. Robert O. Williams III, for kindly accepting me into his excellent research group, and for his patience, motivation, immense knowledge, and advice he has provided throughout my time as his student. The door to Dr. Williams's office was always open whenever I needed his help. Without his guidance, persistent help and encouragement, this degree would not have been possible.

A special thanks to all my kind committee members Dr. James W. McGinity for his insightful professional advices and great classes. I would like to extend my gratitude to Dr. Feng Zhang for his supports with my experiments and valuable advices. Thanks also to Dr. Zhenrong Cui for his helpful comments and Dr. Christopher R. Frei for the best statistic class ever. I would like to thank Dr. Hugh D. Smyth and Dr. Alan B. Watts for all their kindness and for sharing laboratory equipment. My appreciation must also go to Dr. Salomon A. Stavchansky who constantly asked me (with smile) about my graduation.

I am grateful to Dr. Andrey A. Komissarov and Dr. Galina Florova, at University of Texas at Tyler for contributing significantly towards the training on the experiments and scientific discussions. The proteins and peptide projects would not have been done without their contributions. I am very much appreciated their collaboration. Also, I would like to thank Dr. Steven Idell and Dr. Sreerama Shetty for their kind advices and supports.

I would also like to thank Dr. Jason McConville for kindly accepting me to be a graduate student in College of Pharmacy, the University of Texas at Austin. I am grateful for his patience since he had waited for me since 2010. Albeit a brief period, I had a chance to work in his group, that was an enjoyable memory.

I would like to express my respect to all of my teachers in Thailand, including my teachers at Bodindecha (Sing Singhaseni) School, my professors at Chulalongkorn University, and my previous bosses at Department of Medical Sciences for teaching me. My special appreciation is also extended to Dr. Eric Tsai (previously at Merck & Co., Inc., West Point, PA) for encouraging me to further study at the University of Texas at Austin.

My time at College of Pharmacy was made enjoyable in large part due to the many friends and groups that became a part of my life. I would like to thank my friends Dr. Ping Du, Dr. Ju du, Dr. Zachary N. Warnken, Tania Bahamóndez and Danial F. Moraga-Espinoza, Solange Valdes Curiquen, Dr. Javier O. Morales, Dr. Matthew Herpin, Dr. Silvia Ferrati, Dr. Bo Lang, Dr. Youssef Naguib, Dr. Justin M. Keen and many other past and present graduate students.

I am especially grateful for nice conversations with Dr. Xinran Li, Dr. Sha Liu, Abbe J. Haser, Julien Maincent, Xu Liu and Chaeho Moon. I also would like to express my sincere thanks to Siyuan Huang and Dr. Ashkan K. Yazdi for their help with the scientific and non-scientific matters. Specifically, I would like to thank two of my best friends, Dr. Simone Raffa Carvalho and her husband, Dr. Thiago Carvalho, who have supported me academically and emotionally through the road to finish this degree.

I am grateful for time spent with the high-school and undergraduate students who worked with me. Many thanks go to Wilson Chiu, Elizabeth Brigham, Paul Twomey and Brian Beasley for their lovely friendships. I am also thankful to May Chiravisit for her nice friendship and delicious dishes. I am indebted to Ing-Orn Prasanchaimontri and Chanida

Karnpracha, who are my little best friends, for their honest supports. I would like to thank Dr. Vorapann Mahakuna, my unofficial big sister, for her advices and a sincere friendship.

I wish to express my great appreciation to administrative staff including Yolanda L. Camacho, Herman B. Schwarzer IV, Jay M. Hamman, Joe D. Adcock and many others for their kind assistance. Special thanks to Stephanie W. Crouch for her heartfelt and continued help since my first day in Austin. I wish you have a wonderful retirement, my Totoro!!

I gratefully acknowledge the full scholarship received towards my Ph.D. study from the Royal Thai Government. Without such financial support, I would not have come to the United States. Thank you very much. I also would like to thank my colleagues at the Department of Medical Sciences and my friends in Thailand for their moral supports.

I must express my very profound gratitude to my respectful parents, Jirawat and Lawan Hengsawas, who raised me with the endless love, care and supports in all my pursuits. They have faith in me and always be by my side. They are a tremendous source of energy for me and their prayer for me was what sustained me thus far. Thank you, papa mama. I am back!!

Besides, I owe a particular debt of gratitude to my beloved brother and sister, Sarawut Hengsawad and Soranun Kanawaree and their families, who always take great care of my parents while I am 10,000 miles away from home, till I have this day.

At the end, I would like to express appreciation to my beloved husband, Anak Surasarang, for providing me with unfailing support and continuous encouragement throughout my years of study even when it involved long distance and long period apart. Thank you for always being there and waiting for me. You will never know how much I appreciate your supports via our daily FaceTime. Last but not least, special thanks to my husband's family who all have been supporting and caring me.

Importance of Stability of Pharmaceutical Formulations

Soraya Hengsawas, Ph.D.

The University of Texas at Austin, 2016

Supervisor: Robert O. Williams III

Stability is an essential quality attribute for pharmaceutical formulations. Evaluation of drug stability can prevent toxicity and increase safety, efficacy and quality of the final drug product. In this work, various factors affecting stability of both small molecule and biopharmaceutical compounds were investigated. In the first study, we initially hypothesized that albendazole, a poorly water soluble drug, could be prepared by melt extrusion to enhance its dissolution and bioavailability. However, it was found that albendazole was severely degraded by heat and shear during extrusion. When combined with methanesulfonic acid and Kollidon VA 64, amorphous albendazole solid dispersion was successfully prepared by an alternative process, spray drying, to enhance dissolution and shelf-stability. In the second study, the stability of a caveolin-1 scaffolding domain (CSP7), which is a newly developed peptide for the treatment of idiopathic pulmonary fibrosis, was investigated in order to achieve an optimal formulation for *in vivo* clinical studies. This study showed the physical instability of the peptide, which was aggregation induced by moisture, and the crystallization of bulking agent on its stabilizing effect. It was found that the moisture-induced aggregates were reversible and could be prevented by pH adjustment and incorporation of lactose in the composition. Lactose, a reducing sugar, stabilized the peptide possibly as a result of chemical interactions with CSP7 (e.g.,

formation of a Schiff base with the N-terminal amino group of CSP7). Based on these results, lactose stabilized CSP7 against moisture-induced aggregation in the solid state to a greater degree than mannitol. Additionally, stability of the CSP7-bulking agent formulations was not affected by nebulization using vibrating mesh nebulizers. Lastly, the effect of nebulization using vibrating mesh nebulizers on stability of tissue-type plasminogen activator (tPA) and single-chain urokinase plasminogen activator (scuPA), being studied for the treatment of inhalational smoke-induced acute lung injury (ISALI), was evaluated. For scuPA, the effect of lyophilization on its stability was also studied. The results showed that scuPA was stable after lyophilization (scuPA) and that both proteins were stable following reconstitution and nebulization. There were only slightly differences between the active and passive vibrating mesh nebulizers. In conclusion, from our work, the physical and chemical stability of small- and macromolecules was affected by formulation composition, processing and post-processing factors.

Table of Contents

List of Tables	xvi
List of Figures	xvii
Chapter 1: Stability of Pharmaceutical Formulations	1
1.1 Introduction.....	1
1.2 Factors influencing stability of pharmaceutical formulations	2
1.2.1 Temperature	3
1.2.2 pH	4
1.2.3 Moisture	5
1.2.4 Oxygen (Oxidation)	6
1.2.5 Shear stress.....	6
1.2.6 Excipients.....	7
1.2.7 Processing methods.....	9
1.3 Stability of small molecule drugs	10
1.3.1 Chemical stability of small molecules	10
1.3.2 Physical stability of small molecule drugs.....	11
1.4 Stability of therapeutic peptides and proteins	12
1.4.1 Chemical Stability of macromolecules	13
1.4.2 Physical Stability of macromolecules	14
1.5 Stability of the nebulized biopharmaceuticals	14
1.6 Conclusions.....	16
References.....	17
Chapter 2: Hot Melt Extrusion versus Spray Drying: Hot Melt Extrusion Degrades Albendazole	31
Abstract	31
2.1 Introduction.....	32
2.2 Materials and Methods.....	34
2.2.1 Materials	34
2.2.2 Preformulation studies	35

2.2.2.1	pH solubility profile and pKa	35
2.2.2.2	Forced degradation study	35
2.2.2.3	Thermal stability profile	36
2.2.3	Drug-polymer miscibility model.....	37
2.2.3.1	Melting point depression approach.....	37
2.2.3.2	Hansen solubility parameter (δ).....	37
2.2.3.3	Flory–Huggins Theory	38
2.2.3.4	Glass transition temperature (T _g) of the solid dispersion	40
2.2.3.5	Experimental model	40
2.2.4	Formulation of solid dispersions.....	41
2.2.4.1	Hot melt extrusion.....	41
2.2.4.2	Spray drying.....	44
2.2.5	Characterization of solid dispersions	44
2.2.5.1	Powder X-Ray Diffractometry (PXRD)	44
2.2.5.2	Differential Scanning Calorimetry (DSC)	45
2.2.5.3	Thermogravimetric Analysis (TGA).....	45
2.2.5.4	Scanning electron microscope (SEM)	45
2.2.5.5	Particle size distribution of spray-dried particles.....	46
2.2.6	ABZ salt preparation	46
2.2.7	Non-sink dissolution	47
2.2.8	Chromatographic analysis.....	47
2.2.9	Long term stability study of spray-dried formulation	48
2.3	Results and Discussion	48
2.3.1	pH solubility profile and pKa value.....	48
2.3.2	Forced degradation study	49
2.3.3	Thermal stability profile	51
2.3.4	Drug-polymer miscibility.....	53
2.3.5	Hansen solubility parameter	53
2.3.6	Flory-Huggins Theory and Gibbs free energy of mixing	53
2.3.7	Temperature – Composition phase diagram	56

2.3.8	Hot melt extrusion.....	59
2.3.9	Spray-dried formulation.....	62
2.3.10	Characterization of spray-dried formulations	62
2.3.10.1	PXRD	62
2.3.10.2	DSC.....	63
2.3.10.3	SEM images	64
2.3.10.4	Particle size distribution (PSD) of spray-dried formulations	64
2.3.11	Recrystallization of ABZ in spray-dried formulations	67
2.3.12	ABZ salts	68
2.3.13	Non-sink dissolution	69
2.3.14	Long term stability study of spray-dried formulations	75
2.4.	Conclusions.....	76
	References.....	77

Chapter 3: Optimization of Formulation for Novel Inhaled Anti-Idiopathic Pulmonary Fibrosis Therapeutics

	Pulmonary Fibrosis Therapeutics	87
	Abstract.....	87
3.1	Introduction.....	88
3.2	Materials and Methods.....	91
3.2.1	Materials	91
3.2.2	Chromatographic analysis.....	91
3.2.3	Preformulation studies	92
3.2.3.1	Aggregation and chemical stability of peptide solution.....	92
3.2.3.2	Effect of agitation	92
3.2.3.3	Effect of multiple freeze-thaw cycles	92
3.2.3.4	Effect of storage temperature	93
3.2.4	Formulation preparation.....	93
3.2.5	Chemical stability of peptide	94
3.2.5.1	Chemical stability of peptide in reconstituted solution.....	94
3.2.5.2	Chemical Stability of peptide in lyophilized state	94

3.2.6 Karl Fischer Titration.....	94
3.2.7 Osmolality measurements	95
3.2.8 Measurement of reconstitution time	95
3.2.9 Moisture-induced aggregation and quantitation of CSP7 aggregates	96
3.2.10 Powder X-ray diffractometry (PXRD).....	96
3.2.11 Differential scanning calorimetry (DSC).....	97
3.2.12 Determination of water sorption isotherm	97
3.2.13 Long-term stability study (mannitol- and lactose-based formulations).....	98
3.2.14 Nebulization of peptide.....	98
3.3 Results and Discussion	99
3.3.1 Preformulation studies	99
3.3.2 Appearance and residual moisture content of lyophilized cakes	102
3.3.3 Chemical stability of peptide in reconstituted solution.....	103
3.3.4 Chemical stability of peptide in lyophilized state with mannitol	103
3.3.5 Long term stability of the lyophilized CSP7-bulking agent cakes	105
3.3.6 Determination of water sorption isotherm	107
3.3.7 Effect of bulking agent on moisture-induced lyophilized CSP7 aggregation.....	110
3.3.8 Moisture content after exposure to high humidity environment	111
3.3.9 Powder X-ray diffraction (PXRD) analysis	113
3.3.10 Differential scanning calorimeter (DSC) analysis	116
3.3.11 Moisture-induced aggregation of lyophilized CSP7 (mannitol- and lactose-based formulations) is reversible	120
3.3.12 Chemical assay of the aggregates	121
3.3.13 Effect of nebulization on chemical stability of CSP7	125
3.4 Conclusion	126
References	127

Chapter 4: Optimal Nebulizer for Inhaled Tissue-Type Plasminogen Activator (tPA) and Single-Chain Urokinase Plasminogen Activator (scuPA) for Treatment of Inhalational Smoke-Induced Acute Lung Injury (ISALI)	138
Abstract	138
4.1 Introduction.....	139
4.2 Materials and Methods.....	141
4.2.1 Materials	141
4.2.2 Solid-state preparation of scuPA	142
4.2.3 Karl Fischer titration	143
4.2.4 Osmolality measurements	143
4.2.5 Droplet size distribution.....	144
4.2.6 Nebulization of tPA and scuPA solutions.....	144
4.2.7 Kinetic activity assay	145
4.2.8 Sodium dodecyl sulfate-polyacrylamide gel electrophoresis (SDS-PAGE) analysis	146
4.2.9 Residual volume of Aeroneb® Pro nebulizer	146
4.3 Results and Discussion	147
4.3.1 Appearance of lyophilized cakes, residual moisture content, and tonicity of scuPA formulation.....	147
4.3.2 Droplet size distribution.....	148
4.3.3 Nebulization of tPA and scuPA	151
4.3.4 Residual solution remaining in the medication cup	154
4.4 Conclusion	156
References	157
Appendices.....	166
Appendix A.: Proteins in perfluorocarbon suspensions.....	167
Appendix B.: Delivery of tPA and scuPA into a cold 1 gallon plastic bag with vibrating mesh nebulizer and mechanical ventilator	172
References.....	179
Chapter 1 References	179

Chapter 2 References	192
Chapter 3 References	202
Chapter 4 References	212
Vita	222

List of Tables

Table 2.1: Process parameters of hot melt extrusion	43
Table 2.2: Drug content, crystallinity and physical appearance of hot-melt extruded ABZ-Kollidon® VA 64 extrudate	61
Table 2.3: Summary of supersaturation values of the area under the dissolution curve (AUDC) for the USP simulated gastric fluid (without pepsin) at 37°C	75
Table 2.4: Assay and impurity content of ABZ mesylate-Kollidon® VA 64 formulation after 6-month and 1-year storage in a desiccator at 25°C	76
Table 4.1: Lyophilization cycle parameters	143

List of Figures

- Figure 2.1:** Screw design for melt extrusion42
- Figure 2.2:** pH solubility profile of bulk ABZ at 37 °C (A), and pH solubility profile of bulk ABZ at 37°C (concentration are in log S values, the dashed lines were linear interpolation of the experimental data) (B).....49
- Figure 2.3:** Proposed degradation pathway of ABZ – oxidation (A), basic hydrolysis (B)50
- Figure 2.4:** Percentage of drug remaining following 5 minutes storage at various temperature – crystalline drug substance (A), and physical mixture of drug and polymer at 20:80 ratio (B).....52
- Figure 2.5:** Gibbs free energy diagram of the mixture of ABZ–Kollidon® VA 64 (A), Soluplus® (B), and Eudragit® E PO (C).....55
- Figure 2.6:** Phase diagrams of ABZ–polymer binary systems and the appearance of the extrudates at different drug fractions (\varnothing ABZ); ABZ–Kollidon® VA 64 (A), ABZ–Soluplus® (B), and ABZ–Eudragit® E PO (C) at extrusion temperature of 140°C, 140°C and 120°C, respectively58
- Figure 2.7:** DSC thermograms of bulk ABZ and spray dried ABZ-polymer systems from a plot of heat flow (W/g) versus temperature (°C) (A), and glass transition temperatures (T_g(s)) of bulk ABZ and spray dried ABZ-polymer systems from a plot of reverse heat flow (W/g) versus temperature (°C) (B)65

Figure 2.8: SEM images of bulk ABZ (A), Kollidon® VA 64 (B), physical mixture of ABZ and Kollidon® VA 64 (C), spray-dried formulations (ABZ–polymer 20:80) as follows; ABZ–Kollidon® VA 64 (D), ABZ–Soluplus® (E), and ABZ–Eudragit® E PO (F), magnification of 2,000X for (A)-(C) and 10,000X for (D)-(F)	66
Figure 2.9: (A) Non-sink dissolution of bulk ABZ and ABZ salts in 100 mL USP simulated gastric fluid (without pepsin) at 37°C (<i>n</i> =3)	72
Figure 2.9: (B) Non-sink dissolution of bulk ABZ and spray-dried ABZ mesylate:polymer (20:80) in 100 mL USP simulated gastric fluid (without pepsin) at 37°C (<i>n</i> =3).....	73
Figure 2.9: (C) Non-sink dissolution of bulk ABZ, physical mixture of ABZ:Kollidon® VA 64 (20:80), and spray-dried ABZ salt:Kollidon® VA 64 (20:80) in 100 mL USP simulated gastric fluid (without pepsin) at 37°C (<i>n</i> =3)	74
Figure 3.1: Effect of agitation (A), freeze-thaw cycles (B), storage temperature (C) on chemical stability of CSP7 (% recovery), (<i>n</i> =2)	101
Figure 3.2: Chemical stability data of reconstituted CSP7 solutions after storage at 5°C and 25°C for 8 hours (A), and of lyophilized cakes after storage at 5°C and 25°C for 4 weeks. (B)	105
Figure 3.3: Chemical analysis of CSP7-bulking agent after 10-month storage without exposure to humidity at 5°C, no data of CSP7-Mannitol (1:5) presented due to its aggregation (<i>n</i> =3)	107
Figure 3.4: Sorption and desorption isotherms of lyophilized neat CSP7 and lyophilized CSP7:mannitol formulations (A), and CSP7:lactose formulations (B).....	110

Figure 3.5: Residual moisture content of the lyophilized CSP7, (<i>n</i> =3).....	112
Figure 3.6: PXRD of CSP7:bulking agent; CSP7:mannitol (A), CSP7:lactose (B), before (a, b, d, f, and h) and after exposure to 75% RH (c, e, g and i)	115
Figure 3.7: DSC thermograms of lyophilized CSP7:bulking agent before (A and C) and after exposure to 75% RH for 12 hours (B and D); mannitol based formulations ((1) and (2)) - bulk mannitol (a), α mannitol (b), lyophilized neat CSP7 (c), 1:5 (d), 1:70 (e), 1:140 (f) and lactose based formulations ((3) and (4)) - bulk lactose monohydrate (a), lyophilized neat CSP7 (b), 1:5 (c), 1:70 (d), and 1:140 (e).....	119
Figure 3.8: Chemical analysis of aggregates CSP7-bulking agent after exposure to 75% RH at room temperature for 12 hours, (<i>n</i> =2).....	125
Figure 4.1: Droplet size distribution of tPA solutions (A) and scuPA solutions (B) by Aeroneb® Pro (open circle) and EZ Breathe® (closed circle) nebulizers, respectively (<i>n</i> =2)	150
Figure 4.2: Enzymatic activity of tPA after nebulization by Aeroneb® Pro and EZ Breathe® nebulizers.....	152
Figure 4.3: SDS-PAGE results of tPA samples before and after nebulization by Aeroneb® Pro and EZ Breathe® nebulizers (<i>n</i> =2).....	153
Figure 4.4: Enzymatic activity of scuPA after sterile filtration, lyophilization, and nebulization by Aerone® Pro and EZ Breathe® nebulizers as compared with the bulk solution (<i>n</i> =2).....	153

Figure 4.5: (A) Mass (%) of residual DPBS solution in medication reservoir, collected solution in collecting tube, and lost mass ($n=3$), (B) enzymatic activity of tPA and scuPA of the residual solution in the medication reservoir, collected solution in collecting tube, and lost activity ($n=2$).155

Chapter 1: Stability of Pharmaceutical Formulations

1.1 INTRODUCTION

The term “pharmaceutical formulations” is defined as “the processes whereby a drug is transformed into a suitable drug product for administration to a patient by a particular route” (1). During formulation development, clinical studies and marketing, stability is the critical quantity, playing an essential role as performance attributes, that needs to be evaluated (2). The instability of the drug not only impacts the potency, purity and safety of the drug formulation, but can also lead to formation of toxic degradants (3). Stability assessment of drugs since early phase of product development plays a crucial role in providing evidence to explain the root causes or mechanisms of product instability. Thus, the purpose of the following discussion is to give an overview considering chemical and physical stability of both small- and macromolecules (biologics/biopharmaceuticals, peptide/protein are used interchangeably throughout this chapter) during formulation development. For small molecule drugs, stability of amorphous solid dispersions of poorly water soluble drugs will be primarily discussed. On the other hand, for macromolecules, stability of nebulized biologics will be highlighted.

1.2 FACTORS INFLUENCING STABILITY OF PHARMACEUTICAL FORMULATIONS

A variety of factors influencing the stability of a pharmaceutical product include the stability of active ingredient(s), drug-excipient interaction, manufacturing process, dosage form, packaging, shipping, storage and handling (4). Drugs exposed to many conditions, such as heat, pH and moisture during the development process can also cause instability (4). In addition, degradation reactions such as hydrolysis, oxidation, reduction, or racemization are also induced by some conditions such as concentration of reactants, pH, radiation, catalysts as well as aging of the raw materials themselves (4).

Similar to the small molecule drugs, stability of the macromolecules is also affected by the common factors such as temperature, light, moisture, pH, shear (agitation), oxidation and protein concentration (5,6). However, there are some other factors such as buffer components and concentration, ionic strength and the presence of excipients that also affect the stability of the macromolecules (7–11).

Therefore, a basic understanding of the most common factors affecting a drug and its formulation stability is needed for process design, storage and packaging of the drug product (6,12,13). In particular, the understanding of the cause and mechanism of drug instability/inactivity provides the rational development of formulations to minimize degradation and therefore maximize the storage stability of the drug product (14). Examples of the factors affecting the stability of formulations are provided below.

1.2.1 Temperature

The most significant variable affecting drug stability is temperature (15). Relationship between temperature and the rate constant of degradation reactions has basically been expressed by the Arrhenius equation (15). From this equation, as temperature is elevated higher, the chemical reactions are accelerated.

Small molecules: The use of thermal processing (e.g. melt extrusion) can cause the degradation reactions of thermally sensitive drugs. For example, Δ^9 -tetrahydrocannabinol (THC) is thermally unstable. The drug itself undergoes severe thermal degradation. Its chemical stability in thermal-processed polymer films was studied. In combination with carriers such as polyethylene oxide, hydroxypropyl cellulose or antioxidant such as ascorbic acid can protect the THC thermal stability (16–18). In Chapter 1, the thermal degradation of albendazole by hot melt extrusion is discussed.

Biopharmaceuticals: For peptide/protein, chemical degradation, physical denaturation or both can occur at high temperature. Chemical stability of the peptide/protein in solid formulations decreases when exposed to elevated temperature (19). Most of the chemical reactions such as deamidation (20), peptide bond cleavage (9), and oxidation (21) are accelerated by high temperature. Protein inactivation by high temperature is often due to the destruction of disulfide bonds in cystine by β -elimination (22). Oliyai et al. reported that the deamidation of the Asn-hexapeptide increases when temperature in the solid-state increases (20). For physical stability, when temperature

increases, aggregation of insulin also increases (23). It seems that the increase of mobility of the system or the reduction of the activation barrier of the reaction substantially attribute to the increase of instability at elevated temperatures. The mobility significantly increases with increasing temperature, which may associate with the Tg of an amorphous solid (19).

In the liquid phase, proteins can be destabilized at low temperatures (such as during freeze-drying process). However, unlike most high-temperature denaturation, cold denaturation is generally reversible and does not cause much practical problems (24). Moreover, temperature during administration such as using some types of nebulizers can also generate heat resulting in protein degradation. Temperature control devices may be required for the thermolabile drugs (25).

1.2.2 pH

Small molecules: pH is the second most important factor affecting drug decomposition. Most drug substances are practically stable at the neutral pH, which is the pH value in the small intestine. On the other hand, drugs can be decomposed at extremely acidic (of the stomach) or alkaline pH (15). pH normally impacts degradation rates of drug substances because hydronium and/or hydroxide ions catalyze most degradation pathways (15). As mentioned, drug may degrade to the toxic degradants. Pralidoxime degrades by two pH-sensitive pathways (acidic and alkaline). However, under alkaline pH conditions, cyanide, a toxic product is formed (15,26). The other example is the rearrangement of structure of penicillins to penicillenic acids, which are suspected to cause the allergenicity, under acidic pH conditions (pH 2 or below) (27).

Biopharmaceuticals: pH is also one of the most powerful variables affecting stability of the protein formulations. Most protein formulations will survive at pH values between 4-9 (28). An extreme pH can cause protein degradation (29). The degradation of an Asp-hexapeptide depends on pH of the bulk solution prior to lyophilization. It was reported that this peptide degraded under acidic pH conditions (pH 3.5-5.0) and under neutral and alkaline conditions (pH 6.5-8.0), however, via the different decomposition pathways (9).

1.2.3 Moisture

Small molecules: Molecular mobility is a significant factor influencing solid state reactivity. Water can act as a plasticizer, which increases the mobility of the matrix and this is associated with a higher general reactivity of the matrix components. Consequently, to control the moisture, limits for moisture levels of the blend components should be set up and monitored. The introduction of water into amorphous molecular level solid dispersions at room temperature irreversibly disrupted interactions between the drug and polymer resulting in amorphous-amorphous phase separation followed by crystallization (30).

Biopharmaceuticals: Moisture content is a major issue impacting the chemical and physical stability of peptide/protein in the solid state (19). Several studies reported moisture-induced aggregation of lyophilized biopharmaceuticals (e.g. insulin, bovine serum albumin, DNA, and tetanus toxoid) (23,31–35). Chapter 3 also reports the results of moisture-induced aggregation of the peptide studied.

1.2.4 Oxygen (Oxidation)

Small molecules: Oxidation reactions occur when oxygen is presented, and tend to be catalyzed by metal ions. Impurities often catalyze the autoxidation relating reactive oxygen-species, which may be hard to reproduce (36). Force degradation study of oxidation can be examined under an oxygen atmosphere in the presence of peroxides. However, a model of using oxygen is more realistic (37). To characterize the behavior of materials stressed by both heat and oxygen, thermo-oxidative stability is tested (38). In addition, oxidation reactions can be affected by light. A photosensitizer, which absorbed light, can react with molecular oxygen to form the more reactive singlet oxygen species.

Biopharmaceuticals: In general, oxidation occurs because the side chains of amino acids expose to air, residual peroxide from excipients or to visible ultraviolet light. Methionine, cysteine, tryptophan, and tyrosine are particularly prone to oxidation. Oxidation and other degradation processes can also be catalyzed by metal ions such as iron, zinc, copper, or tungsten from metals that are used in the manufacturing process (39,40).

1.2.5 Shear stress

Small molecules: A screw extruder, particularly counter-rotating extruder, provides high shear stress and intense mixing (41). The energy from the heaters and shearing promotes melting. On the other hand, this high energy can lead to degradation of the drug as well. Effect of shear stress on drug instability was discussed in Chapter 2.

Biopharmaceuticals: Regarding biologics, vortexing and shaking can cause shear

stresses, which lead to partition proteins to the air-water interface. This promotes physical changes such as partial unfolding when exposed to the more hydrophobic air phase (42). Interestingly, the human growth hormone remained intact in the absence of any air-liquid interface; although, using the homogenizer at the highest shear rate. While in the presence of air-liquid interface, the extent of the aggregates increased with higher shear rates during homogenization. This is largely attributable to the surface area of the finer dispersion of the air in the liquid phase being expanded, due to higher shear (43).

1.2.6 Excipients

Excipients can also affect drug stability by various mechanisms (15). Since the excipients can act as reactants in chemical reactions, the stability of the drug in formulation may be lower than the bulk material (44). Other components in the formulation and/or variables can induce chemical reactions between drug and excipient. Therefore, drug-excipient incompatibility must be studied at the early stage of drug development.

Small molecules: Several other excipients in melt-extruded formulations are needed for specific purposes. A high temperature and shear stress imposed on materials are unavoidable in a thermal and mechanical process, particularly hot melt extrusion. For the purpose of studying the stability of the formulation, therefore, close monitoring is required as not only drug substance but also other excipients would undergo chemical reactions.

The polymeric carrier, a major excipient in melt-extruded formulations, melts during extrusion, encompassing all other components to form the matrix. To achieve the successful development of formulation and manufacturing processes, selection of the

polymer is critical. The mechanisms of chemical degradation of polymers were reviewed (45). Solubility parameters and miscibility of drug-polymer mixtures play an important role in prediction of the physical stability of the products. Drug-polymer miscibility will be discussed in the following chapter.

Other excipients such as plasticizer, melt solubilizer, release modifiers, glidants, or pigments may also be added to assist processing or modify formulations (46,47). To achieve the desired process temperature and to minimize the thermal degradation during hot-melt extrusion formulation, plasticizers are added. In some scenarios, however, glass transition temperature (T_g) of the formulation was found to be reduced by some plasticizers, thus affecting the physical stability of the product. (48,49).

Selection of excipient is very crucial. As presented above, adding an antioxidant, such as ascorbic acid, into the THC formulation helps stabilize the thermolabile drug. In contrast, the authors also reported that the other antioxidant, vitamin E succinate gave the opposite results. The degradation remarkably increased and the stability of the THC formulation was reduced (18).

Biopharmaceuticals: Excipients in peptide/protein formulations are often used to stabilize the drugs during processing and/or storage or to serve as a matrix for controlled release (40). Several reports presented that crystallization of stabilizing agents such as mannitol and glycine, influences the stability of the drugs (11,50–52). The other main concern is buffer used since certain buffer salts potentially precipitate during lyophilization

and lead to large pH changes (53). The effects of excipients on aggregation of peptide are also investigated in Chapter 3.

1.2.7 Processing methods

Amorphous solids can be prepared by different pharmaceutical processes, such as melt extrusion, spray- and freeze-drying (54). Melting of the drug-polymer mixtures is attributed to the heat and shear force of the hot melt extrusion (41). Thus, either high temperature or shear stress or their combination can generally cause drug degradation. In addition, other variables such as residence time can have an influence on physical and chemical stability of the product as well. This will be discussed in Chapter 2.

Besides the melt processing, spray drying is also widely used to produce solid dispersions. Typical inlet and outlet temperatures of the spray dryer are 60-160°C and 40-90°C, respectively. As discussed in Chapter 2, even though the inlet temperature of the spray dryer is high, the drying of the particles is typically very quick (a second up to a few seconds) (55). Thus, the high speed vaporization and low outlet temperature of the drying chamber can avoid crystallization, and instability of the drug during processing.

Lyophilization or freeze-drying is another well-known manufacturing approach used to prepare both small molecule and biological formulations. In particular, for heat-sensitive compounds like biologics, lyophilization is often selected. Even if a number of peptides/proteins survive the freeze-drying process, some proteins suffer irreversible damage during processing (56). Because lyophilization is a multistage process that

generates dry materials by removing the solvent(s) and each step is critical (57,58), the optimal cycle conditions will lead to a stable formulation.

1.3 STABILITY OF SMALL MOLECULE DRUGS

Drug stability and degradation reactions are reviewed in several books (3,15,59). Drug that loses potency and contains degradants over the acceptance criteria may be considered as unacceptable product. The significant changes of product appearance such as color or odor may indicate the instability of the product. The chemical and physical stability should be continuously studied to determine the suitable formulation components, optimized processing conditions, storage condition, and long-term-stability of the drug products.

1.3.1 Chemical stability of small molecules

Potency of the drug decreases when it degrades through the chemical reactions. Since the drug may degrade to a toxic substance, it is valuable to identify the relevant degradants. Several chemical reactions causing degradation include hydrolysis, dehydration, isomerization and racemization, elimination, oxidation, photodegradation, as well as complex interactions with excipients and other drugs. Drugs are susceptible to various degradation mechanisms due to the diversity of molecular structures. Prediction of the chemical instability of a drug based on its molecular structure would be beneficial (15).

1.3.2 Physical stability of small molecule drugs

Physical stability such as drug crystallization should be a major concern since it generally decreases the dissolution of the amorphous system (30). There are several factors affecting physical stability of drug formulation in solid state, particularly amorphous pharmaceuticals, such as crystallization, and structure collapse. Amorphous solids are physically unstable, which can transform to the crystalline state. Since the advantages of amorphous solids are negated by crystallization, the stability of amorphous drugs against crystallization is critical for pharmaceutical development (60). However, crystallization from the amorphous state can be localized by including some excipients in the formulations to stabilize the amorphous state (54).

Marsac et al. (2010) reported that the miscibility of formulation components impacted the physical stability of amorphous solid dispersion (30). Therefore, studying the solubility parameters and miscibility of the drug and components prior to formulating the amorphous solid dispersions would be very useful to anticipate the physical stability of the products. Also, the glass transition temperature (T_g) of the amorphous material is one of the most important properties associated with its physical stability.

T_g is defined as “a temperature at which an amorphous material undergoes a transition from a glassy state to a rubbery state” (61). The major cause of physical instability of the amorphous systems is the high molecular mobility (62). Therefore, the T_g of amorphous materials is correlated with their molecular mobility and physical stability. When the temperature is below the T_g of the drug-polymer system, mobility of the

molecules is limited and the system remains in the glassy state. Relationship between the molecular mobility of small molecules and polymers and their Tg(s) was reported. Considerable molecular mobility of amorphous solids exists at the temperatures up to 50°C below their Tg(s) (60). As a Tg-50 rule, the amorphous systems are more physically stable when the Tg of the system is 50°C above the storage temperature (54).

1.4 STABILITY OF THERAPEUTIC PEPTIDES AND PROTEINS

The therapeutic activity of proteins highly depends on their conformational structure (57). Owing to their complex structure, the development of stable peptide/protein formulations generally require even more resources and effort than the conventional small molecule drugs (28). Stability requirements for biologics are also more restrictive than for small molecules (63). Therefore, one of the difficulties in commercial development of therapeutic peptides/proteins is achieving stability (22). Peptide/protein stabilities can be divided into two general groups: chemical stability and physical stability (64). Following such physical instability such as denaturation or unfolding, chemical instability of peptide/protein in the solid state can also occur (40). Hence, an understanding of the chemical and physical stability of biopharmaceuticals can avoid stability problems and develop the suitable analytical methods for characterization of drugs and their related compounds. It would be more beneficial if the interrelationship between chemical and physical instability is known. However, as a result of the smaller size and lesser ordered structure, peptides may behave differently from proteins (65). Moreover, each protein may also perform differently as well due to their large and complex three-dimensional

structures.

1.4.1 Chemical Stability of macromolecules

Chemical instabilities of proteins involve covalent modification (make or break bonds, rearrangement, or substitution) to generate new molecules (40). There are several chemical processes that contribute instability of biopharmaceuticals such as deamidation (66), oxidation (67), hydrolysis (68), aspartate (Asp) isomerization (69), racemization (70), Maillard reaction (71), β -elimination (23), and glycation of proteins (72). The susceptibility of peptide/protein to chemical degradation in solution challenges scientists in the development of the stable formulations (22). As a consequence, lyophilization has been used to prolong shelf life of the protein formulation (73,74). Although lyophilized formulation is generally more stable than the corresponding aqueous formulation, chemical degradation reactions can still occur (73,74) as reported in some cases that protein stability in the solid state is less than or similar to that in solution (75,76). Since peptide/protein are frequently prepared in solid-state formulations to prolong the shelf life, this section focuses on the chemical degradation of the proteins and peptides in the solid state. The factors affecting to chemical stability of proteins/peptide in solid-state are, for example, temperature, residual moisture and the excipient(s) included in a formulation (40) as described above.

1.4.2 Physical Stability of macromolecules

Owing to the polymeric nature of the proteins and their ability to adopt some forms of superstructure (secondary, tertiary, and quaternary), proteins can undergo various types of structural changes (22). The physical stability of a protein relates to maintaining the native secondary and higher order structure. The meaning of physical instability of protein is any process by which the physical state (three-dimensional conformational integrity) of the protein changes without any change in the chemical composition (64). However, physical instabilities may result from chemical instabilities such as deamidation and disulfide bond cleavage and vice versa (40). Typically physical instability of proteins includes four processes: denaturation, aggregation, precipitation and surface adsorption (22). “Precipitation” is the term used to denote insolubility rather than insoluble aggregate formation.

1.5 STABILITY OF THE NEBULIZED BIOPHARMACEUTICALS

Direct drug delivery to the site of action provides high drug concentrations, minimizes systemic exposure and increases therapeutic effects and safety (77–79). Comparing with other devices for pulmonary delivery, nebulization of biologics directly to the lung is easier, faster and most used to formulate and test a new drug model (80). However, there was a report on stability issue with biopharmaceuticals when using nebulizer (81). In some atomization process, shear stress and heat may damage the drugs (80). Since the biopharmaceuticals are more susceptible to the physical stress (shear stress and heat) produced by the atomizers than small molecule, their pharmacological activity could be

affected during nebulization (29,80). In addition, the solution formulations are more susceptible to the effect of the factors than suspension formulations (29). Thus, the challenge of inhalation technologies for biopharmaceutical compounds is to maintain their therapeutic activity until the drugs access to the lung. The evaluation of nebulization process is significant for the development of peptide/protein formulations.

The nebulizers are categorized according to the mechanism of atomization into three types; jet, ultrasonic, and vibrating-mesh nebulizers (29,80). Relevant factors affecting biopharmaceutics degradation and inactivation depend on the basic mechanism of aerosol generation (29). Air-jet and ultrasonic nebulizers by design suffer from recirculation. In brief, the droplets are repeatedly nebulized for at least 10-15 times resulting in an increase in interfacial stress (82,83). Ultrasonic nebulizers can also generate heat, which can cause negative effects on heat-labile compounds such as proteins or peptides (84). On the other hand, the vibrating mesh nebulizers are single-pass devices by design that can prevent the repetition of nebulization stress (85) and do not generate heat during operation (86). Thus, vibrating mesh nebulizers are currently the most suitable devices for pulmonary protein/peptide delivery. In conclusion, owing to factors of biologics degradation and inactivation, the vibrating mesh nebulizers have been recommended to aerosolize peptide/protein formulations (87,88) since they gently generate the aerosol plume (89,90) with low shear stress (91). In Chapter 3 and Chapter 4, the nebulization of the biologics (peptide and protein) was examined.

1.6 CONCLUSIONS

Stability is a critical issue that must be assessed during the drug development process. Drug instability can occur not only in the liquid state, but also in the solid state. The common factors that must be studied include temperature, pH, moisture, oxygen, shear stress and excipients. Processing technique and device type for drug delivery can also cause drug degradation. The small- and macromolecules have both similar and different relevant factors affecting the stability of their formulations. Macromolecules tend to be less stable than the small molecules due to their complex structures and various functional groups.

REFERENCES

1. Shaika RH, Sial AA. Stability of pharmaceutical formulations. *Pak J Pharm Sci.* 1996;9(2):83–86.
2. Guo Y, Shalaev E, Smith S. Solid-state analysis and amorphous dispersions in assessing the physical stability of pharmaceutical formulations. *TrAC Trends Anal Chem.* 2013;49:137.
3. Huynh-Ba K. Handbook of stability testing in pharmaceutical development: regulations, methodologies, and best practices. 1. Aufl. New York: Springer; 2009.
4. Bajaj S, Singla D, Sakhuja N. Stability Testing of Pharmaceutical Products. *J Appl Pharm Sci.* 2012;2(3):129.
5. Wang W. Protein aggregation and its inhibition in biopharmaceutics. *Int J Pharm.* 2005;289(1–2):1–30.
6. Briscoe CJ, Hage DS. Factors affecting the stability of drugs and drug metabolites in biological matrices. *Bioanalysis.* 2009;1(1):205.
7. Asahara K, Yamada H, Yoshida S. Stability of human insulin in solutions containing sodium bisulfite. *Chem Pharm Bull (Tokyo).* 1991;39(10):2662–6.
8. Helm VJ, Müller BW. Stability of the synthetic pentapeptide thymopentin in aqueous solution: Effect of pH and buffer on degradation. *Int J Pharm.* 1991;70(1):29–34.

9. Oliyai C, Patel JP, Carr L, Borchardt RT. Chemical pathways of peptide degradation. VII. Solid state chemical instability of an aspartyl residue in a model hexapeptide. *Pharm Res.* 1994;11(6):901–908.
10. Paborji M, Pochopin NL, Coppola WP, Bogardus JB. Chemical and physical stability of chimeric L6, a mouse-human monoclonal antibody. *Pharm Res.* 1994;11(5):764.
11. Akers MJ, Milton N, Byrn SR, Nail SL. Glycine crystallization during freezing: the effects of salt form, pH, and ionic strength. *Pharm Res.* 1995;12(10):1457–1461.
12. Melveger AJ, Huynh-Ba K. Critical Regulatory Requirements for a Stability Program. In: *Handbook of stability testing in pharmaceutical development: regulations, methodologies, and best practices.* 2nd ed. New York: Springer; 2009. p. 9–19.
13. <1150> Pharmaceutical Stability. In: *US Pharmacopeia 35-NF30* [Internet]. Pharmacopeial Convention, Rockville, MD.; 2012. Available from: www.uspnf.com
14. Volkin DB, Middaugh CR. The effect of temperature on protein structure. In: *Stability of protein pharmaceuticals part A chemical and physical pathways of protein degradation.* New York: Plenum Press; 1992. p. 215–47.
15. Yoshioka S, Stella VJ, NetLibrary, Inc. *Stability of drugs and dosage forms.* New York: Kluwer Academic; 2002.

16. Munjal M, Stodghill SP, ElSohly MA, Repka MA. Polymeric systems for amorphous Δ^9 -tetrahydrocannabinol produced by a hot-melt method. Part I: Chemical and thermal stability during processing. *J Pharm Sci.* 2006;95(8):1841–1853.
17. Munjal M, ElSohly MA, Repka MA. Chemical stabilization of a Delta9-tetrahydrocannabinol prodrug in polymeric matrix systems produced by a hot-melt method: role of microenvironment pH. *AAPS PharmSciTech.* 2006;7(3):71.
18. Munjal M, Elsohly MA, Repka MA. Polymeric systems for amorphous Delta9-tetrahydrocannabinol produced by a hot-melt method. Part II: Effect of oxidation mechanisms and chemical interactions on stability. *J Pharm Sci.* 2006;95(11):2473.
19. Lai MC, Topp EM. Solid-state chemical stability of proteins and peptides. *J Pharm Sci.* 1999;88(5):489–500.
20. Oliyai C, Patel JP, Carr L, Borchardt RT. Solid state chemical instability of an asparaginy residue in a model hexapeptide. *J Pharm Sci Technol.* 1994;48(3):167.
21. Karel M, Yong S. Autoxidation-initiated reactions in foods. In: *Water activity: influences on food quality.* 1981. p. 511–29.
22. Manning MC, Patel K, Borchardt RT. Stability of protein pharmaceuticals. *Pharm Res.* 1989;6(11):903–918.

23. Costantino HR, Langer R, Klibanov AM. Moisture-induced aggregation of lyophilized insulin. *Pharm Res.* 1994;11(1):21–29.
24. Franks F. Protein destabilization at low temperatures. *Adv Protein Chem.* 1995;46:105.
25. Hertel S, Pohl T, Friess W, Winter G. That’s cool!--Nebulization of thermolabile proteins with a cooled vibrating mesh nebulizer. *Eur J Pharm Biopharm.* 2014 Jul;87(2):357.
26. Ellin RI, Henry Wills J. Oximes Antagonistic to Inhibitors of Cholinesterase: Part I. *J Pharm Sci.* 1964;53(9):995–1007.
27. Deshpande AD, Baheti KG, Chatterjee NR. Degradation of b-lactam antibiotics. *Curr Sci.* 2004;87:1684–1695.
28. Chang BS, Hershenson S. Practical approaches to protein formulation development. In: *Rational design of stable protein formulations: theory and practice.* New York: Kluwer Academic; 2002. p. 1–23.
29. Hertel SP, Winter G, Friess W. Protein stability in pulmonary drug delivery via nebulization. *Adv Drug Deliv Rev.* 2015;93:79–94.

30. Marsac PJ, Rumondor AC, Nivens DE, Kestur US, Stanciu L, Taylor LS. Effect of temperature and moisture on the miscibility of amorphous dispersions of felodipine and poly (vinyl pyrrolidone). *J Pharm Sci.* 2010;99(1):169–185.
31. Flores-Fernández GM, Solá RJ, Griebenow K. The relation between moisture-induced aggregation and structural changes in lyophilized insulin. *J Pharm Pharmacol.* 2009;61(11):1555–61.
32. Jain NK, Roy I. Role of trehalose in moisture-induced aggregation of bovine serum albumin. *Eur J Pharm Biopharm.* 2008;69(3):824–34.
33. Sharma V, Klibanov A. Moisture-Induced Aggregation of Lyophilized DNA and its Prevention. *Pharm Res.* 2007;24(1):168–75.
34. Schwendeman SP, Costantino HR, Gupta RK, Siber GR, Klibanov AM, Langer R. Stabilization of Tetanus and Diphtheria Toxoids Against Moisture-Induced Aggregation. *Proc Natl Acad Sci U S A.* 1995;92(24):11234–8.
35. Jain N, Roy I. Accelerated Stability Studies for Moisture-Induced Aggregation of Tetanus Toxoid. *Pharm Res.* 2011;28(3):626–39.
36. Boccardi G. Oxidative susceptibility testing. Taylor& Francis; 2005.

37. Alsante KM, Ando A, Brown R, Ensing J, Hatajik TD, Kong W, et al. The role of degradant profiling in active pharmaceutical ingredients and drug products. *Adv Drug Deliv Rev.* 2007;59(1):29–37.
38. Camacho W, Karlsson S. Assessment of thermal and thermo-oxidative stability of multi-extruded recycled PP, HDPE and a blend thereof. *Polym Degrad Stab.* 2002;78(2):385–91.
39. Shirwaikar A, Srinivasan K, Alex J, Prabu S, Mahalaxmi R, Kumar R, et al. Stability of proteins in aqueous solution and solid state. *Indian J Pharm Sci.* 2006;68(2):154–63.
40. Lai MC, Topp EM. Solid-state chemical stability of proteins and peptides. *J Pharm Sci.* 1999;88(5):489–500.
41. Crowley MM, Zhang F, Repka MA, Thumma S, Upadhye SB, Kumar Battu S, et al. Pharmaceutical applications of hot-melt extrusion: part I. *Drug Dev Ind Pharm.* 2007;33(9):909–926.
42. Gidalevitz D, Huang Z, Rice SA. Protein Folding at the Air-Water Interface Studied with X-Ray Reflectivity. *Proc Natl Acad Sci U S A.* 1999;96(6):2608–11.
43. Maa Y-F, Hsu CC. Protein denaturation by combined effect of shear and air-liquid interface. *Biotechnol Bioeng.* 1997;54(6):503–12.

44. Bruce CD. Recrystallization of guaifenesin from hot-melt extrudates containing Acryl-EZE or Eudragit L100-55. University of Texas at Austin; 2008.
45. Beyler CL, Hirschler MM. Thermal decomposition of polymers. *SFPE Handb Fire Prot Eng.* 2002;2:110–131.
46. Güres S, Kleinebudde P. Dissolution from solid lipid extrudates containing release modifiers. *Int J Pharm.* 2011;412(1):77–84.
47. DiNunzio JC, Martin, Z.F.C., McGinity JW. Melting extrusion. In: Williams III RO, Watts AB Miller, DA, editors. *Formulating poorly water soluble drugs.* Springer, New York, NY; 2012. p. 311–62.
48. El-Gendy NA. Pharmaceutical plasticizers for drug delivery systems. *Curr Drug Deliv.* 2012 Mar;9(2):148.
49. Ghebremeskel A, Vemavarapu C, Lodaya M. Use of surfactants as plasticizers in preparing solid dispersions of poorly soluble API: stability testing of selected solid dispersions. *Pharm Res.* 2006;23(8):1928–36.
50. Costantino HR, Andya JD, Nguyen P-A, Dasovich N, Sweeney TD, Shire SJ, et al. Effect of mannitol crystallization on the stability and aerosol performance of a spray-dried pharmaceutical protein, recombinant humanized anti-IgE monoclonal antibody. *J Pharm Sci.* 1998;87(11):1406–1411.

51. Cavatur R, Vemuri N, Pyne A, Chrzan Z, Toledo-Velasquez D, Suryanarayanan R. Crystallization behavior of mannitol in frozen aqueous solutions. *Pharm Res.* 2002;19(6):894–900.
52. Al-Hussein A, Gieseler H. The effect of mannitol crystallization in mannitol-sucrose systems on LDH stability during freeze-drying. *J Pharm Sci.* 2012;101(7):2534–44.
53. Carpenter JF, Chang BS, Garzon-Rodriguez W, Randolph TW. Rational design of stable lyophilized protein formulations: theory and practice. In: *Rational design of stable protein formulations.* Springer; 2002. p. 109–133.
54. Yu L. Amorphous pharmaceutical solids: preparation, characterization and stabilization. *Adv Drug Deliv Rev.* 2001;48(1):27–42.
55. Kolter K, Karl M, Gryczke A. Hot-melt extrusion with BASF pharma polymers: extrusion compendium. 2nd ed. 2012.
56. Pikal MJ. Mechanisms of protein stabilization during freeze-drying storage: the relative importance of thermodynamic stabilization and glassy state relaxation dynamics. In: *Freeze-drying/lyophilization of pharmaceutical and biological products.* New York: Marcel Dekker; 1999. p. 198–232.

57. Frokjaer S, Otzen DE. Protein drug stability: a formulation challenge. *Nat Rev Drug Discov.* 2005;4(4):298–306.
58. Yang W, Owens III DE, Williams III RO. Pharmaceutical cryogenic technologies. In: *Formulating poorly water soluble drugs.* New York: Springer; p. 443–500.
59. Carstensen JT, Rhodes CT. *Drug stability: principles and practices.* 3rd ed., and expanded. New York: Marcel Dekker; 2000. (Drugs and the pharmaceutical sciences; vol. 107).
60. Hancock BC, Shamblin SL, Zografi G. Molecular mobility of amorphous pharmaceutical solids below their glass transition temperatures. *Pharm Res.* 1995;12(6):799–806.
61. Shah N, Sandhu H, Choi DS, Kalb O, Page S, Wytenbach N. Structured development approach for amorphous systems. In: *Formulating poorly water soluble drugs.* New York, NY: AAPS Press; 2012. p. 267–310.
62. Bhardwaj SP, Arora KK, Kwong E, Templeton A, Clas S-D, Suryanarayanan R. Correlation between Molecular Mobility and Physical Stability of Amorphous Itraconazole. *Mol Pharm.* 2013;10(2):694–700.

63. McNally EJ, Hastedt JE. Development of Drug Products: Similarities and Differences Between Protein Biologics and Small Synthetic Molecules. In: Protein Formulation and Delivery. 2nd ed. Informa Healthcare New York, NY; 2007. p. 332.
64. Manning MC, Chou DK, Murphy BM, Payne RW, Katayama DS. Stability of protein pharmaceuticals: an update. *Pharm Res.* 2010;27(4):544–575.
65. Fang W-J, Qi W, Kinzell J, Prestrelski S, Carpenter J. Effects of excipients on the chemical and physical stability of glucagon during freeze-drying and storage in dried formulations. *Pharm Res.* 2012;29(12):3278–91.
66. Pikal M, Rigsbee D. The stability of insulin in crystalline and amorphous solids: observation of greater stability for the amorphous form. *Pharm Res.* 1997;14(10):1379–87.
67. Hovorka SW, Schöneich C. Oxidative degradation of pharmaceuticals: Theory, mechanisms and inhibition. *J Pharm Sci.* 2001;90(3):253–69.
68. Tarelli E, Corran PH. Ammonia cleaves polypeptides at asparagine proline bonds. *J Pept Res.* 2003;62(6):245–251.
69. Chu G, Chelius D, Xiao G, Khor H, Coulibaly S, Bondarenko P. Accumulation of Succinimide in a Recombinant Monoclonal Antibody in Mildly Acidic Buffers Under Elevated Temperatures. *Pharm Res.* 2007;24(6):1145–56.

70. Ueno K, Ueda T, Sakai K, Abe Y, Hamasaki N, Okamoto M, et al. Evidence for a novel racemization process of an asparaginyl residue in mouse lysozyme under physiological conditions. *Cell Mol Life Sci.* 2005;62(2):199–205.
71. Lan X, Liu P, Xia S, Xia W, Jia C, Mukunzi D, et al. Temperature effect on the non-volatile compounds of Maillard reaction products derived from xylose–soybean peptide system: Further insights into thermal degradation and cross-linking. *Food Chem.* 2010;120(4):967–72.
72. Hawe A, Friess W. Development of HSA-free formulations for a hydrophobic cytokine with improved stability. *Eur J Pharm Biopharm.* 2008;68(2):169–82.
73. Carpenter J, Pikal M, Chang B, Randolph T. Rational design of stable lyophilized protein formulations: some practical advice. *Pharm Res.* 1997;14(8):969–75.
74. Pikal MJ, Dellerman KM, Roy ML, Riggin RM. The effects of formulation variables on the stability of freeze-dried human growth hormone. *Pharm Res.* 1991;8(4):427–436.
75. Strickley RG, Visor GC, Lin LH, Gu L. An unexpected pH effect on the stability of moexipril lyophilized powder. *Pharm Res.* 1989;6(11):971.
76. Pearlman R, Nguyen T. Pharmaceutics of protein drugs. *J Pharm Pharmacol.* 1992;44:178.

77. Geller DE. The science of aerosol delivery in cystic fibrosis. *Pediatr Pulmonol.* 2008 Sep 1;43(S9):S5–17.
78. Pilcer G, Amighi K. Formulation strategy and use of excipients in pulmonary drug delivery. *Int J Pharm.* 2010;392(1):1–19.
79. Maillet A, Guilleminault L, Lemarié E, Lerondel S, Azzopardi N, Montharu J, et al. The Airways, a Novel Route for Delivering Monoclonal Antibodies to Treat Lung Tumors. *Pharm Res.* 2011;28(9):2147–56.
80. Fathe K, Ferrati S, Moraga-Espinoza D, Yazdi A, Smyth HDC. Inhaled Biologics: From Preclinical to Product Approval. *Curr Pharm Des.* 2016;22(17):2501.
81. Niven RW, Prestrelski SJ, Treuheit MJ, Ip AY, Arakawa T. Protein nebulization II. Stabilization of G-CSF to air-jet nebulization and the role of protectants. *Int J Pharm.* 1996;127(2):191–201.
82. Uchenna Agu R, Ikechukwu Ugwoke M, Armand M, Kinget R, Verbeke N. The lung as a route for systemic delivery of therapeutic proteins and peptides. *Respir Res.* 2001;2:198.
83. Niven RW. Delivery of biotherapeutics by inhalation aerosol. *Crit Rev Ther Drug Carrier Syst.* 1995;12(2–3):151–231.

84. Niven RW, Ip AY, Mittelman S, Prestrelski SJ, Arakawa T. Some factors associated with the ultrasonic nebulization of proteins. *Pharm Res.* 1995;12(1):53–59.
85. Lass JS, Sant A, Knoch M. New advances in aerosolised drug delivery: vibrating membrane nebuliser technology. *Expert Opin Drug Deliv.* 2006;3(5):693–702.
86. Fink JB, Schmidt D, Power J. Comparison of a nebulizer using a novel aerosol generator with a standard ultrasonic nebulizer designed for use during mechanical ventilation. American Thoracic Society 97th International Conference, San Francisco, CA; 2001.
87. Elhissi AMA, Taylor KMG. Delivery of liposomes generated from proliposomes using air-jet, ultrasonic, and vibrating-mesh nebulisers. *J Drug Deliv Sci Technol.* 2005;15(4):261–5.
88. Hertel S, Pohl T, Friess W, Winter G. Prediction of protein degradation during vibrating mesh nebulization via a high throughput screening method. *Eur J Pharm Biopharm.* 2014;87(2):386–394.
89. Waldrep JC, Dhand R. Advanced nebulizer designs employing vibrating mesh/aperture plate technologies for aerosol generation. *Curr Drug Deliv.* 2008;5(2):114–119.

90. Watts AB, McConville JT, Williams RO. Current Therapies and Technological Advances in Aqueous Aerosol Drug Delivery. *Drug Dev Ind Pharm.* 2008;34(9):913–22.
91. Knoch M, Keller M. The customised electronic nebuliser: a new category of liquid aerosol drug delivery systems. *Expert Opin Drug Deliv.* 2005;2(2):377–90.

Chapter 2: Hot Melt Extrusion versus Spray Drying: Hot Melt Extrusion Degrades Albendazole

ABSTRACT

The purpose of this study was to enhance the dissolution properties of albendazole (ABZ) by the use of amorphous solid dispersions. Phase diagrams of ABZ-polymer binary mixtures generated from Flory-Huggins theory were used to assess miscibility and processability. Forced degradation studies showed that ABZ degraded upon exposure to hydrogen peroxide and 1 N NaOH at 80°C for 5 min, and the degradants were albendazole sulfoxide (ABZSX), and ABZ impurity A, respectively. ABZ was chemically stable following exposure to 1 N HCl at 80°C for one hour. Thermal degradation profiles show that ABZ, with and without Kollidon® VA 64, degraded at 180°C and 140°C, respectively, which indicated that ABZ could likely be processed by thermal processing. Following hot melt extrusion ABZ degraded up to 97.4%, while the amorphous ABZ solid dispersion was successfully prepared by spray drying. Spray-dried ABZ formulations using various types of acids (methanesulfonic acid, sulfuric acid and hydrochloric acid), and polymers (Kollidon® VA 64, Soluplus® and Eudragit® E PO) were studied. The spray-dried ABZ with methanesulfonic acid and Kollidon® VA 64 substantially improved non-sink dissolution in acidic media as compared to bulk ABZ (8-fold), physical mixture of ABZ:Kollidon® VA 64 (5.6-fold) and ABZ mesylate salt (1.6-fold). No degradation was

observed in the spray-dried product for up to 6 months and less than 5% after 1-year storage. In conclusion, amorphous ABZ solid dispersions in combination with an acid and polymer can be prepared by spray drying to enhance dissolution and shelf-stability, whereas those made by melt extrusion are degraded.

2.1 INTRODUCTION

Successful treatment of infections of the liver, lung, and peritoneum caused by worms with drugs in the benzimidazole group, including albendazole (ABZ), depends on the plasma concentration of the drug [1]. However, ABZ is practically insoluble in water as a BCS class II drug [2]. Its low water solubility leads to an extremely low (< 5%) systemic absorption [3]. Dissolution is an important limiting step of ABZ absorption, so enhancement of the dissolution is expected to result in greater bioavailability [4]. Various strategies have been developed to improve oral bioavailability of ABZ, such as administering the drug with a fatty meal [5] or using surfactants [6], nanosuspensions [7], co-grinding with water soluble polymers [8], nanocrystals [9], salt formation [10] and solid dispersions [11,12]. However, to our knowledge, combinations of salt and amorphous solid dispersions of ABZ have not been reported.

Amorphous solid dispersions are desirable to improve drug solubility since amorphous drugs exist in a high energy form which contributes to the increased solubility, however, they are not thermodynamically stable and are prone to recrystallization. The solubility parameters and thermodynamic models have been recognized as the logical and

rational approaches for guiding the selection of drug-polymer compositions and processing parameters to obtain stable amorphous solid dispersions [13–16].

Ideally, a water-insoluble drug and hydrophilic carrier(s) are homogeneously mixed at the molecular level to form an amorphous solid dispersion. Hot melt extrusion (HME) and spray drying are well-known processing techniques for preparing solid dispersions [17,18]. HME is a solvent-free continuous thermal process, which transforms discrete particles of drug and polymeric carrier(s) into a glassy state product. The quality of the extruded product depends on the processing parameters (e.g., screw configuration, processing temperature, screw speed, and feed rate) and properties of the components (e.g., glass transition temperature (T_g), solubility and stability) [18,19]. For higher melting point drugs (normally those with high molecular weight), the drug particles may not be melted during processing, but dissolved into the rubbery polymer. The high molecular weight drugs containing various types of atoms and functional groups can lead to higher propensity to degradation including thermal degradation. The balance between mixing efficiency and thermal exposure to achieve the desirable safety and efficacy of the products must be evaluated [19]. On the other hand, spray drying is a solvent-based method that transforms a solution (or suspension) of drug and excipient(s) into a glassy state. Process parameters of spray drying (e.g., inlet and outlet temperatures, feed flow rate and types of atomization nozzles) and properties of compositions of the formulation (e.g., carrier, solvent, and solid content) also substantially affect product quality [20]. HME has many advantages over the solvent-based techniques, however it poses a challenge on thermolabile and shear sensitive

drugs [21]. The drug candidates processed by HME have to be exposed to elevated temperatures and shear stress in the equipment for a long period of time, so they may decompose during the process [21,22]. A recent study mentioned about the shear stress and energy input affecting the recovery of carbamazepine during the extrusion [23].

The present study compares dissolution performance and purity of solid dispersions of ABZ made by HME and spray drying. The objective of this study is to enhance the dissolution performance of ABZ by preparing solid dispersions made by spray drying and hot melt extrusion. To our knowledge, there are no reports of thermal degradation, solubility parameters, or phase diagrams of binary mixtures of ABZ and carriers. Therefore, the applicability of modeling ABZ and polymer miscibility based on Flory-Huggins theory is studied.

2.2 MATERIALS AND METHODS

2.2.1 Materials

Albendazole (ABZ) was purchased from Molecular (Irvine, CA). Kollidon® VA 64 and Soluplus® were kindly donated from BASF (Florham Park, NJ). Eudragit® E PO was generously donated from Degussa GmbH (Linden, NJ). Tetrahydrofuran (THF) with butylated hydroxytoluene (BHT) was purchased from Thermo Fisher Scientific (Hudson, NH). All other chemicals and solvents used were American Chemical Society (ACS) reagent or high performance liquid chromatography (HPLC) grade.

2.2.2 Preformulation studies

2.2.2.1 pH solubility profile and pKa

Buffer species were prepared as per USP 36 [24], ranging in pH values from 1.2 to 9. For pH 1.2, USP-simulated gastric fluid (without pepsin) was used. An excess of crystalline ABZ was added to each glass vial containing buffer media. The vials were placed in the shaker (Environ Orbital Shaker, Lab-Line Instruments, Melrose Park, IL, USA) at 100 rpm shaking speed, at 37°C, in the absence of light. The aliquot samples were collected after 12, and 24 hours, centrifuged and filtered through 0.22 µm, 13-mm polyvinylidene difluoride (PVDF) syringe filters. Samples were properly diluted with methanol, and the concentration of ABZ was measured using HPLC as described below. The pKa of ABZ in buffer at 37°C was calculated from the pH solubility profile and the modified Henderson-Hasselbalch equation [25].

$$\log S = \log S_0 + \log(1 + 10^{pKa-pH})$$

where S_0 is the intrinsic solubility, S is the solubility at a given pH, and pKa is a pH at which the concentration of unionized and ionized forms of a monoprotic drug in the solution are equal.

2.2.2.2 Forced degradation study

ABZ was exposed to stressed conditions including acid, basic, oxidation, and thermal degradation [26]. Firstly, a stock solution of 1 mg/mL ABZ was prepared by dissolving the drug with 1% sulfuric acid in methanol and diluting to volume with

methanol. For acid stressed degradation, 1 mL of the stock solution was exposed to 1 mL of 1 N HCl for 2 hours and 1 hour at 25°C and 80°C, respectively. The reaction was then stopped with 1 mL of 1 N NaOH and diluted to volume (10 mL) with methanol. On the other hand, the alkaline stressed condition was achieved by adding 1 mL of 1 N NaOH to the ABZ stock solution. The exposure times were 1 hour, and 5 min, at 25°C and 80°C, respectively. The reaction was quenched by 1 mL of 1 N HCl and the sample was diluted with methanol. Oxidative degradation was carried out by reacting 1 mL of ABZ stock solution with 1 mL of 3% hydrogen peroxide (H₂O₂) solution at 25°C and 80°C for 1 hour and 5 min, respectively, and diluted with methanol. For the thermal degradation, the sample solution was heated to 80°C for 2 hours and diluted with methanol before being tested. All samples were analyzed using HPLC and LC/MS.

2.2.2.3 Thermal stability profile

Thermal analysis was performed using a Q20 modulated differential scanning calorimeter (mDSC) (TA Instruments, New Castle, DE, USA) to determine the thermal degradation profile of ABZ with or without a polymer. The instrument was calibrated using the standard, indium, prior to use. Bulk ABZ and its physical mixture with Kollidon® VA 64 (20:80) of 6.0 ± 0.1 mg were weighed into the aluminum DSC pans and heated and equilibrated at each temperature for 5 min with 50 mL/min of nitrogen flow. Samples were studied at 10°C intervals over a range of 80°C to 220°C. After 5 min, the sample was removed from the pan and dissolved with 1% sulfuric acid in methanol and diluted to

volume with methanol. Sample solutions were analyzed by HPLC to investigate the influence of polymers on the degradation temperature of ABZ.

2.2.3 Drug-polymer miscibility model

2.2.3.1 Melting point depression approach

Prior to running the experiments, drugs and polymers were dried in a vacuum oven for 24 hours. The test method was adapted from a previous study [19]. In short, physical mixtures of ABZ and each polymer were prepared at concentrations of 0%, 5%, 10%, 15%, 20%, and 25% polymer by volume for ABZ systems. Each composition was weighed into an aluminum pan at 6.0 ± 0.1 mg. Triplicate samples were prepared at each concentration. The onset of melting endotherm and the melting temperature of the ABZ, in the presence of a polymer, were measured with an mDSC equipped with a refrigerated cooling accessory (DSC 2920, TA Instruments, New Castle, DE, USA). A ramp rate of 1°C/min, from 30°C to 250°C modulating every 60 sec at an amplitude of 1°C with 50 mL/min of nitrogen gas, were exploited as a running condition for all samples. Glass transition temperatures (T_g) were also determined for the drug concentration–T_g profile. The heat–cool–heat cycle was used to heat the sample to 210°C, quench-cool to remove thermal history, and re-heat to measure the T_g of samples at different drug–polymer ratios.

2.2.3.2 Hansen solubility parameter (δ)

Solubility parameters of ABZ were calculated based on chemical structure and

group contributions using Molecular Modeling Pro software (Chem SW Inc., Fairfield, CA). The summary of the three fractions is shown in Equation 1 [27].

$$\delta^2 = \delta_d^2 + \delta_p^2 + \delta_h^2 \quad \text{Equation 1}$$

where δ is the total solubility parameter, δ_d is dispersion forces, δ_p is polar interactions of the functional groups in the molecule, and δ_h is hydrogen bonding energy. Miscibility of the binary mixture system was evaluated from the difference in solubility parameters between ABZ and polymer ($\Delta\delta$).

2.2.3.3 Flory–Huggins Theory

Flory–Huggins theory was applied to generate the Gibbs free energy of mixing and a phase diagram of the ABZ–polymer binary system. The relative contribution of entropy and enthalpy to the mixing free energy of ABZ-polymer systems is as described in Equation 2.

$$G_{mix} = \Delta H_{mix} - T\Delta S_{mix} \quad \text{Equation 2}$$

where G_{mix} is the free energy of mixing, ΔH_{mix} is the enthalpy of mixing, T is the absolute temperature, and ΔS_{mix} is the entropy of mixing.

In addition, Equation 3, Gibbs free energy of mixing was evaluated in terms of the volume fractions of the drug, ϕ , and the Flory–Huggins interaction parameter, χ .

$$\frac{\Delta G_{mix}}{RT} = n_{drug} \ln \phi_{drug} + n_{polymer} \ln \phi_{polymer} + n_{drug} \phi_{polymer} \chi \quad \text{Equation 3}$$

where G_{mix} is the free energy of mixing, R is the universal gas constant, T is the absolute temperature, n_{drug} and $n_{polymer}$ are the number of moles of the drug and the polymer, respectively, ϕ_{drug} is the volume fraction of the drug and $\phi_{polymer}$ is the volume fraction of the polymer [28–30]. Molar volume per Flory–Huggins lattice size, was also calculated using Molecular Modeling Pro software and the χ is considered as a function of temperature as described in the literature [16,31]. The values of χ at various temperatures were calculated by a linear equation of two points of data (χ) at ambient temperature (about 25 °C). Gibbs free energy of different temperatures was diagrammed.

The second derivative of Equation 3 was set to 0 and ϕ was defined as a function of χ . This equation determines the spinodal curve, which is the borderline between metastable and unstable zones. Equations 4 and 5 result in the binodal curve, which is the phase boundary between metastable and stable zones. The curve is plotted by building the common tangents of the free energy at the compositions and corresponding to the equilibrium of two phases [19,32].

$$\left(\frac{\partial \frac{G}{RT}}{\partial \phi}\right)^{Phase 1} = \left(\frac{\partial \frac{G}{RT}}{\partial \phi}\right)^{Phase 2} \quad \text{Equation 4}$$

and

$$\left(\frac{\partial \frac{G}{RT}}{\partial (1-\phi)}\right)^{Phase 1} = \left(\frac{\partial \frac{G}{RT}}{\partial (1-\phi)}\right)^{Phase 2} \quad \text{Equation 5}$$

The spinodal and binodal curves intersect at the critical point, which was calculated from the third derivative of Equation 2.

2.2.3.4 Glass transition temperature (T_g) of the solid dispersion

The T_g of the solid dispersion is given by the Gordon-Taylor equation [33].

$$T_g = \frac{w_1 T_{g1} + K w_2 T_{g2}}{w_1 + K w_2} \quad \text{Equation 6}$$

where T_g, T_{g1}, and T_{g2} are the glass transition temperatures of the solid states and the two different components, respectively: *w* is the weight fraction, and the *K* is a constant approximately calculated from Equation 7.

$$K \approx \frac{\rho_1 T_{g1}}{\rho_2 T_{g2}} \quad \text{Equation 7}$$

2.2.3.5 Experimental model

Solid dispersions of ABZ-Kollidon® VA 64 and ABZ-Soluplus® at 10%, 20% and 30% drug loadings and 1%, 5%, 10% and 20% drug in Eudragit® E PO matrices were produced. The HAAKE Mini-Lab Micro Compounder (Thermo Electron, Germany) was run at 140°C for the Kollidon® VA64 and Soluplus® formulations, and at 120°C for Eudragit® E PO with a screw speed of 150 rpm. Forming of the single-phase, metastable or two-phase unstable mixture was confirmed using visual observation and a powder X-ray diffractometer (Phillips Electronic Instrument, NY) at the 2θ range of 10-40°, step width of 0.04° and a dwell time of 2 sec/step.

2.2.4 Formulation of solid dispersions

2.2.4.1 Hot melt extrusion

ABZ and Kollidon® VA 64 were dried in an oven (ON-12G, Jero Tech, Kyunggi-do, Korea) for 24 hours prior to extrusion. The homogeneous blend of 20% w/w ABZ was fed at a feed rate of 1.5 g/min to a Nano-16 twin-screw extruder (American Leistritz Extruder Corp. USA, Somerville, NJ) equipped with a 5-mm diameter die. The screw design used is shown in Figure 2.1.

During the extrusion process, ethanol (absolute, 99.5% v/v dehydrated with molecular sieve) was injected into the injection zone, and a vent to atmosphere was located in the venting zone (Figure 2.1) using an HPLC pump. The barrel temperature, screw speed, and flow rate of solvent were varied as listed in Table 2.1. Upon ejection, the extrudate was air-cooled on a conveyor to room temperature, dried in an oven overnight, and subsequently milled. Particles smaller than 250 µm were stored in airtight glass containers for further analysis.

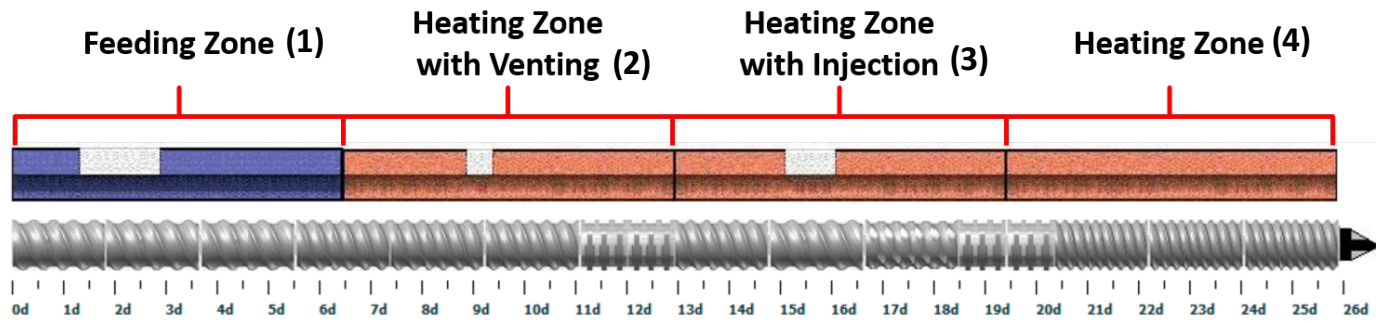


Figure 2.1: Screw design for melt extrusion

Formulation	Temperature (°C)					Screw speed (RPM)	Feed rate (g/min)	Solvent	Solvent Flow rate (ml/min)	Torque (Nm)	Melt pressure (psi)
	Die	4	3	2	1						
1	120	120	120	110	X	100	1.5	-	-	14.2	300
2	120	120	120	110	X	200	1.5	-	-	13.2	200
3	120	120	120	110	X	300	1.5	-	-	11.3	200
4	120	120	120	110	X	150	1.5	Ethanol	0.2	7.4	50
5	120	120	120	110	X	150	1.5	Ethanol	0.5	6.4	65
6	120	120	120	110	X	300	1.5	Ethanol	0.5	5.4	45
7	110	110	110	100	X	300	1.5	Ethanol	0.5	5.9	40
8	100	100	100	100	X	300	1.5	Ethanol	0.5	6.6	30

Table 2.1: Process parameters of hot melt extrusion

2.2.4.2 Spray drying

ABZ and polymer(s) (20:80 w/w) were dissolved in THF containing hydrochloric acid, sulfuric acid or methanesulfonic acid. The weight ratio of ABZ:acid was 1:1, and the total solid content of each solution was 5% w/v. Solutions were fed into a Buchi Mini Spray Dryer 290 (Buchi, Flawil, Switzerland) with a co-axial nozzle with co-current flow. The inlet temperature at the drying chamber was maintained at $100 \pm 5^\circ\text{C}$ and the outlet temperature was $60 \pm 5^\circ\text{C}$. The aspirator and pump were set at $100 \text{ m}^3/\text{h}$ and 20%, respectively. The resulting particles were collected by a cyclone and then vacuum dried at 30°C for 24 h. The fine powder was stored in airtight glass containers in a desiccator. Physical mixtures (PM) of ABZ and polymer(s) in the same weight ratio were used as controls.

2.2.5 Characterization of solid dispersions

2.2.5.1 Powder X-Ray Diffractometry (PXRD)

Morphology of the powder samples was investigated using a Benchtop X-ray diffraction instrument; Model Miniflex 600 (Rigaku, Woodlands, TX) with primary monochromated radiation (CuK radiation source, $\lambda = 1.54056 \text{ \AA}$). The instrument was operated at an accelerating voltage of 40 kV and 15 mA. All samples were subjected to the same program; scanned over a 2θ range of 5° to 40° at a step size of $0.04^\circ/\text{sec}$, a dwell time of 2 sec and scan speed of $1^\circ/\text{min}$.

2.2.5.2 Differential Scanning Calorimetry (DSC)

The thermal properties of formulations were conducted using a modulated differential scanning calorimetry. Each sample of approximately 3 mg was loaded into a standard aluminum pan. Experiments were performed at a heating ramp rate of 10°C/min in the range of 30-250°C, with a modulation temperature amplitude of 1°C/min and nitrogen purge of 50 mL/min.

2.2.5.3 Thermogravimetric Analysis (TGA)

Thermal stability of ABZ, each polymer and the resulting formulations were determined using a thermogravimetric Analyzer (TGA/DSC 1, Mettler Toledo, Columbus, OH). Approximately 3 mg of each sample was weighed into a separate crucible and covered with a lid. The crucible was placed in the chamber with a constant flow of nitrogen (50 mL/min), and equilibrated at 30°C. Once equilibrated, the sample mass was monitored and plotted as a function of temperature from 30°C to 250°C at a scan rate of 10°C/min.

2.2.5.4 Scanning electron microscope (SEM)

The morphology of spray-dried particles was evaluated using a scanning electron microscope (SEM). Prior to imaging, samples were coated with platinum/palladium, targeted for 12 nm thickness, under high vacuum using a Cressington 208 Benchtop Sputter Coater (Watford, England). The images were captured using a Carl Zeiss Supra[®] 40VP

(Carl Zeiss, Oberkochen, Germany) operated under vacuum, at an accelerating voltage of 5 kV of Electron High Tension (EHT).

2.2.5.5 Particle size distribution of spray-dried particles

The particle size distribution of ABZ and the spray-dried formulations was determined using a particle size analyzer with laser diffraction, Helos and Rodos T4.1 dispenser (Sympatec, Clausthal-Zellerfeld, Germany). The powders were dispersed at the primary pressure of 3 bar and a rotation speed of 50%.

2.2.6 ABZ salt preparation

Three ABZ salts (mesylate, sulfate and hydrochloride) were produced in order to compare the non-sink dissolution with the spray-dried ABZ (non-salt form) solid dispersions. The preparation methods were adapted from [10]. Five grams of bulk ABZ was dispersed in 500 mL THF. Each acid (methanesulfonic acid, sulfuric acid or hydrochloric acid) in a 1:1 molar ratio (ABZ:acid) was added into the slurry and stirred at room temperature until the solution was clear. Dried materials were obtained when THF completely evaporated in a fume hood at ambient temperature. In particular, the off-white ABZ hydrochloride was received after re-dissolving the material yielded from the first step by 500 mL of ethanol. The ethanol was again evaporated at ambient temperature to obtain the final hydrochloride salt. The milled powders (250 μm) were characterized by ^1H NMR, XRD, DSC, TGA, HPLC and LC/MS.

2.2.7 Non-sink dissolution

Non-sink dissolution analysis was performed using an SR8 Plus dissolution tester (Hanson Research Corp., Chatsworth, CA) equipped with mini paddles. Spray-dried formulations equivalent of 700 mg ABZ were added into dissolution vessels containing 100 mL of simulated gastric fluid without pepsin (10X equilibrium solubility). The vessels were maintained at $37 \pm 0.5^\circ\text{C}$ with rotating speed of 50 rpm. Test samples were studied in triplicate, with 3-ml samples withdrawn from the vessels at 5, 10, 15, 30, 45, 60, 90 and 120 min. The drawn volume was replaced with the warmed blank medium. All samples were immediately filtered through $0.22 \mu\text{m}$ PVDF syringe filters, and diluted with the dissolution medium. Samples were then analyzed as described in Section 2.2.8.

2.2.8 Chromatographic analysis

ABZ samples were tested using a Dionex 3000 (Thermo Fisher Scientific, Fair Lawn, NJ) HPLC system. The analytical method was modified from the USP 36 monograph for albendazole tablets [34]. The HPLC system was equipped with a UV-Vis detector and run at ambient conditions. ABZ was eluted by an Inertsil® ODS-2 ($4.6 \times 150 \text{ mm}$) column (GL Sciences, Tokyo, Japan). The mobile phase was 4.35 mM monobasic ammonium phosphate and methanol (40:60 %v/v) and the flow rate was 1.5 ml/min. A $20 \mu\text{L}$ aliquot was injected onto the column and chromatograms were acquired at a detection wavelength of 210 nm. Duplicate determinations were made for each of the samples.

2.2.9 Long term stability study of spray-dried formulation

Long-term stability studies of the spray-dried formulation were conducted by storing samples in a desiccator at 25°C.

2.3 RESULTS AND DISCUSSION

2.3.1 pH solubility profile and pKa value

Figure 2.2A shows the pH solubility profile of bulk ABZ at 37°C. The solubility of ABZ was higher at pH values less than 2. ABZ is a weakly basic compound [10] that exhibits two pKa's of 2.8 and 10.26 [3] so the drug is in neutral species between the two pKa. It was also observed that ABZ was relatively chemically stable under acidic conditions at 37°C for at least 24 hours. ABZ appeared to be more soluble and stable at lower pH values. The pKa of ABZ at 37°C was 3.2 (Figure 2.2B), which compared favorably to reported values (pKa 3.6) and the calculated pKa of 2.8 from the Hammett equation [3,10].

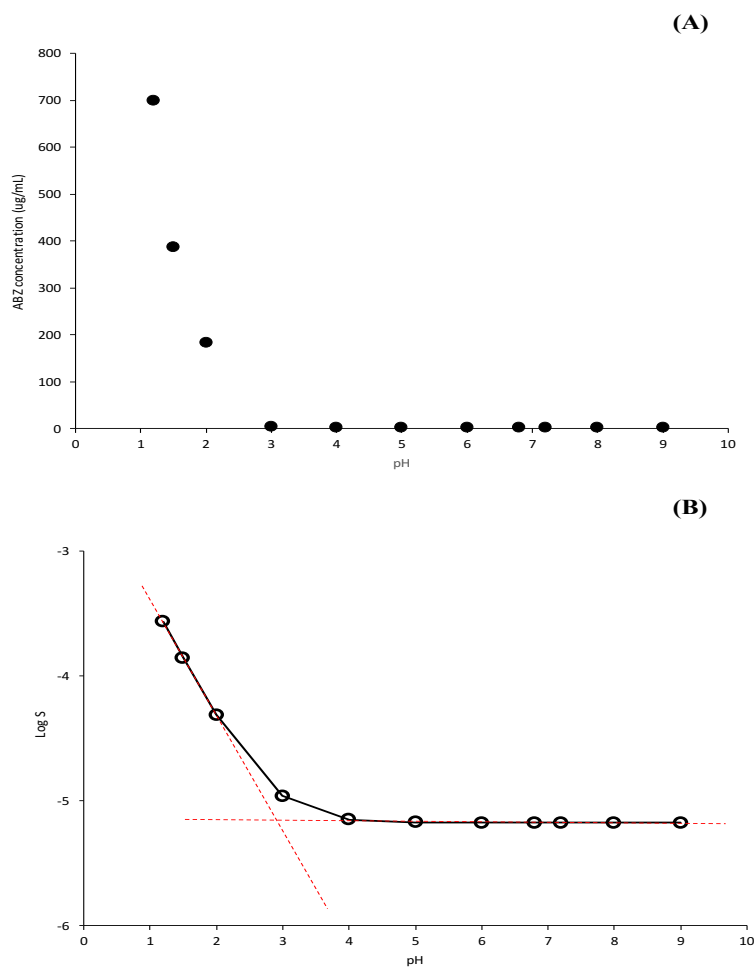


Figure 2.2: pH solubility profile of bulk ABZ at 37 °C (A), and pH solubility profile of bulk ABZ at 37°C (concentration are in log S values, the dashed lines were linear interpolation of the experimental data) (B)

2.3.2 Forced degradation study

The results showed that ABZ was degraded primarily upon exposure to H₂O₂ and 1 N NaOH at 80 °C for 5 min. As expected, albendazole sulfoxide (ABZSX) or ricobendazole, which is a major active metabolite of ABZ, was the degradation product

from the oxidative stress condition [35]. ABZ impurity A is a product from alkaline catalyzed hydrolysis of the bond in the ABZ molecule. An important by-product from this degradation mechanism is methanol. The chemical degradation pathways of these two stressed conditions are proposed in Figure 2.3.

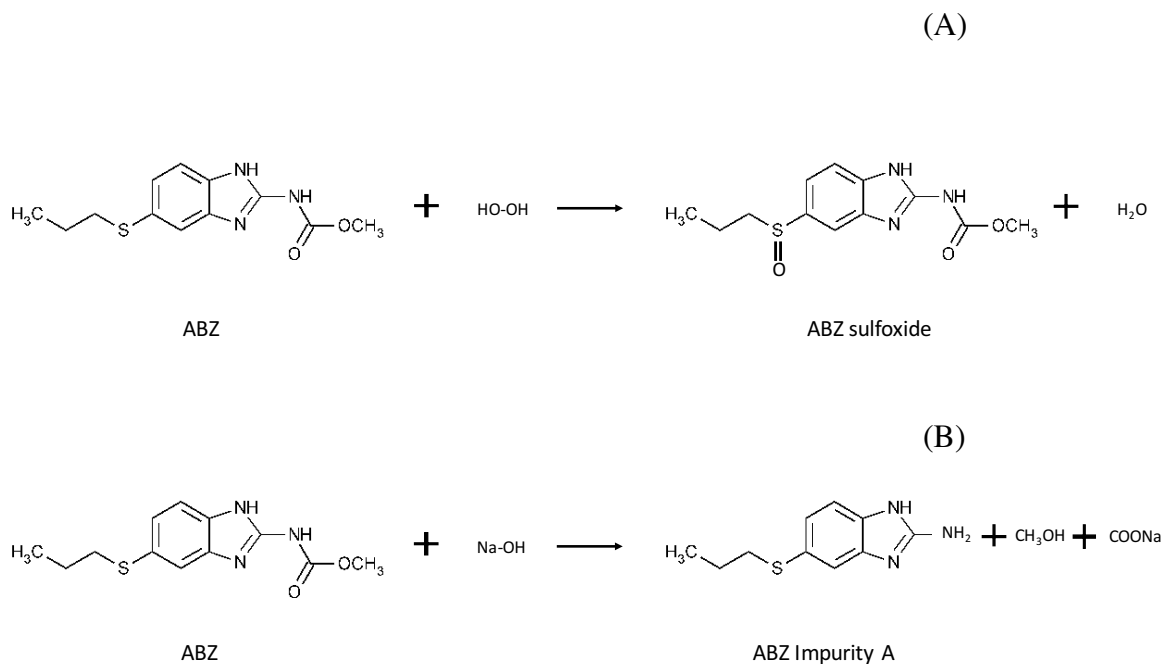


Figure 2.3: Proposed degradation pathway of ABZ – oxidation (A), basic hydrolysis (B)

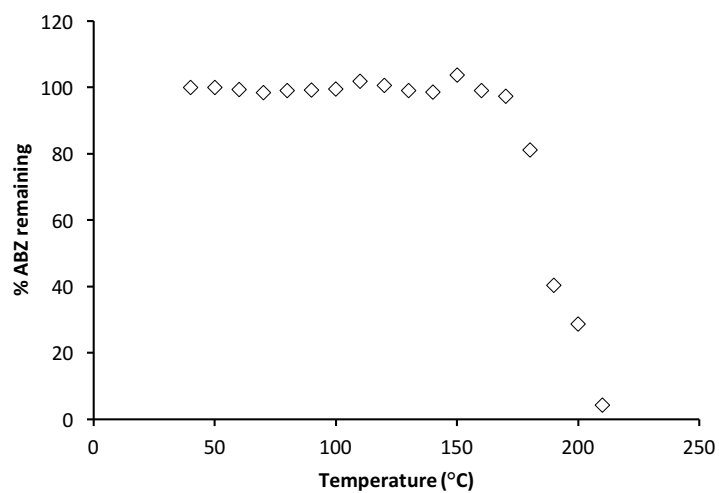
Degradation was not observed following incubation in 1 N HCl at both room temperature and 80°C for 2 hours and 1 hour, respectively. ABZ exhibited greater acid resistance probably due to the overlapping electron clouds within the amide functional groups in the molecule and the corresponding multiple resonance forms [36]. As recommended by Blessy et al. (2014) [37], the thermal degradation study was carried out

at 80°C and ABZ was chemically stable following exposure at this elevated temperature for 2 hours. Nonetheless, the temperatures used with HME and spray drying were higher than 80°C, therefore the thermal stability profiles of ABZ at various elevated temperatures was studied.

2.3.3 Thermal stability profile

Figure 2.4 shows the extent of the remaining drug, as a function of temperature. Bulk ABZ and ABZ in combination with Kollidon® VA 64 degraded after storage for only 5 min at 180°C and 140°C, respectively. The lower degradation temperature of ABZ in the polymer mixture may result from the effect of polymer-induced melting point depression [38]. Kollidon® VA 64 began softening at its glass transition temperature (101°C) and induced drug solubilization at a lower temperature than its melting point (210°C). The increase of molecular mobility after the drug melts leads to the enhancement of drug decomposition [39,40].

(A)



(B)

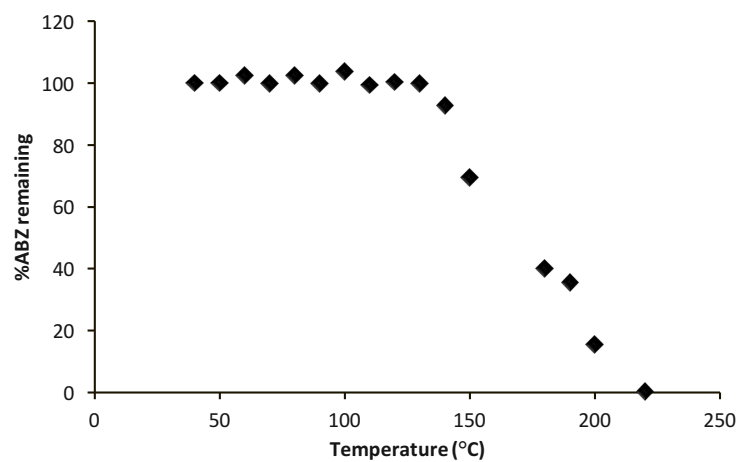


Figure 2.4: Percentage of drug remaining following 5 minutes storage at various temperature – crystalline drug substance (A), and physical mixture of drug and polymer at 20:80 ratio (B)

2.3.4 Drug-polymer miscibility

To produce stable amorphous molecular dispersions, the miscibility between drug and polymer(s) must be understood. Hansen solubility parameters and Flory-Huggins interaction parameters were used to model the phase diagrams of binary mixtures.

2.3.5 Hansen solubility parameter

The miscibility criteria suggested by Greenhalgh et al. (1999) [41] categorizes the level of miscibility between two compounds, based on the $\Delta\delta$, into three groups. If the $\Delta\delta < 2 \text{ MPa}^{1/2}$, the drug and carrier are likely to be miscible and produce a glass solution when molten. If the $\Delta\delta < 7 \text{ MPa}^{1/2}$, the drug and polymer are also likely to be miscible and possibly form a glass solution in a liquid state. Whereas the $\Delta\delta > 10 \text{ MPa}^{1/2}$ show some signs of immiscibility and may not form the glass solution. These solubility parameters were utilized as a tool for carrier selection.

The solubility parameters of ABZ, Kollidon® VA 64, Soluplus® and Eudragit® E PO were calculated of 25.96, 23.52, 22.19, and 19.60 $\text{MPa}^{1/2}$, respectively and the $\Delta\delta$ between ABZ and these three polymers were 2.44, 3.77 and 6.36 $\text{MPa}^{1/2}$, respectively, which were less than 7 $\text{MPa}^{1/2}$. ABZ is likely to be more miscible with Kollidon® VA 64 than the other two polymers at 25°C.

2.3.6 Flory-Huggins Theory and Gibbs free energy of mixing

The Flory-Huggins theory is used to evaluate thermodynamic miscibility of a binary mixture between a drug substance and polymer matrix [14,16,42]. The plots

between free energy of mixing versus drug ratio are shown in Figure 2.5A-C. The positive energy of mixing indicates that the energy of the mixed state is greater than that of the phase-separated state, which results in the drug and polymer spontaneously separating into two phases in order to reduce the free energy. On the other hand, the negative energy of mixing demonstrates that the energy of the mixed state is less than that of the phase-separation state, which leads to the promotion of mixing and results in homogeneous mixtures of drugs and polymers [16,42]. It is apparent that the free energy of mixing is negative and convexed at the elevated temperatures of 150°C and above for the binary systems of ABZ-Kollidon® VA 64 and ABZ-Soluplus®, and 100°C and above for the ABZ-Eudragit® E PO system. Therefore, at these temperatures, the mixtures are homogeneous and thermodynamically stable at all drug-polymer ratios.

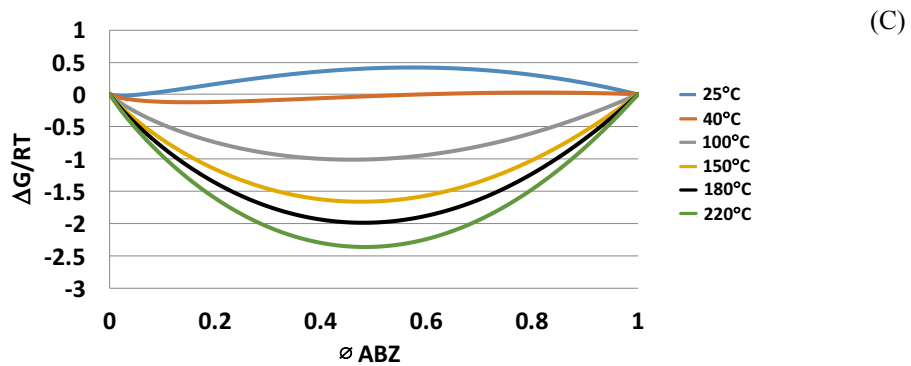
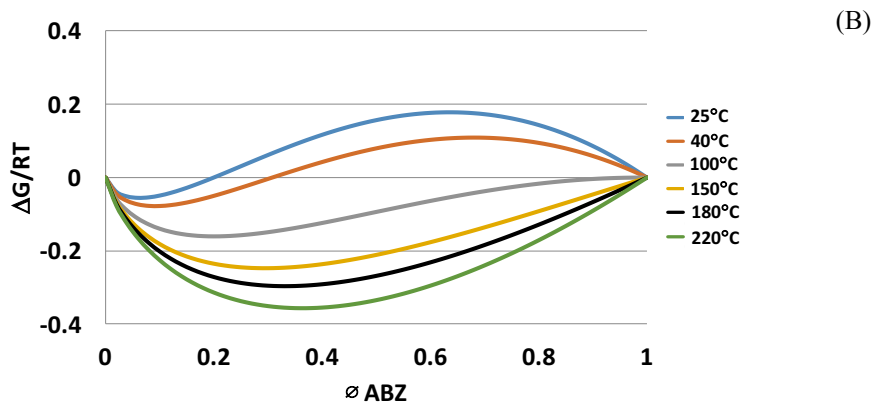
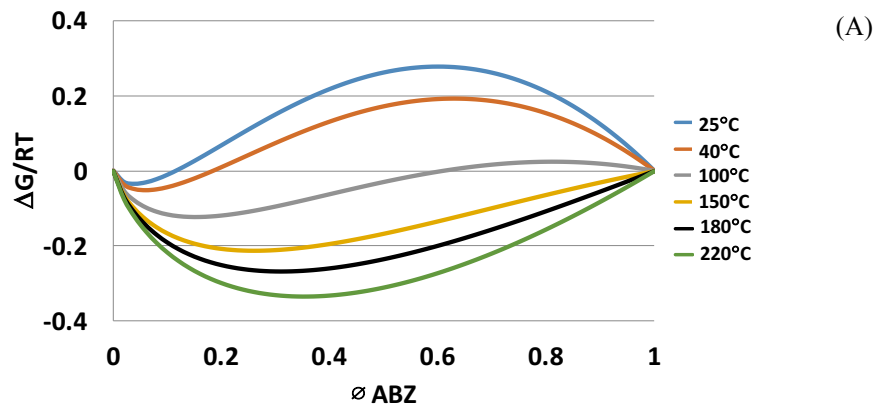


Figure 2.5: Gibbs free energy diagram of the mixture of ABZ–Kollidon® VA 64 (A), Soluplus® (B), and Eudragit® E PO (C)

2.3.7 Temperature – Composition phase diagram

Phase diagrams are potentially useful for the prediction of the physical stability of solid dispersions [16]. Figure 2.6 shows the phase diagrams of three drug-polymer mixtures, the appearance of extrudates and the PXRD patterns. The phase diagrams demonstrate the stable, metastable and unstable zones of the systems as a function of temperature. Drug-polymer miscibility and drug-polymer solubility are indicated by spinodal and binodal curves, respectively [43]. These two curves and the T_g also imply the viscosity change of the systems which are related to their molecular mobility [39]. The mixtures under the T_g curve have low molecular mobility. In contrast, above the T_g curve, molecular mobility of the system is high which results in the increasing of molecular motion and demixing of the systems. The systems, however, may remain crystal-free over pharmaceutically relevant timescales [14,16,42,43].

The amorphous solid dispersions are typically transparent, and the degree of crystallinity increases the opacity of the systems [44]. The solid dispersions of ABZ-Kollidon® VA 64 and ABZ-Soluplus® at 10% drug loading, which falls in the metastable zone, were clear and transparent. While the formulations with higher drug content (20% and 30%) were more opaque. At ambient temperature, the 20% ABZ in the Soluplus® matrix is the point that is closest to the boundary between the metastable and the two-phase unstable zone, and the extrudate was not as clear as the one containing 10% ABZ. This observation was confirmed by the PXRD results (peaks at $2\theta = 17.5^\circ$, 22.5° , 24.5° and about 27°). The appearance of the ABZ-Eudragit® E PO dispersions were clear at very

low drug levels (1% and 5%) and also became more opaque when the drug loadings increased (10% and 20%). The observation was again corroborated by PXRD (crystalline ABZ peak at $2\theta = 24.5^\circ$). The discharged extrudates were opaque at the outlet. This suggested that the drug in polymer dissolution process simply takes longer at the higher drug loadings and was incomplete. Therefore, Flory-Huggins modeling indicated that the amorphous state of ABZ in each of the polymer systems would exist at low drug loadings. The results from this study prove that phase diagrams are a powerful tool to model the phase separation of binary mixtures. Interestingly, even though a majority of drug degraded during processing (e.g. 71.4% of ABZ degraded from the ABZ-Kollidon® VA 64 (20:80) formulation), the phase diagram was still valid. The solubility parameter of the degradant, which was ABZ impurity A, was calculated as $26.87 \text{ MPa}^{1/2}$. The value is very similar to the drug itself ($25.96 \text{ MPa}^{1/2}$), therefore this supports that the results are still relevant regardless of the chemical change.

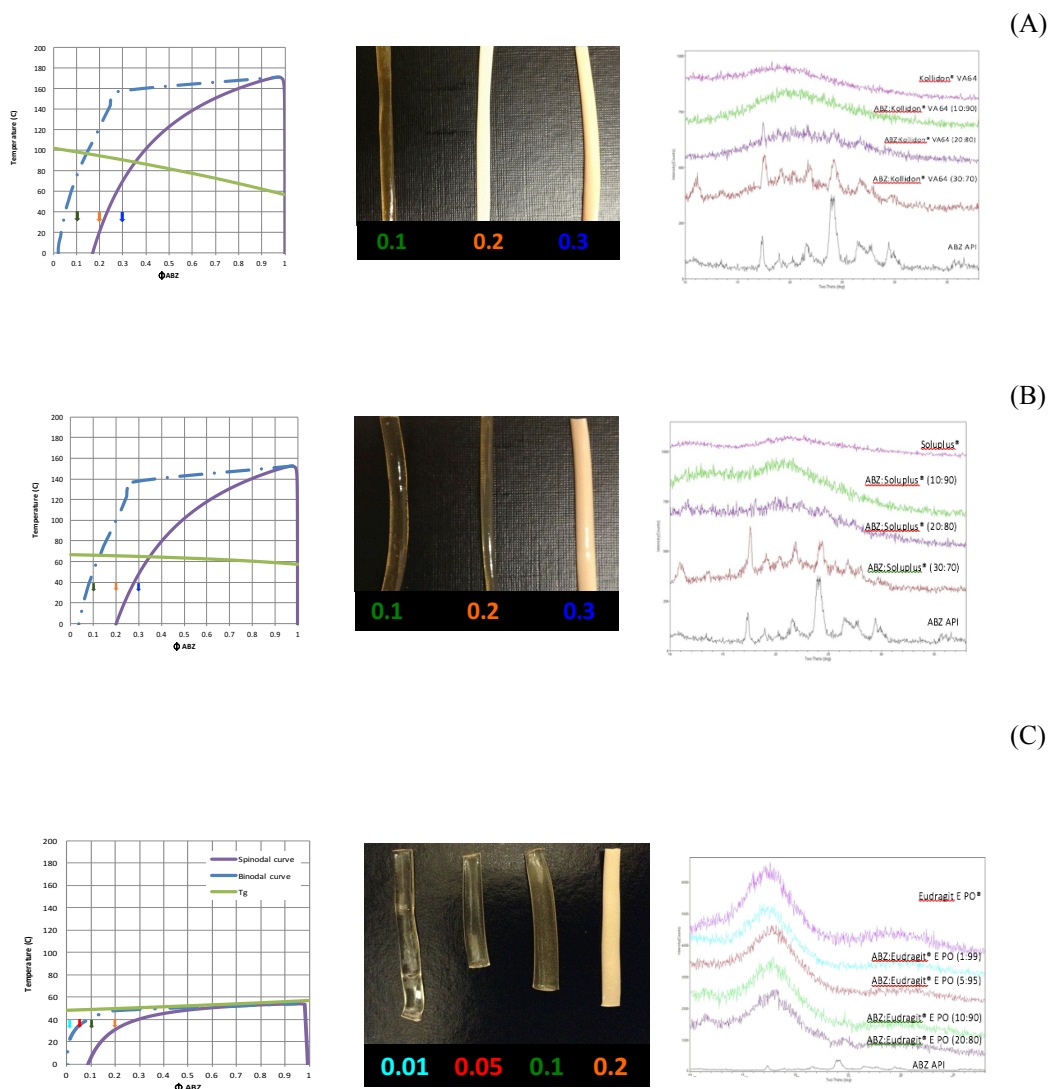


Figure 2.6: Phase diagrams of ABZ–polymer binary systems and the appearance of the extrudates at different drug fractions (ϕ_{ABZ}); ABZ–Kollidon® VA 64 (A), ABZ–Soluplus® (B), and ABZ–Eudragit® E PO (C) at extrusion temperature of 140°C, 140°C and 120°C, respectively

2.3.8 Hot melt extrusion

Based on the preformulation studies, particularly the thermal stability profile and phase diagram, we hypothesize that amorphous solid dispersions of ABZ could be prepared by thermal processing. Table 2.2 presents the results of the extrusion products including the extent of ABZ remaining, PXRD, and physical appearance of the extrudates. The thermal degradation profiles of ABZ-Kollidon® VA 64 mixtures show that the onset of the degradation occurs at 140°C. In addition, preliminary studies in which the barrel temperature was below 120°C did not convert crystalline ABZ to the amorphous state (data not shown). Thus, formulations 1-3 were run at 120°C with different screw speeds and unexpectedly more than 90% of ABZ was degraded during the extrusion process. The increase in screw speed induces higher mechanical shear force, which increases chemical degradation [45,46]. The hydrolysis degradation product, ABZ impurity A, was detected by HPLC and LC/MS, and methanol, a by-product of ABZ degradation, vaporized and created bubbles in the extrudates. Visual observations supported the chemical assays. Transparency of the extrudates and foam formation during the extrusion process indicated the presence of crystallinity and decomposition of ABZ. A recent study of ABZ solid dispersions produced by HME [12] also observed bubbles in the extrudates. Their dissolution results, under sink conditions measured by UV spectrophotometry at 250 nm, showed only about 70% completion. The authors speculate on why, however, they have not proven this phenomenon. Our results revealed that ABZ is sensitive to both thermal and shear stress from the HME process. Moreover, the long residence time distribution

(RTD) of this study (13 min) also induced ABZ degradation. The RTD is a critical factor that significantly affects the chemical stability of thermal labile compounds like ABZ. Impurity formation, as a result of thermal processing caused by RTD at elevated temperatures, has been reported [21]. Therefore, the long residence time and high shear in this present work seriously strengthened the thermal degradation of ABZ.

Ethanol was introduced to the extrusion process to reduce the processing temperature. In a comparison between formulations 3 and 6, the percent drug remaining increased about 11 fold (from 2.63% to 28.17%). However, the percent drug remaining was still unacceptably low. The use of a lower screw speed of 150 rpm with ethanol injection in formulations 4 and 5 still did not sufficiently reduce drug degradation. Formulations 7 and 8 were then processed at lower barrel temperatures (110 °C and 100 °C). Unfortunately, at temperature of 100 °C with solvent assistance did not produce ABZ amorphous solid dispersion. Therefore, HME is not a suitable process for preparing ABZ amorphous solid dispersions due to significant chemical degradation from heat and shear stress.

Formulation	%ABZ remaining	XRD	Physical Appearance
Blend	100.00		
1	9.49	Amorphous	Clear glass extrudate with bubbles
2	4.45	Amorphous	Clear glass extrudate with bubbles
3	2.63	Amorphous	Clear glass extrudate with bubbles
4	26.54	Amorphous	Clear glass extrudate with bubbles
5	35.46	Amorphous	Clear glass extrudate with bubbles
6	28.17	Amorphous	Clear glass extrudate with bubbles
7	28.95	Amorphous	Translucent extrudate with bubbles
8	56.62	Crystalline	Opaque extrudate with bubbles

Table 2.2: Drug content, crystallinity and physical appearance of hot-melt extruded ABZ-Kollidon® VA 64 extrudate

2.3.9 Spray-dried formulation

Spray drying is another prevalent technique to produce amorphous solid dispersions of ABZ in a polymer matrix. The acids used to prepare ABZ salts were also added to the spray dried formulations. Without assistance of the acids, the ABZ-polymer solutions for spray drying cannot be obtained. The results indicate that there was no degradation product detected in all spray-dried formulations. Spray drying also utilizes high temperatures during processing, the liquid droplets are typically in contact with the hot air inlet in the drying chamber for short periods of time [47]. In addition, the temperature of the droplets remained low due to the high evaporation rate of the solvent. The temperature of the products exiting the dryer was slightly less than the outlet air temperature [47]. The outlet temperature of all formulations was in the range of 55-65 °C. When the droplets dried in the chamber, the moisture content and air temperature were reduced, which resulted in the temperature of the particles not markedly increasing. As previously reported, a spray dryer with a co-current configuration is appropriate for thermally sensitive drugs due to the short evaporation time which results in less thermal degradation of the products [48,49]. Therefore, spray drying was better than HME as it avoided thermal degradation of ABZ.

2.3.10 Characterization of spray-dried formulations

2.3.10.1 PXRD

PXRD reportedly quantifies to a limit of about 5% or less crystallinity in solid dispersions, depending on the size and shape of the crystals [50,51]. The broad halo

scattering profiles of the spray-dried ABZ in Kollidon® VA 64 and Soluplus® indicated the amorphous morphology of the spray-dried matrices. Interestingly, partially crystalline ABZ remained in the spray-dried ABZ-Eudragit® E PO formulation (peaks at $2\theta = 7.5^\circ$, 17.5° , and 24.5°).

2.3.10.2 DSC

DSC determines the extent of mixing in polymer systems [52]. If an amorphous drug is molecularly dispersed in the polymer matrix, the solid dispersion system exhibits a single T_g [53]. The calculated T_g value of each of the molecular dispersions is between that of the pure amorphous drug and pure polymer. A single T_g for each spray-dried ABZ formulation was detected. However, a small melting peak at about 210°C was still observed in the ABZ-Eudragit® E PO sample (Figure 2.7A). The predicted and experimental T_g of the spray-dried ABZ-Kollidon® VA 64, ABZ-Soluplus®, and ABZ-Eudragit® E PO were $91.3^\circ\text{C}/91.1^\circ\text{C}$, $67.3^\circ\text{C}/70.0^\circ\text{C}$, and $49.8^\circ\text{C}/55.8^\circ\text{C}$, respectively (Figure 2.7B). The prediction of T_g was very accurate for the ABZ-Kollidon® VA 64 samples. It was difficult to notice the multiple T_g (s) from the ABZ-Eudragit® E PO formulation since their T_g (s) are close to each other (T_g pure ABZ is 57°C and T_g of Eudragit® E PO is 48°C). However, the large difference (about 6°C) between the predicted and experimental T_g of ABZ-Eudragit® E PO might imply the lack of homogeneity of the system. Hence, the higher experimental T_g of the ABZ-Eudragit® E PO formulation than the predicted T_g was attributed to partially crystalline ABZ in the mixture.

2.3.10.3 SEM images

The SEM image has a high sensitivity and is able to detect a very low crystalline level (1% or less) of the drug in spray-dried formulations [14]. Figure 2.8 shows the morphology and size of bulk ABZ, pure Kollidon® VA 64, physical mixtures, and the spray-dried products. Overall, the spray-dried formulations appeared in a good spherical shape without any collapse of skin. The SEM images revealed a reduction in the particle size of the solid dispersions from the physical mixtures (for example, Figure 2.8D and C). Interestingly, the irregular-shaped particles of crystalline ABZ were observed in the ABZ-Eudragit® E PO formulation. This confirmed the XRD results that the ABZ-Eudragit® E PO formulation contained fractions of crystalline drug.

2.3.10.4 Particle size distribution (PSD) of spray-dried formulations

The upper diameter of the smallest 90%, $x(90\%)$, of bulk ABZ, spray-dried ABZ-Kollidon® VA 64, ABZ-Soluplus® and ABZ-Eudragit® E PO were 14.75, 15.81, 14.82 and 10.58, respectively. The Eudragit® E PO formulation gave the smallest particle size while the particle size of the other spray-dried formulations was not significantly different from the crystalline drug. The poor water solubility of the bulk ABZ was attributed to low wettability capability rather than particle size.

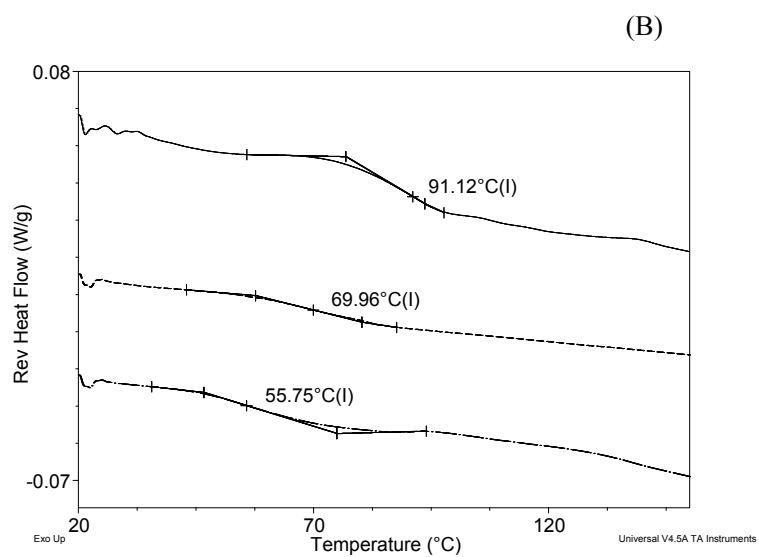
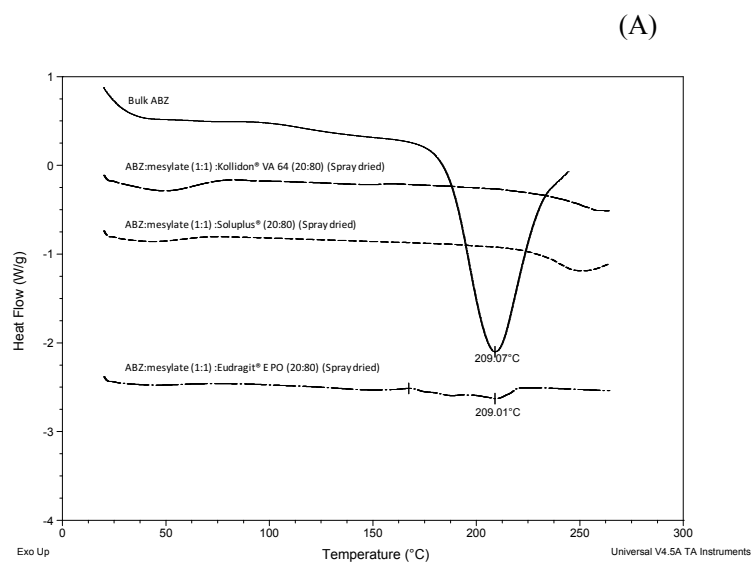


Figure 2.7: DSC thermograms of bulk ABZ and spray dried ABZ-polymer systems from a plot of heat flow (W/g) versus temperature (°C) (A), and glass transition temperatures (T_g(s)) of bulk ABZ and spray dried ABZ-polymer systems from a plot of reverse heat flow (W/g) versus temperature (°C) (B)

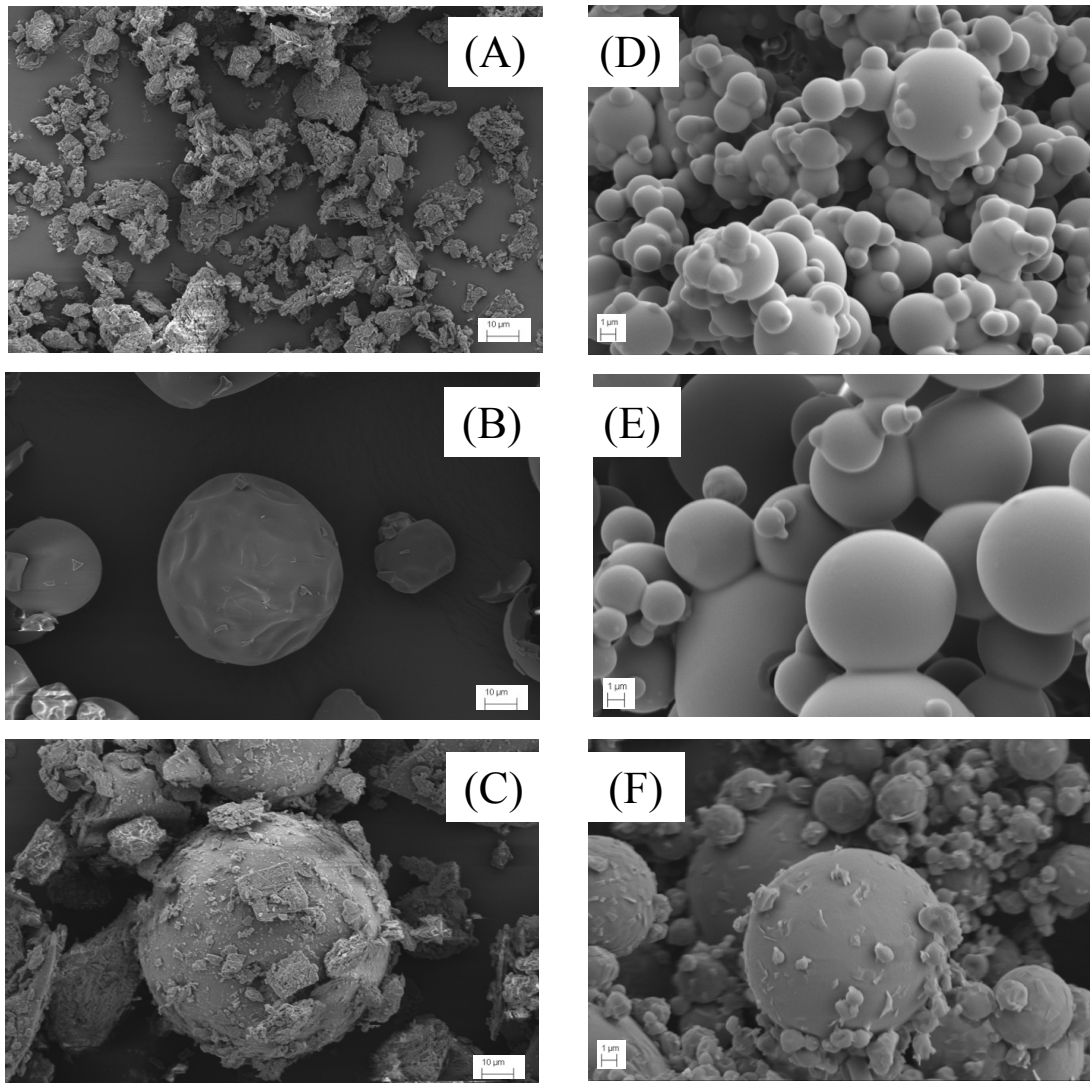


Figure 2.8: SEM images of bulk ABZ (A), Kollidon® VA 64 (B), physical mixture of ABZ and Kollidon® VA 64 (C), spray-dried formulations (ABZ-polymer 20:80) as follows; ABZ-Kollidon® VA 64 (D), ABZ-Soluplus® (E), and ABZ-Eudragit® E PO (F), magnification of 2,000X for (A)-(C) and 10,000X for (D)-(F)

2.3.11 Recrystallization of ABZ in spray-dried formulations

In reference to the crystalline ABZ detected in the spray-dried ABZ-Eudragit® E PO, the recrystallization of ABZ was discussed. Crystallization of an amorphous material depends mostly on molecular mobility [40,53] and the molecular mobility also relies on both thermodynamic and kinetic factors [54,55]. The $\Delta\delta$ of ABZ and polymers, which determine the solubility and miscibility of a drug in polymer matrices, were ranked. The spray-dried ABZ-Eudragit® E PO formulation has the highest difference value and was observed in the recrystallization. In the phase diagrams (Figure 2.6), within the pharmaceutically relevant temperature range (0-50°C), the dispersions of amorphous ABZ in Kollidon® VA 64 and Soluplus® at 20% drug loading are in the metastable region, where the drug achieved a supersaturated state in the polymer matrices. If a formulation in this metastable zone is appropriately engineered, the kinetic barrier will be high enough to prevent phase separation. The ABZ-Eudragit® E PO (20:80) system at temperatures below 30°C clearly falls within the two-phase unstable zone, where the drug is supersaturated but immiscible with the polymer carrier. The high driving force of the drug toward recrystallization at this supersaturated state resulted in the increase of crystalline drug particles in the polymeric dispersions [16].

From the kinetic perspective, molecular mobility of the amorphous material is high at the area above the T_g curve. The differences between the T_g of the spray-dried formulations (ABZ-Kollidon® VA 64, ABZ-Soluplus®, and ABZ-Eudragit® E PO) and room temperature (25°C) were 66, 45 and 31°C, respectively. A rule of thumb for

determining the storage temperature of the amorphous solid dispersions is that the physical stability of the amorphous dispersions is considered to be stable if the T_g of the system is 50°C above the storage temperature [56]. The amorphous material exhibits substantial molecular mobility at temperatures up to 50°C below the T_g of the system, which initiates the recrystallization of the amorphous drug in the ABZ-Eudragit® E PO system.

The ratio of the ABZ melting point to the T_g of the ABZ-Eudragit® E PO was highest. This melting point to T_g ratio indicates the ability of glass formation [57] and relates to the physical stability of the drug in solid dispersions [14]. Harmon et al. (2009) [54] reported that ‘the higher this ratio, the greater is the risk of crystallization.’ Drugs with high melting temperatures are more likely to recrystallize since the melting temperature exhibits the crystal lattice energy and can be a tool to indicate the thermodynamic driving force toward recrystallization. On the other hand, T_g can reflect molecular mobility of the dispersion system. Material with low T_g has a high risk of recrystallization at room temperature due to its high molecular mobility [54].

2.3.12 ABZ salts

In brief, the ABZ salts (ABZ mesylate, sulfate and hydrochloride) were prepared and agreed to those reported by Paulekuhn et al. (2013) [10] (data not presented). In addition, there was no degradation products of ABZ detected.

2.3.13 Non-sink dissolution

The non-sink dissolution was conducted to evaluate the *in vitro* dissolution performance of the solid dispersions. ABZ exhibits significantly higher solubility in the ionized form in acidic conditions. Hence, all dissolution studies were demonstrated in USP simulated gastric fluid. Results of the dissolution analysis are presented in Figure 2.9A-C, and the area under the dissolution curves (AUDC) values were summarized in Table 2.3.

Figure 2.9A shows the non-sink dissolution profiles of the free base and salts of ABZ. The mesylate salt showed immediate dissolution within 5 min and exhibited the highest dissolution enhancement of about 5-fold as compared to the free base form. Enhanced wettability of the mesylate salt contributed to this dissolution enhancement [10]. Nonetheless, the extent of ABZ dissolved was decreased over time because the salt was not able to maintain the supersaturated state. Referring to the study by Paulekuhn et al. (2013), ABZ mesylate, sulfate and hydrochloride salts were the anhydrate, hydrate and hemihydrate, respectively [10]. Therefore, the slower rate of the sulfate salt may be attributed to its hydrate form [58]. ABZ hydrochloride exhibited the lowest rate and extent of dissolution in comparison to the other two salts due to the common ion effect of the chloride ion [10,59]. Paulekuhn et al. (2013) also suggested that the formulation development of ABZ should be considered since ABZ salts did not have an effect on the microenvironmental pH for a long period of time in the media used and may not achieve the expected dissolution result in the patient's stomach [10].

To maintain the supersaturation of the drug, spray-dried formulations of ABZ and methanesulfonic acid with various types of polymers were prepared. Figure 2.9B shows that all three polymers (Kollidon® VA 64, Soluplus® and Eudragit® EPO) were capable of promoting drug release and prolonging the drug supersaturation in the acidic medium. The spray-dried formulation with Kollidon® VA 64 matrix proved to be superior to the other two polymers. The AUC of the Kollidon® VA 64 formulation was 2- and 3-fold higher than the Soluplus® and the Eudragit® E PO formulations, respectively. Since the drug still partially existed in a crystalline state in the spray-dried ABZ-Eudragit® E PO dispersion, this formulation exhibited the lowest dissolution rate and extent compared to the complete amorphous dispersions.

There are a few possible explanations for the slower dissolution rate and lower drug release of the spray-dried ABZ-Soluplus® than the Kollidon® formulation. First, as discussed earlier, $\Delta\delta$ between ABZ and Soluplus® is slightly greater than ABZ and Kollidon® VA 64, therefore the miscibility of ABZ with Soluplus® is likely to be poorer than with the Kollidon® VA 64. Second, the T_g of the spray-dried ABZ-Soluplus® was about 20°C below the ABZ-Kollidon® VA 64. In the presence of the dissolution media, amorphous solid dispersion systems spontaneously absorbed water from the surroundings, and water usually acted as a potent plasticizer of the system. The T_g of the system rapidly decreased from the dry state after absorption of water into the system. Thus, when the T_g of the system decreases, the molecular mobility of the drug molecule in the polymer matrix is likely increased, leading to recrystallization [60]. Lastly, slower ABZ diffusion and

dissolution from the solid dispersion of the Soluplus® formulation was attributed to the swelling effect of Soluplus®, which should occur in the patients as well [61].

As spray drying is a particle engineering technique, the PSD of these formulations was taken into account. The particle size of the ABZ-Eudragit® E PO was the smallest; however, in contrast, the dissolution performance was slowest among these three formulations. There was no significant difference in the particle size between ABZ-Kollidon® VA 64 and ABZ-Soluplus® spray-dried dispersions, while the dissolution results were substantially different. Thus, it can be concluded that the particle size of the spray-dried formulations did not have an effect on the dissolution, whereas the type of polymer was played an important role in the improvement of ABZ dissolution.

Since the spray-dried ABZ mesylate formulation with Kollidon® VA 64 exhibited the greatest dissolution performance (both rate and extent), Kollidon® VA 64 was selected for the acid salt study. Figure 2.9C shows the dissolution profiles of the spray-dried formulations with acids. Overall, the spray-dried formulations showed improved non-sink dissolution compare to the ABZ free base, salts and the physical mixture of ABZ and Kollidon® VA 64. The formulation containing methanesulfonic acid exhibited the best performance, that was about 8-, 1.6- and 5.6-fold (AUDC) greater than the bulk material, ABZ mesylate salt, and physical mixture of ABZ-Kollidon® VA 64 (20:80), respectively. This can be attributed to a combination of the mesylate salt and polymer used. Again, the lower dissolution improvement of spray-dried ABZ hydrochloride:Kollidon® VA 64 as

compared to the mesylate formulation was attributed to the common ion effect of the chloride ion.

(A)

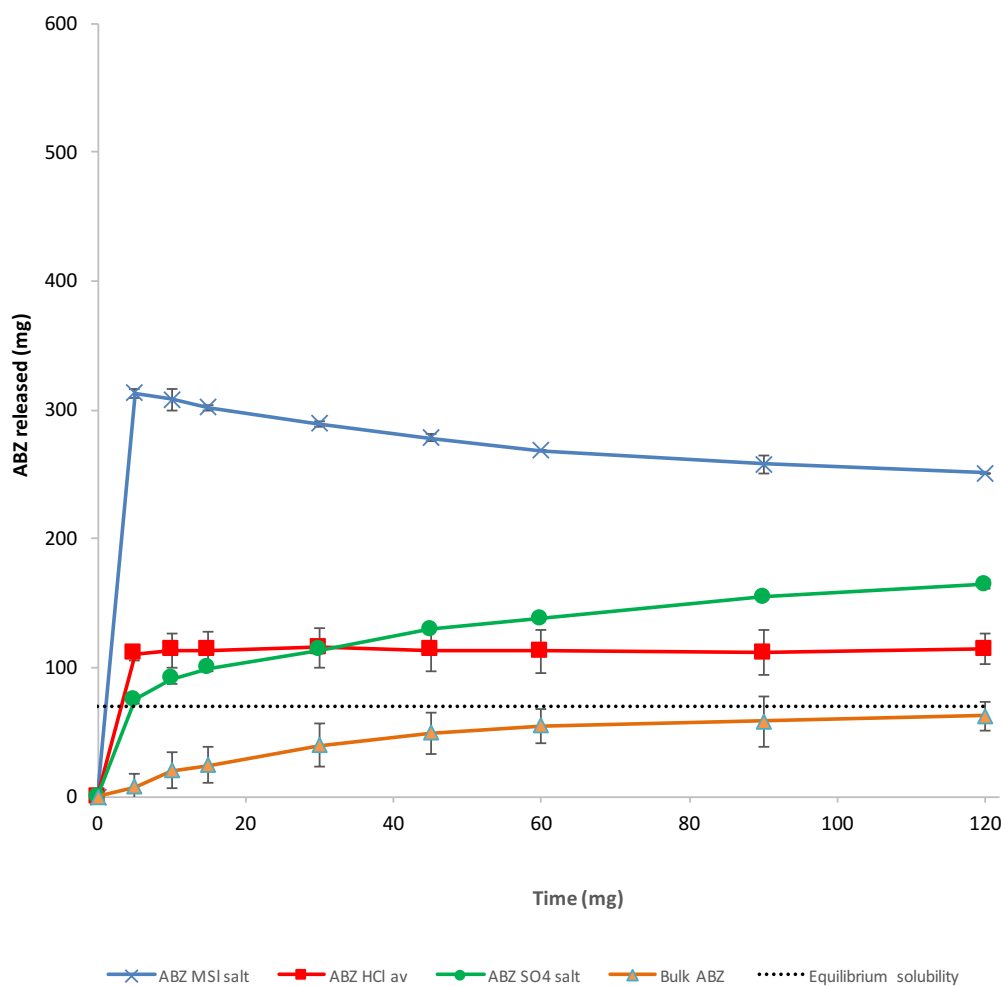


Figure 2.9: (A) Non-sink dissolution of bulk ABZ and ABZ salts in 100 mL USP simulated gastric fluid (without pepsin) at 37°C ($n=3$)

(B)

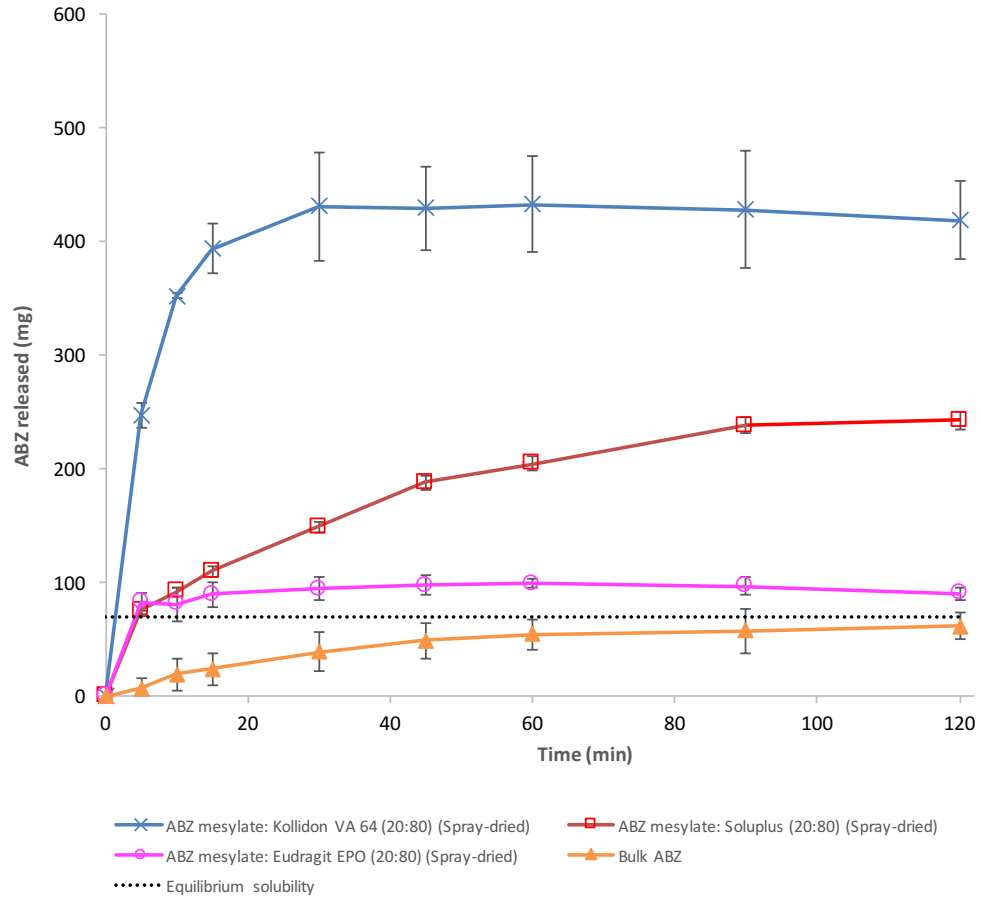


Figure 2.9: (B) Non-sink dissolution of bulk ABZ and spray-dried ABZ mesylate:polymer (20:80) in 100 mL USP simulated gastric fluid (without pepsin) at 37°C ($n=3$)

(C)

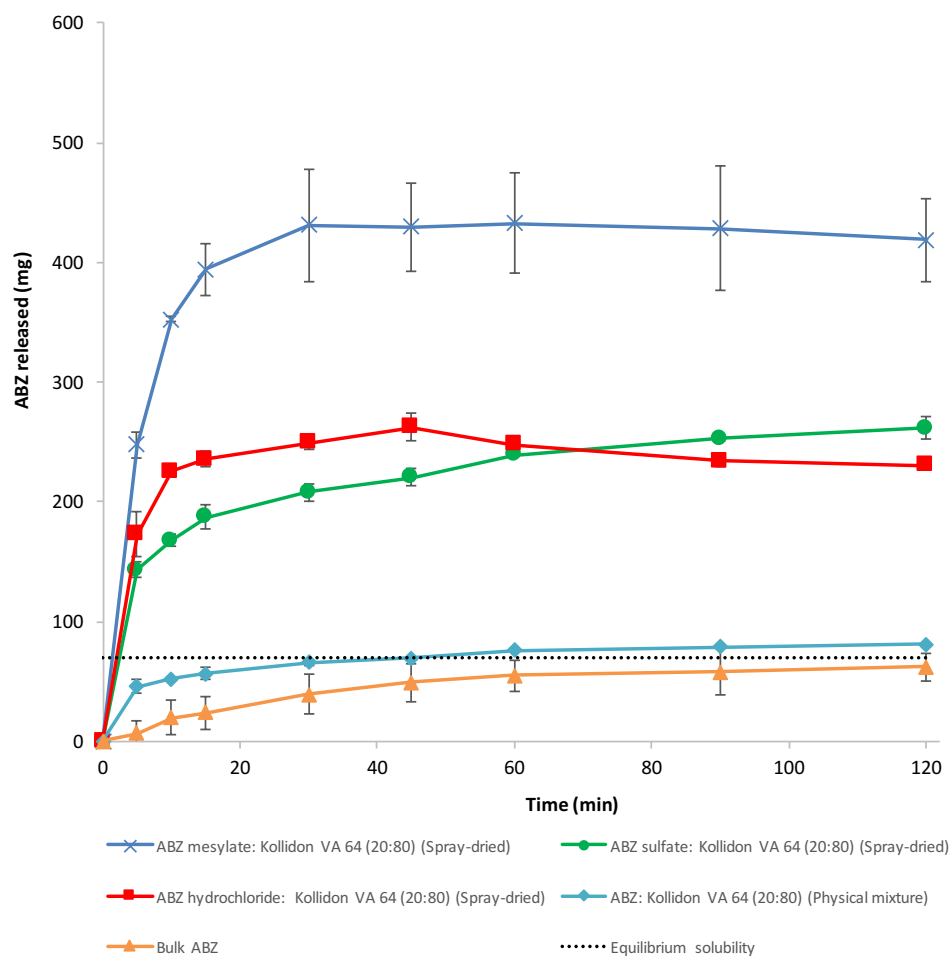


Figure 2.9: (C) Non-sink dissolution of bulk ABZ, physical mixture of ABZ:Kollidon® VA 64 (20:80), and spray-dried ABZ salt:Kollidon® VA 64 (20:80) in 100 mL USP simulated gastric fluid (without pepsin) at 37°C ($n=3$)

Formulation	AUDC (mg.min)
Bulk ABZ	6,376±319
ABZ hydrochloride salt	14,621±1,847
ABZ sulfate salt	17,175±298
ABZ mesylate salt	32,161±328
Physical mixture ABZ:Kollidon® VA 64 (20:80)	9109±219
Spray-dried ABZ hydrochloride:Kollidon® VA 64 (20:80)	29,665±726
Spray-dried ABZ sulfate:Kollidon® VA 64 (20:80)	29,127±656
Spray-dried ABZ mesylate:Kollidon® VA 64 (20:80)	51,303±4,937
Spray-dried ABZ mesylate:Soluplus® (20:80)	25,529±814
Spray-dried ABZ mesylate:Eudragit® E PO (20:80)	11,749±853

Table 2.3: Summary of supersaturation values of the area under the dissolution curve (AUDC) for the USP simulated gastric fluid (without pepsin) at 37°C

2.3.14 Long term stability study of spray-dried formulations

As the spray-dried ABZ mesylate:Kollidon® VA 64 formulation showed the best performance, this formulation was selected for the long term stability study. The drug still remained in the sample after 6-months and 1-year storage as 99.24% and 96.87%, respectively. The two degradation products (ABZSX and ABZ impurity A) were detected at a very low level (less than 2%) after 1 year (Table 2.4). There was no recrystallization of ABZ observed in the X-ray patterns. This great stability data can be used as a guideline for designing a package for the product, and recommended storage conditions.

Duration of storage	ABZ (% label claim)	ABZ sulfoxide (Oxidation) (% of ABZ)	ABZ Imp A (Hydrolysis) (% of ABZ)
Initial	100.00	-	-
6-month storage	99.24	0.34	0.42
1-year storage	96.87	1.47	1.67

Table 2.4: Assay and impurity content of ABZ mesylate-Kollidon® VA 64 formulation after 6-month and 1-year storage in a desiccator at 25°C

2.4.CONCLUSIONS

ABZ solid dispersions prepared by spray drying were amorphous and showed enhanced dissolution and shelf-stability, whereas those made by hot melt extrusion were degraded by heat and shear stress. The dissolution enhancement is attributed to the effects of salt formation and hydrophilic polymer used in the spray-dried formulation. Thermodynamic models of drug-polymer systems based on the Flory-Huggins theory provided useful information of the solubility and miscibility between the drug and polymer, which helps elucidate the physical stability of each system.

REFERENCES

- [1] S.E. Marriner, D.L. Morris, B. Dickson and J.A. Bogan, *Pharmacokinetics of albendazole in man*, Eur. J. Clin. Pharmacol. 30 (1986), pp. 705–708.
- [2] M. Lindenberg, S. Kopp and J.B. Dressman, *Classification of orally administered drugs on the World Health Organization Model list of Essential Medicines according to the biopharmaceutics classification system*, Eur. J. Pharm. Biopharm. 58 (2004), pp. 265–278.
- [3] H. Jung, L. Medina, L. García, I. Fuentes and R. Moreno-Esparza, *Biopharmaceutics: Absorption Studies of Albendazole and Some Physicochemical Properties of the Drug and Its Metabolite Albendazole Sulphoxide*, J. Pharm. Pharmacol. 50 (1998), pp. 43–48.
- [4] K. Daniel-Mwambete, S. Torrado, C. Cuesta-Bandera, F. Ponce-Gordo and J.J. Torrado, *The effect of solubilization on the oral bioavailability of three benzimidazole carbamate drugs*, Int. J. Pharm. 272 (2004), pp. 29–36.
- [5] H. Lange, R. Eggers and J. Bircher, *Increased systemic availability of albendazole when taken with a fatty meal*, Eur. J. Clin. Pharmacol. 34 (1988), pp. 315–317.
- [6] J.L. del Estal, A.I. Alvarez, C. Villaverde, A. Justel and J.G. Prieto, *Increased systemic bioavailability of albendazol when administered with surfactants in rats*, Int. J. Pharm. 102 (1994), pp. 257–260.

- [7] M. Pavan Kumar, Y. Madhusudan Rao and S. Apte, *Improved bioavailability of albendazole following oral administration of nanosuspension in rats*, *Curr. Nanosci.* 3 (2007), pp. 191–194.
- [8] M. Vogt, K. Kunath and J.B. Dressman, *Dissolution enhancement of fenofibrate by micronization, cogrinding and spray-drying: Comparison with commercial preparations*, *Eur. J. Pharm. Biopharm.* 68 (2008), pp. 283–288.
- [9] R. Ravichandran, *In Vivo Pharmacokinetic Studies of Albendazole Nanoparticulate Oral Formulations for Improved Bioavailability*, *Int. J. Green Nanotechnol. Biomed.* 2 (2010), pp. B46–B53.
- [10] G.S. Paulekuhn, J.B. Dressman and C. Saal, *Salt screening and characterization for poorly soluble, weak basic compounds: case study albendazole*, *Pharm. - Int. J. Pharm. Sci.* 68 (2013), pp. 555–564.
- [11] F.K. Alanazi, M. El-Badry, M.O. Ahmed and I.A. Alsarra, *Improvement of albendazole dissolution by preparing microparticles using spray-drying technique*, *Sci. Pharm.* 75 (2007), pp. 63.
- [12] L. Martinez-Marcos, D.A. Lamprou, R.T. McBurney and G.W. Halbert, *A novel hot-melt extrusion formulation of albendazole for increasing dissolution properties*, *Int. J. Pharm.* 499 (2016), pp. 175–185.

- [13] D. Zhou, G.G.Z. Zhang, D. Law, D.J.W. Grant and E.A. Schmitt, *Physical stability of amorphous pharmaceuticals: Importance of configurational thermodynamic quantities and molecular mobility*, J. Pharm. Sci. 91 (2002), pp. 1863–1872.
- [14] D.T. Friesen, R. Shanker, M. Crew, D.T. Smithey, W.J. Curatolo and J.A.S. Nightingale, *Hydroxypropyl methylcellulose acetate succinate-based spray-dried dispersions: an overview*, Mol. Pharm. 5 (2008), pp. 1003–1019.
- [15] K. Pajula, M. Taskinen, V.-P. Lehto, J. Ketolainen and O. Korhonen, *Predicting the Formation and Stability of Amorphous Small Molecule Binary Mixtures from Computationally Determined Flory–Huggins Interaction Parameter and Phase Diagram*, Mol. Pharm. 7 (2010), pp. 795–804.
- [16] Y. Tian, J. Booth, E. Meehan, D.S. Jones, S. Li and G.P. Andrews, *Construction of drug–polymer thermodynamic phase diagrams using Flory–Huggins interaction theory: identifying the relevance of temperature and drug weight fraction to phase separation within solid dispersions*, Mol. Pharm. 10 (2012), pp. 236–248.
- [17] R.P. Patel, M.P. Patel and A.M. Suthar, *Spray drying technology: an overview*, Indian J. Sci. Technol. 2 (2009), pp. 44–47.
- [18] M.M. Crowley, F. Zhang, M.A. Repka, S. Thumma, S.B. Upadhye, S. Kumar Battu et al., *Pharmaceutical applications of hot-melt extrusion: part I*, Drug Dev. Ind. Pharm. 33 (2007), pp. 909–926.

- [19] J.M. Keen, C. Martin, A. Machado, H. Sandhu, J.W. McGinity and J.C. DiNunzio, *Investigation of process temperature and screw speed on properties of a pharmaceutical solid dispersion using corotating and counter-rotating twin-screw extruders*, J. Pharm. Pharmacol. 66 (2014), pp. 204–217.
- [20] A. Paudel, Z.A. Worku, J. Meeus, S. Guns and G. Van den Mooter, *Manufacturing of solid dispersions of poorly water soluble drugs by spray drying: Formulation and process considerations*, Int. J. Pharm. 453 (2013), pp. 253–284.
- [21] J.R. Hughey, J.C. DiNunzio, R.C. Bennett, C. Brough, D.A. Miller, H. Ma et al., *Dissolution Enhancement of a Drug Exhibiting Thermal and Acidic Decomposition Characteristics by Fusion Processing: A Comparative Study of Hot Melt Extrusion and KinetiSol® Dispersing*, AAPS PharmSciTech 11 (2010), pp. 760–774.
- [22] D.J. am Ende, *Achieving a Hot Melt Extrusion Design Space for the Production of Solid Solutions*, in *Chemical Engineering in the Pharmaceutical Industry*, John Wiley & Sons, Inc, Hoboken, NJ, USA, pp. 819–836.
- [23] S. Huang, K. O'Donnell, J. Keen, M. Rickard, J. McGinity and R. Williams III, *A New Extrudable Form of Hypromellose: AFFINISOL™ HPMC HME*, AAPS PharmSciTech 17 (2016), pp. 106–119.
- [24] *US Pharmacopeia 36-NF31*, 2013.

- [25] A. Pobudkowska and U. Domańska, *Study of pH-dependent drugs solubility in water*, Chem. Ind. Chem. Eng. Q. 20 (2014), pp. 115–126.
- [26] FDA, *Stability Testing: Drug substance stress testing*, Int. Conf. Harmon. Tech. Requir. Regist. Pharm. Hum. Use Rockv. MD USA (2003), .
- [27] A. Forster, J. Hempenstall, I. Tucker and T. Rades, *Selection of excipients for melt extrusion with two poorly water-soluble drugs by solubility parameter calculation and thermal analysis*, Int. J. Pharm. 226 (2001), pp. 147–161.
- [28] P.J. Flory, *Thermodynamics of High Polymer Solutions*, J. Chem. Phys. 10 (1942), pp. 51–61.
- [29] M.L. Huggins, *Thermodynamic Properties of Solutions of Long-Chain Compounds*, Vol. 43, 1., Annals of the New York Academy of Sciences New York Academy of Sciences, New York, 1942.
- [30] P.J. Marsac, S.L. Shamblin and L.S. Taylor, *Theoretical and Practical Approaches for Prediction of Drug–Polymer Miscibility and Solubility*, Pharm. Res. 23 (2006), pp. 2417–2426.
- [31] P.J. Marsac, T. Li and L.S. Taylor, *Estimation of drug–polymer miscibility and solubility in amorphous solid dispersions using experimentally determined interaction parameters*, Pharm. Res. 26 (2009), pp. 139–151.

- [32] M. Rubinstein and R.H. Colby, *Polymer Physics*, Oxford University Press, Oxford, 2007.
- [33] M. Gordon and J.S. Taylor, *Ideal copolymers and the second-order transitions of synthetic rubbers. i. non-crystalline copolymers*, J. Appl. Chem. 2 (1952), pp. 493–500.
- [34] *Albendazole Tablets*, in *US Pharmacopeia 36-NF 31*, US Pharmacopeia, US Pharmacopeial Convention, Rockville, MD., 2013, .
- [35] P. Venkatesan, *Albendazole.*, J. Antimicrob. Chemother. 41 (1998), pp. 145–147.
- [36] T. Nogrady and D.F. Weaver, *Medicinal Chemistry: A Molecular and Biochemical Approach*, 3rd ed. Oxford University Press, New York, N.Y, 2005.
- [37] M. Blessy, R.D. Patel, P.N. Prajapati and Y.K. Agrawal, *Development of forced degradation and stability indicating studies of drugs—A review*, J. Pharm. Anal. 4 (2014), pp. 159–165.
- [38] N. Shah, H. Sandhu, D.S. Choi, H. Chokshi and A.W. Malick, *Amorphous Solid Dispersions: Theory and Practice*, Springer, 2014.
- [39] D.Q. Craig, P.G. Royall, V.L. Kett and M.L. Hopton, *The relevance of the amorphous state to pharmaceutical dosage forms: glassy drugs and freeze dried systems*, Int. J. Pharm. 179 (1999), pp. 179–207.

- [40] S. Yoshioka and Y. Aso, *Correlations between molecular mobility and chemical stability during storage of amorphous pharmaceuticals*, J. Pharm. Sci. 96 (2007), pp. 960–981.
- [41] D.J. Greenhalgh, A.C. Williams, P. Timmins and P. York, *Solubility parameters as predictors of miscibility in solid dispersions*, J. Pharm. Sci. 88 (1999), pp. 1182–1190.
- [42] Y. Zhao, P. Inbar, H.P. Chokshi, A.W. Malick and D.S. Choi, *Prediction of the thermal phase diagram of amorphous solid dispersions by Flory–Huggins theory*, J. Pharm. Sci. 100 (2011), pp. 3196–3207.
- [43] F. Qian, J. Huang and M.A. Hussain, *Drug–polymer solubility and miscibility: Stability consideration and practical challenges in amorphous solid dispersion development*, J. Pharm. Sci. 99 (2010), pp. 2941–2947.
- [44] A. Forster, J. Hempenstall and T. Rades, *Characterization of glass solutions of poorly water-soluble drugs produced by melt extrusion with hydrophilic amorphous polymers*, J. Pharm. Pharmacol. 53 (2001), pp. 303–315.
- [45] *Polymer Extrusion (2nd ed.)*. Hanser Publishers, Munchen, 1990.
- [46] S. Govindasamy, O.H. Campanella and C.G. Oates, *High moisture twin-screw extrusion of sago starch: 1. Influence on granule morphology and structure*, Carbohydr. Polym. 30 (1996), pp. 275–286.

- [47] C. Anandharamakrishnan, *Computational Fluid Dynamics Applications in Food Processing*, Springer Science & Business Media, 2013.
- [48] K. Masters, *Impact of spray dryer design on powder properties*, *Drying* 91 (1991), pp. 56–73.
- [49] C. Anandharamakrishnan, C.D. Rielly and A.G.F. Stapley, *Effects of process variables on the denaturation of whey proteins during spray drying*, *Dry. Technol.* 25 (2007), pp. 799–807.
- [50] S.-D. Clas, R. Faizer, R. O’Connor and E. Vadas, *Quantification of crystallinity in blends of lyophilized and crystalline MK-0591 using x-ray powder diffraction*, *Int. J. Pharm.* 121 (1995), pp. 73–79.
- [51] M.M. de Villiers, D.E. Wurster, J.G. Van der Watt and A. Ketkar, *X-Ray powder diffraction determination of the relative amount of crystalline acetaminophen in solid dispersions with polyvinylpyrrolidone*, *Int. J. Pharm.* 163 (1998), pp. 219–224.
- [52] L.A. Utracki, *Polymer Alloys and Blends: Thermodynamics and Rheology*, Hanser, Munich, 1990.
- [53] G. Van den Mooter, M. Wuyts, N. Blaton, R. Busson, P. Grobet, P. Augustijns et al., *Physical stabilisation of amorphous ketoconazole in solid dispersions with polyvinylpyrrolidone K25*, *Eur. J. Pharm. Sci.* 12 (2001), pp. 261–269.

- [54] P. Harmon, L. Li, P.J. Marsac, C. McKelvey, N. Variankaval and W. Xu, *Amorphous Solid Dispersions: Analytical Challenges and Opportunities*, AAPS Newsmagazine Sept (2009), pp. 14–20.
- [55] A.C. Rumondor and L.S. Taylor, *Effect of polymer hygroscopicity on the phase behavior of amorphous solid dispersions in the presence of moisture*, Mol. Pharm. 7 (2010), pp. 477–490.
- [56] L. Yu, *Amorphous pharmaceutical solids: preparation, characterization and stabilization*, Adv. Drug Deliv. Rev. 48 (2001), pp. 27–42.
- [57] D. Turnbull, *On the relationa between crystallization rate and liquid structure*, J. Phys. Chem. 66 (1962), pp. 609–613.
- [58] K.T. Savjani, A.K. Gajjar and J.K. Savjani, *Drug solubility: importance and enhancement techniques*, ISRN Pharm. 2012 (2012), .
- [59] M. Shozo, O. Midori and N. Tanekazu, *Unusual solubility and dissolution behavior of pharmaceutical hydrochloride salts in chloride-containing media*, Int. J. Pharm. 6 (1980), pp. 77–85.
- [60] B.C. Hancock and G. Zografi, *The Relationship Between the Glass Transition Temperature and the Water Content of Amorphous Pharmaceutical Solids*, Pharm. Res. 11 (1994), pp. 471–477.

- [61] T. Taupitz, J.B. Dressman and S. Klein, *New formulation approaches to improve solubility and drug release from fixed dose combinations: case examples pioglitazone/glimepiride and ezetimibe/simvastatin*, Eur. J. Pharm. Biopharm. 84 (2013), pp. 208–218.

Chapter 3: Optimization of Formulation for Novel Inhaled Anti-Idiopathic Pulmonary Fibrosis Therapeutics

ABSTRACT

A caveolin-1 scaffolding domain, CSP7, is a newly developed peptide for the treatment of idiopathic pulmonary fibrosis. To optimize the formulation for further use we have obtained, characterized and compared a number of lyophilized formulations of CSP7 with DPBS and in combination with excipients (mannitol and lactose at molar ratios 1:5, 70 and 140). CSP7 was stable (>95%) in solution at 5 and 25°C for up to 48 hours and tolerated at least 5 freeze/thaw cycles. Lyophilized cakes of CSP7 with excipients were stable (>96%) for up to 4 weeks at room temperature (RT), and retained more than 98% of the CSP7 in the solution at 8 hours after reconstitution at RT. The lyophilized CSP7 formulations were stable for up to 10 months at 5°C protected from moisture. Exposure of the lyophilized cakes of CSP7 to 75% relative humidity (RH) resulted in an increase in the absorbed moisture, promoted crystallization of the excipients and induced reversible formation of CSP7 aggregates. Increased molar ratio of mannitol slightly affected formation of the aggregates. In contrast, lactose significantly decreased (up to 20-times) aggregate formation with apparent saturation at the molar ratio of 1:70. The possible mechanisms of stabilization of CSP7 in solid state by lactose include physical state of the bulking agent and the interactions between lactose and CSP7 (e.g., formation of a Schiff base with the N-terminal amino group of CSP7). Finally, CSP7 exhibited excellent stability

during nebulization of formulations containing mannitol or lactose. Thus, a combination of CSP7 and lactose (1:70 molar ratio) exhibited the greatest stability and is considered the lead formulation for future testing *in vivo*.

3.1 INTRODUCTION

Idiopathic Pulmonary Fibrosis (IPF) is a serious, chronic and progressive interstitial lung disease. By definition, IPF is a build-up of scar tissue in the lung parenchyma from unknown origins (1). This condition often occurs in elderly male smokers or ex-smokers and results in restrictive lung dysfunction (2–4). In the general population, prevalence estimates for IPF have varied from 14 to 43 cases per 100,000 people per year and it is known to be increasing (1). Median survival is about three years after the condition is diagnosed (5) and mortality usually results from respiratory failure (6). While not well-appreciated, survival from IPF is actually lower than many malignancies (4). Current treatments for IPF include nintedanib (7), pirfenedone (8), oxygen therapy (1), and in advanced cases, lung transplantation (9). Unfortunately, none of these interventions are curative and lung transplantation is invasive, expensive and carries its own co-morbidities.

Recently identified pharmacotherapy can slow the progression of disease indicating that better treatment is possible. A caveolin-1 scaffolding domain 7-mer peptide (CSP7), FTTFTVT, is being developed by Lung Therapeutics Inc. for testing for treatment of patients with IPF. CSP7 can inhibit tumor suppressor protein (p53), alveolar epithelial cell (AEC) apoptosis. In AEC, when expression of p53 increases, AEC apoptosis is augmented. Apoptotic AECs are replaced by activated fibroblasts or fibrotic lung fibroblasts (fLFs)

which proliferate, resist apoptosis and deposit matrix proteins (10). CSP7 has an effect on both pathways to stop or reverse development of PF. These effects of CSP7 result in the prevention of PF development in mice after bleomycin (BLM)-induced lung injury (11–15). Therefore, CSP7 has emerged as a new and promising compound for airway delivery via nebulization to treat IPF. If this treatment is successful in future clinical trial testing, it may benefit thousands of patients suffering from IPF in the US and worldwide. Thus, a stable CSP7 formulation prepared by lyophilization and a reconstituted solution delivered to the lung using a nebulizer was initially investigated for preclinical assessment and for subsequent clinical trial utilization.

Lyophilization is used to enhance the stability of peptides since the molecular mobility and reactivity of the peptides in the solid state are reduced (16). However, it is known that residual or absorbed moisture can induce physical and chemical instability of peptide and protein drugs in the lyophilized state, such as aggregation and degradation (17). Aggregation often leads to unfavorable outcomes (e.g., reduction of biological activity, solubility or enhancement of immunogenicity) (18,19). Residual moisture content of the lyophilized products may depend on the bulking agent(s) used in formulations (20–22). A number of publications document that the physical states of the bulking agents have a strong impact on stabilization of the lyophilized products (23–27). Mannitol and lactose are the most commonly and widely used in lyophilized protein/peptide formulations (27–29). Typically mannitol, a non-reducing sugar, provides a robust cake structure, which undergoes micro-collapse; however, its crystallization behavior leads to an unexpected

protective effect (24,25,29,30). On the other hand, lactose, a disaccharide reducing sugar, usually remains in an amorphous state during the freeze-drying process (31,32).

Biopharmaceuticals for treatment of pulmonary disease can be directly delivered to the lungs to minimize their systemic exposure and to increase their efficiency and safety (33,34). Nebulization is used for airway delivery of protein and peptide drugs. However, during nebulization, thermolabile proteins can be partially denatured leading to loss of its activity, formation of aggregates, which may lead to an unwanted outcomes like increasing in immunogenicity (35). These effects result from stress on proteins in the droplets and bulk reservoir liquid. Hence, the evaluation of the effects of nebulization process on activity and stability of therapeutics is critical to the development of novel protein formulations to use in preclinical and clinical trials. Currently used nebulizers are categorized by their mechanism of nebulization such as jet, ultrasonic and vibrating mesh (or membrane) nebulizers (35). To address/minimize potential degradation and inactivation of biologics, vibrating mesh nebulizers have been recommended to aerosolize protein and peptide formulations (36,37). These devices gently generate the aerosol plume (38,39) with low shear force (40). Thus, vibrating mesh nebulizers are considered suitable/optimal method devices for pulmonary protein/peptide delivery.

The present study was focused on evaluation of stability of CSP7 and finding an optimal formulation for further *in vivo* clinical studies. The physical and chemical stability of CSP7 in both liquid and lyophilized states, and the effect of nebulization on stability of CSP7 solutions were evaluated. Stability assessments include characterization of moisture-

induced aggregates using various techniques such as high performance liquid chromatography (HPLC), liquid chromatography/mass spectroscopy (LC/MS), and matrix-assisted laser desorption/ionization time-of-flight mass spectrometer (MALDI-TOF MS). In addition, effects of moisture-induced crystallization of bulking agents are also reported.

3.2 MATERIALS AND METHODS

3.2.1 Materials

The CSP7 (purity > 95%), was kindly provided by Lung Therapeutics, Inc. (Austin, TX). Lactose monohydrate was purchased from Foremost Farms (Baraboo, WI). Dulbecco's phosphate buffered saline (DPBS) without calcium or magnesium was purchased from Lonza (Walkersville, MD). Mannitol, ammonium hydroxide solution (28%w/w in water) ultrapure water, HPLC grade solvents were purchased from Fisher Scientific (Fair Lawn, NJ). All other chemicals utilized in this study were of ACS grade.

3.2.2 Chromatographic analysis

Samples were chemically analyzed with a Dionex 3000 HPLC system (Thermo Fisher Scientific, Fair Lawn, NJ) with a wavelength of 220 nm. CSP7 was eluted by Phenomenex® Luna 5 μ C18(2) 100 Å, 150 mm x 4.6 mm (Phenomenex®, Torrance, CA) column at a flow rate of 1.0 mL/min. Two mobile phases were A (0.1% trifluoroacetic acid in water) and B (0.09% trifluoroacetic acid in a mixture of 20:80, water and acetonitrile).

The HPLC gradient consisted of 25-35% mobile phase B in 20 min and was run at ambient temperature. 20 μ L of each sample was injected onto the column and chromatograms were acquired at the detection wavelength of 220 nm. Standard curve of the CSP7 (concentrations of 0.1-1 mg/mL) were prepared. Duplicate determinations were made for each sample. LC/MS was used for to confirm identity.

3.2.3 Preformulation studies

3.2.3.1 Aggregation and chemical stability of peptide solution

Aggregation and chemical stability of the peptide solution was studied prior to developing the lyophilized formulation. The solutions of CSP7 dissolved in DPBS with minimal amount of ammonium hydroxide solution (28%w/w in water) (concentration 0.5 mg/mL) were prepared to test the effects of agitation, freeze-thaw cycles and storage temperature as follows:

3.2.3.2 Effect of agitation

The solutions of CSP7 were shaken on an orbital shaker at 200 RPM at 5°C and 25°C. The samples were collected at 0.5, 1, 3, 6, 12 and 24 hours and analyzed by HPLC as described in section 3.2.2.

3.2.3.3 Effect of multiple freeze-thaw cycles

Freeze-thaw cycles were studied at -20°C and -80°C. The peptide solutions were frozen at each temperature for 1 hour and then thawed at room temperature for 1 hour. The

freeze-thaw cycle was repeated for 5 cycles and the samples were collected after each cycle and analyzed by HPLC as described in section 3.2.2.

3.2.3.4 Effect of storage temperature

CSP7 solutions were kept at -80°C, -20°C, 5°C and room temperature (about 25°C). Samples were collected after 24 and 48 hours and analyzed by HPLC as described in section 3.2.2.

3.2.4 Formulation preparation

Solutions of CSP7 were prepared by dissolving the peptide (concentration of 0.5 mg/mL) and bulking agents (mannitol or lactose) in the following CSP7:excipient molar ratios of 1:5, 1:70 and 1:140 in DPBS with pH adjusted to 8.0 by ammonium hydroxide solution (28% w/w). Resulting solutions were filtered through a 0.2 μ m PES filter (Celltreat Scientific Products, Shirley, MA). Aliquots of 2 mL of the solution were filled into 5 mL borosilicate glass vials. Rubber stoppers were placed on top of the vials prior to loading on the lyophilizer. Samples were lyophilized using VirTis BenchTop lyophilizer (Gardiner, NY). Lyophilized cycle parameters are as presented in Table 4.1 (Chapter 4). Primary drying time may vary depending on the number or volume of samples. At the completion of the cycle, nitrogen was introduced into the chamber. Vials were sealed with rubber stoppers and aluminum closure, and kept in a desiccator with desiccant at 5°C until tested.

3.2.5 Chemical stability of peptide

3.2.5.1 Chemical stability of peptide in reconstituted solution

The lyophilized formulation of CSP7-mannitol (1:140) cakes was reconstituted to 0.5 mg/mL and kept at 5°C and 25°C. The samples were collected in duplicate at 0.5, 1, 2, 3, 6, and 8 hours. The aggregation was observed and chemical stability of the peptide was then determined by HPLC as described in section 3.2.2.

3.2.5.2 Chemical Stability of peptide in lyophilized state

Vials of lyophilized CSP7-mannitol (1:140) cakes were stored at 5°C and 25°C and sampled in duplicate after 1, 2, and 4 weeks. The lyophilized cakes were reconstituted (0.5 mg/mL) and the solutions were then investigated for aggregation and chemical stability of the peptide by visually observation, HPLC and LCMS. Residual moisture content, osmolality, reconstitution time and pH of the samples were also monitored at each time point.

3.2.6 Karl Fischer Titration

Measurement of moisture content was demonstrated by Karl Fischer titration using an Aquatest 2000 moisture analyzer (Photovolt Instruments, Minneapolis, MN). Anhydrous methanol (1 mL) was added to the pre-weighed sealed sample vial by syringe through the rubber stopper and mixed using vortex mixer. Sample aliquots were withdrawn and transferred to the Karl Fischer vessel. Moisture content of 1mL anhydrous methanol

was also determined and subtracted from the moisture content of samples. Dry, clean empty vial was weighed. Percentage of moisture content was calculated and compared between freshly prepared lyophilized cakes and the samples after exposure to 75% RH. Moisture analysis was performed in triplicate for each of the samples.

3.2.7 Osmolality measurements

Osmolality of the reconstituted solutions of CSP7-mannitol and lactose (1:140 and 1:70) were performed on a 5004 Micro-osmomete™ High Sensitivity Osmometer (Precision Systems Inc. Natick, MA) with 50 µL sample volume. The equipment was calibrated using osmometry standard solutions of 100 and 500 mOsm/kg H₂O (Precision Systems Inc. Natick, MA) before measurement. The osmolality of the reconstituted CSP7 in sterile water for injection (SWI), DBPS and solutions of mannitol (or lactose) in SWI were measured in triplicate.

3.2.8 Measurement of reconstitution time

Reconstitution time of lyophilized cake was measured by injecting 2.0 mL of SWI into the sample vial. The vial was gently swirled. Two mL of SWI was used as control sample. Clarity of the reconstituted solution was compared with the control every 5 seconds and the reconstitution time was recorded when visual clarity was observed. Samples were tested in duplicate.

3.2.9 Moisture-induced aggregation and quantitation of CSP7 aggregates

Lyophilized formulations of CSP7 with both sugars (molar ratios of 1:5, 1:70 and 1:140) were initially prepared. The sample vials were then opened and placed in a desiccator containing an aqueous saturated sodium chloride solution at constant relative humidity (75% relative humidity (RH)). The desiccator was stored at room temperature for 12 hours. After incubation, two vials of exposed sample powders were resealed before testing moisture content by Karl Fisher titration. The other four vials were reconstituted with SWI to a concentration of 0.5 mg/mL, then shaken on an orbital shaker (Lab-Line Instruments, Inc., Melrose Park, IL) at 100 rpm in a cold room (5°C). After 2 hours of shaking, two vials of the aggregated samples were centrifuged at 12,000 rpm for 15 min in the microcentrifuge (model Microfuge 18, Beckman Coulter, Brea, CA). The clear supernatant and aggregate samples were collected. The separated aggregates were re-dissolved in 2 mL of DPBS with ammonium hydroxide solution (28%w/w in water) to render clear solutions (pH 8). Controls were composed of reconstituted solutions of each freshly prepared sample. All clear sample solutions were analyzed by HPLC and LC/MS.

3.2.10 Powder X-ray diffractometry (PXRD)

Morphology of the powder samples was investigated using a Benchtop X-ray diffraction instrument, model Miniflex 600 (Rigaku, Woodlands, TX) with primary monochromated radiation (CuK radiation source, $\lambda = 1.54056 \text{ \AA}$). The instrument was operated at an accelerating voltage of 40 kV and 15 mA. All samples were subjected to the

same program (scanned over a 2θ range of 5° to 40° at a step size of $0.04^\circ/\text{sec}$ and a dwell time of 2 sec), scan speed $1^\circ/\text{min}$.

3.2.11 Differential scanning calorimetry (DSC)

Thermal properties of formulations were conducted using a modulated differential scanning calorimetry (mDSC) (model Q20, TA Instruments, New Castle, DE) equipped with a refrigerated cooling system. Each sample of approximately 3 mg was loaded into a standard aluminum pan and press-sealed with an aluminum lid (PerkinElmer, Waltham, MA). Another crimped empty pan was used as a reference. Experiments were performed at a heating ramp rate of $10^\circ\text{C}/\text{min}$ in the range of $30\text{-}250^\circ\text{C}$ with a modulation temperature amplitude of $1^\circ\text{C}/\text{min}$ under dynamic flow of nitrogen purge the sample cell at a flow rate of $40\text{ mL}/\text{min}$. Data was analyzed using TA Universal Analysis 2000 software (TA Instruments, New Castle, DE).

3.2.12 Determination of water sorption isotherm

Isotherms of peptide-bound water were determined for lyophilized formulations using dynamic vapor sorption (Surface Measurement Systems Ltd., London, UK). A quartz pan was loaded with approximately 10 mg of the lyophilized powder. Water was absorbed from the samples prior to assay, and was removed by leaving the samples at below 0.5% RH until mass changed by less than 0.002% in dm/dt for 120 min. Each formulation was run for a full sorption/desorption cycle from 0% to 90% RH in steps of 10% RH at 25°C . The instrument was run in step dm/dt mode reach equilibrium, as determined by a dm/dt

less than 0.0075% within an interval of 5 min. Percentage of change in mass was calculated and plotted as sorption isotherm. The following equation was used to calculate percent mass sorption (desorption).

$$\text{mass\% sorption (desorption)} = \left(\frac{\text{increase (decrease) in mass form water sorption (desorption)}}{\text{mass of dry powder at initial equilibration (0\% RH)}} \right) 100$$

3.2.13 Long-term stability study (mannitol- and lactose-based formulations)

To avoid exposure to humidity, the lyophilized CSP7 with mannitol and lactose cakes (1:5, 1:70 and 1:140) in the sealed vials were wrapped with parafilm and aluminum foil and kept in a desiccator in the fridge. After 10-month storage, the cakes were reconstituted and analyzed by HPLC as describe in section 3.2.2.

3.2.14 Nebulization of peptide

The lyophilized CSP7: sugar (mannitol and lactose) in the molar ratio of 1:140 and 1:70, respectively were freshly reconstituted with SWI (concentration of 0.5 mg/mL). The solutions were atomized using two types of vibrating mesh nebulizers, which are Aeroneb® Pro (Aerogen, Mountain View, CA) and EZ Breathe® Atomizer (Model EZ-100, Nephron Pharmaceuticals Corporation, Orlando, FL). Nebulization was performed until dryness. Each atomized sample was collected by condensation in the polypropylene tube (35) and analyzed by HPLC as described in section 3.2.2.

3.3 RESULTS AND DISCUSSION

3.3.1 Preformulation studies

A common challenge of formulating biopharmaceutical products is their instability. Peptide drugs may exhibit a wide range of aggregation phenomena along with chemical instability (41,42). At this relatively early stage of product development, the chemical stability and aggregation of the CSP7 peptide were evaluated at different conditions (Figure 3.1). Figure 3.1A shows the effect of agitation on recovery of CSP7 after shaking at 5°C and 25°C for 24 hours. The level of the peptide decreased about 4% after 24 hours of shaking at both temperatures. The solutions were still clear and colorless. Peptide aggregation was not detected. The assessment of repeated freeze-thaw cycles on quality of the CSP7 solution was also conducted. Figure 3.1B shows that about 100% of the CSP7 remained after 5 freeze-thaw cycles. No aggregation was found in any samples following 5 freeze-thaw cycles. These results indicate that freeze-thaw cycling did not affect the stability of CSP7 solution. In addition, Figure 3.1C shows that the storage temperature (from -80 to 25°C) only slightly affected the stability of CSP7 up to 48 hours. The extent of CSP7 decreased about 3% after storage at 25°C for 48 hours but it was more stable at lower temperatures and shorter storage periods. At -80°C and -20°C, the remaining CSP7 was about 100% after storage for 48 hours. There was no aggregation or precipitation detected in any sample after reconstitution in 2 mL of SWI. These results clearly indicate that CSP7 being lyophilized, dissolved at neutral pH or frozen is stable for a short time at

wide range of temperatures. Next, the effect of excipients (mannitol and lactose) on long-term storage stability of CSP7 was studied.

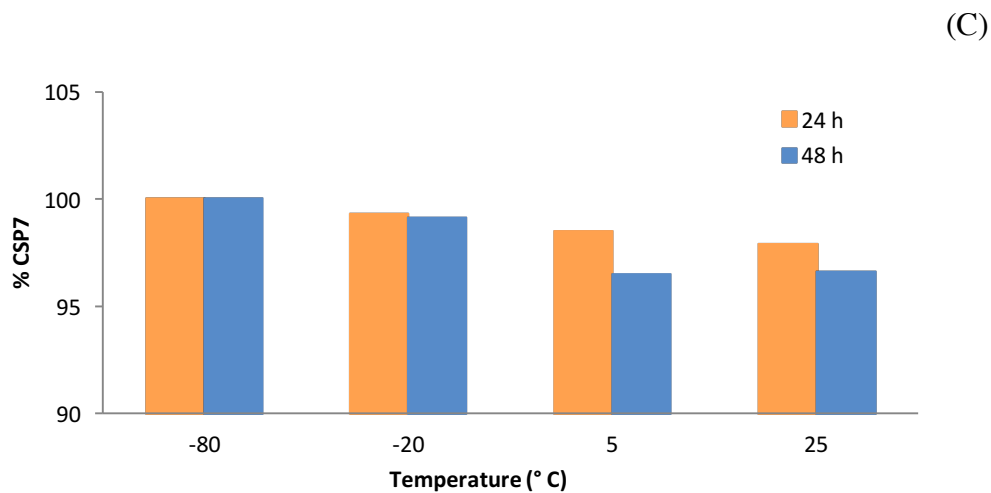
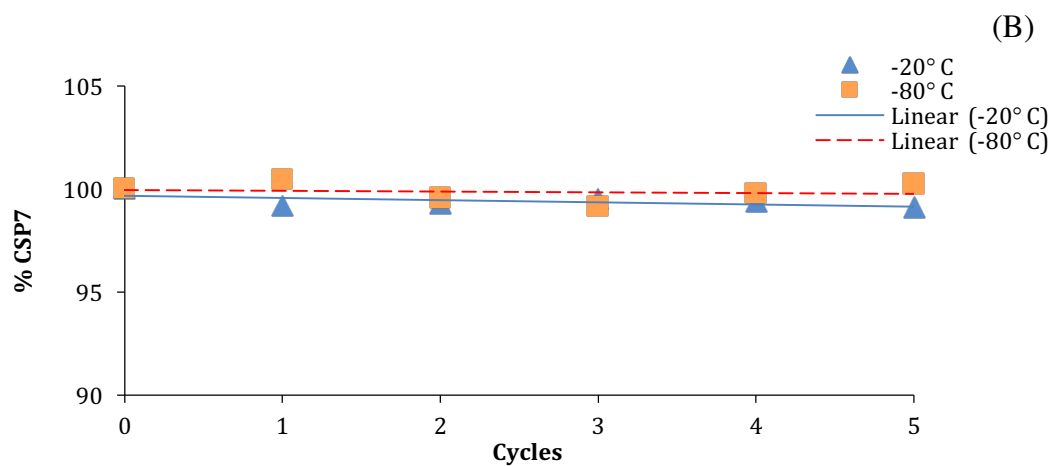
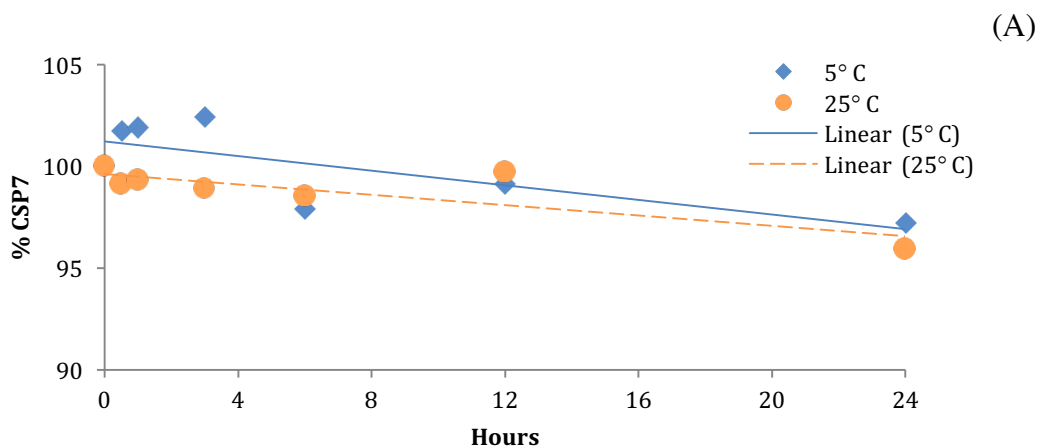


Figure 3.1: Effect of agitation (A), freeze-thaw cycles (B), storage temperature (C) on chemical stability of CSP7 (% recovery), ($n=2$)

3.3.2 Appearance and residual moisture content of lyophilized cakes

The lyophilized CSP7-mannitol (1:70 and 1:140) and CSP7-lactose (1:70) formulations produced smooth and homogeneous cakes. The cakes maintained their structure when tapped and did not exhibit collapse or melt-back after storage at 5°C. The lyophilized products of neat CSP7 without bulking agent and the 1:5 molar ratio of both excipient-based formulations showed a loss of pore structure and broke into pieces while the CSP7-lactose (1:140) cake had minimal shrinkage. Behavior of the lyophilized cake significantly affects the stability of the formulations. Proper cake formation results in proper pore formation, which is associated with water escape and moisture content in the product (43). Compared to the cake, which remains in the microstructure, collapsed mass may contain a higher level of residual moisture since the specific surface area of the shrunken structure is decreased (44).

The residual moisture content from the freshly prepared cakes was in the range of 0.49-4.02% w/w. Overall, residual moisture content of the mannitol- and lactose-based formulations were similar except for the CSP7-lactose (1:140), which contained the highest moisture content (4.02% w/w) approximately 8-fold greater than that of the mannitol-based cake of the same molar ratio (0.53% w/w). The difference in residual moisture content resulted from poor structure and improper pore formation of the CSP7-lactose (1:140) cakes. Generally, lyophilized peptides are more stable at lower water content (< 3%) since high levels of residual moisture frequently lead to higher molecular mobility and chemical instability in the solid state of the protein and peptide (28,45,46). These results demonstrate

that lyophilization of CSP7 alone or with mannitol or lactose (1:5 or 1:70) result in effective removing of moisture from the formulations.

3.3.3 Chemical stability of peptide in reconstituted solution

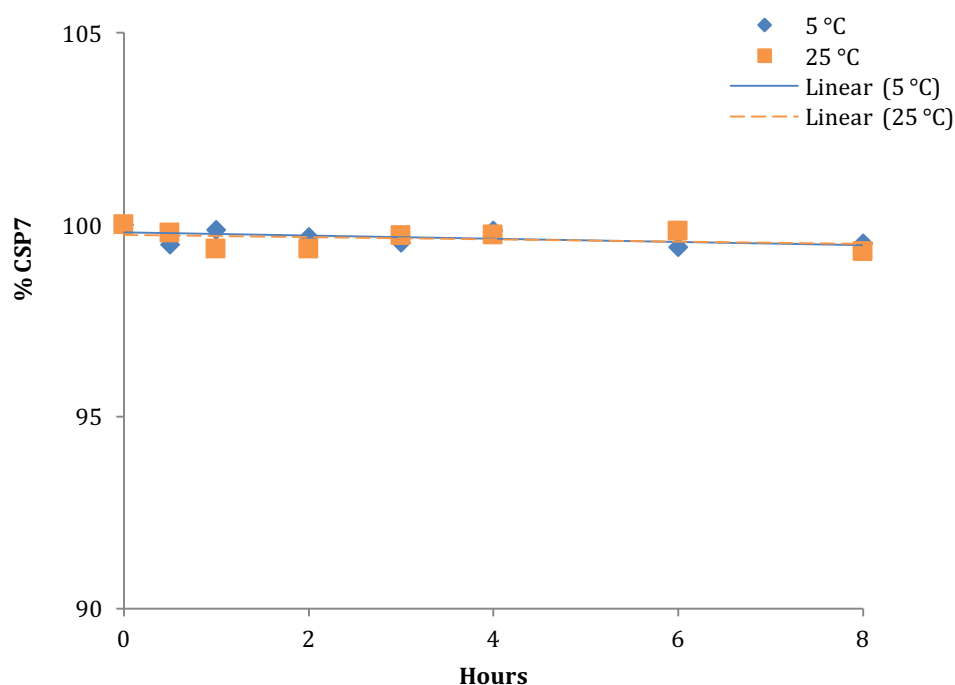
Figure 3.2A shows the stability of CSP7 in reconstituted solutions. Potency, which refers to the amount of peptide in the sample, remained at about 100% after 8 hours at 5°C and 25°C. It is important to obtain isotonic solution after reconstitution of the lyophilized formulations. The non-isotonic solutions can cause the release of histamine, which resulted from changing of the osmotic load around mast cells (47). The release of histamine is responsible for bronchoconstriction (48). Osmolality of the reconstituted solutions of lyophilized CSP7 containing mannitol or lactose was 378 and 328 mOsm/kg (slightly hypertonic). The osmolality of DBPS and solutions of mannitol and lactose in water were 294, 98, and 47 mOsm/kg, respectively. The osmolality of DPBS and sugar solutions were thus very close to the osmolality of the reconstituted CSP7-bulking agent solutions. Although the CSP7 reconstituted solutions were slightly hypertonic, using vibrating mesh nebulizers for drug delivery can markedly improve the treatment time and dose delivery (49).

3.3.4 Chemical stability of peptide in lyophilized state with mannitol

A plot of the percentage remaining CSP7 (potency) versus time is presented in Figure 3.2B. The results show that CSP7 was quite stable in the lyophilized state for 4 weeks at 5°C (98.6%) and 25°C (96.8%). The reconstitution times were between 50-55

seconds and the pH of the samples was about 8. Stability results indicated that the CSP7 in lyophilized cakes containing mannitol (1.5% w/v; 1:140) can resist chemical degradation in the solid state for up to 1 month. In addition, there was no significant change in osmolality (range between 374-378 mOsm/kg) throughout the study period. Residual moisture content of the samples increased from 0.5% at initial to 1.21% and 0.92% after storage at 5°C and 25°C, respectively, however, aggregation of the peptide was not detected when reconstituted after 1-month storage. Thus, storage of mannitol based formulations without exposure to moisture results in both excellent chemical stability of CSP7 and stable osmolality of the solution upon reconstitution.

(A)



(B)

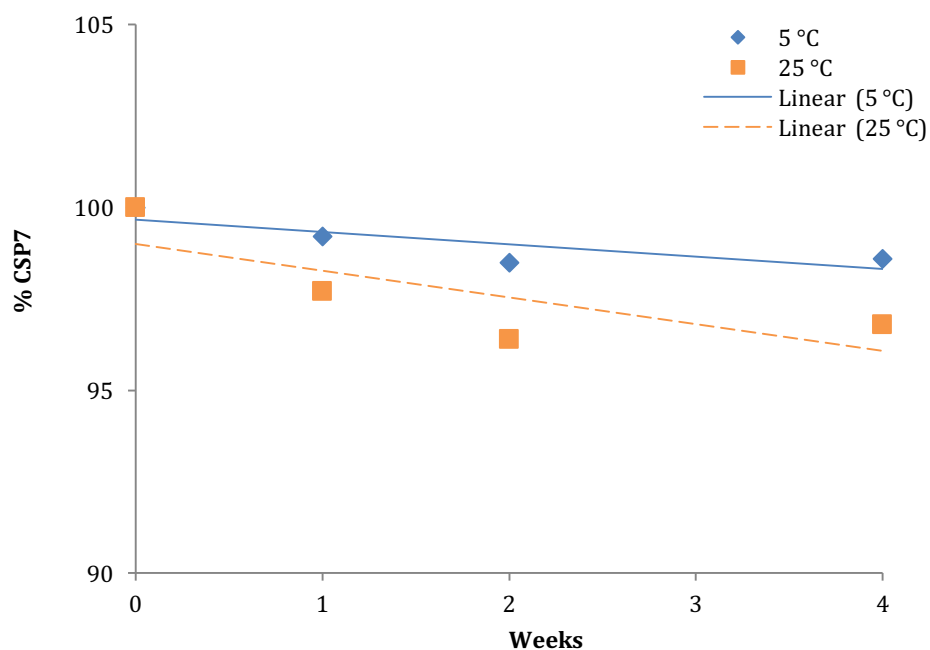


Figure 3.2: Chemical stability data of reconstituted CSP7 solutions after storage at 5°C and 25°C for 8 hours (A), and of lyophilized cakes after storage at 5°C and 25°C for 4 weeks. (B)

3.3.5 Long term stability of the lyophilized CSP7-bulking agent cakes

To test long term stability of CSP7 cakes in the absence of moisture a set of cakes of different formulations was kept at 5°C in a desiccator. Thus, the cakes were protected from humidity during this stability study to avoid an increase of moisture content. After 10 months at 5°C cakes were reconstituted and analyzed for CSP7 using HPLC, as described under Materials and Methods. The results of the analysis (Figure 3.3) demonstrate high stability of the lyophilized cakes of CSP7 with mannitol (1: 70 and 1:140) or lactose (1:5; 1:70 and 1:140) stored without moisture. The slightly aggregates were observed in CSP7-

mannitol (1:5) cakes (not shown) after reconstitution. Thus, this formulation was not analyzed. The other solutions (Figure 3.3) were clear and colorless. Figure 3.3 shows that the percent potency of the samples were between 92.7% (± 1.0) and 97.4% (± 1.9). Regarding this study, without exposure to humidity, the CSP7-bulking agent formulations (except CSP7-mannitol 1:5) were sufficiently stable at 5°C for up to 10 months.

These results demonstrate that mannitol and lactose protect more than 92% of CSP7 up to 10 months at 5°C without exposure to moisture and any of formulations shown in Figure 3.3, if stored properly, could be used for further *in vivo* studies of CSP7. On the other hand, an increase in moisture content in the cake during storage was associated with the lower Tg of the protein formulations. (32,50). The decreased Tg led to an increase in molecular mobility, crystallization of the bulking agent and protein instability (32). Thus, water vapor most likely transferred from around the rubber stoppers could affect the stability of the peptide. Indeed, at 8 weeks, the moisture content of samples stored at 5°C and 25°C without desiccator increased further to 1.99% and 1.36%, respectively. Moreover, both samples exhibited turbidity upon reconstitution due to formation of insoluble aggregates, similar to those observed after 10 months at 5°C in formulation with mannitol (1:5). As the aggregates were observed in the cakes containing higher moisture content, the moisture-induced aggregation became concerned. Water sorption can increase

molecular mobility which leads to a change of physical structure (22). Therefore, the effect of moisture on structure of the cake and aggregate formation of CSP7 was further studied.

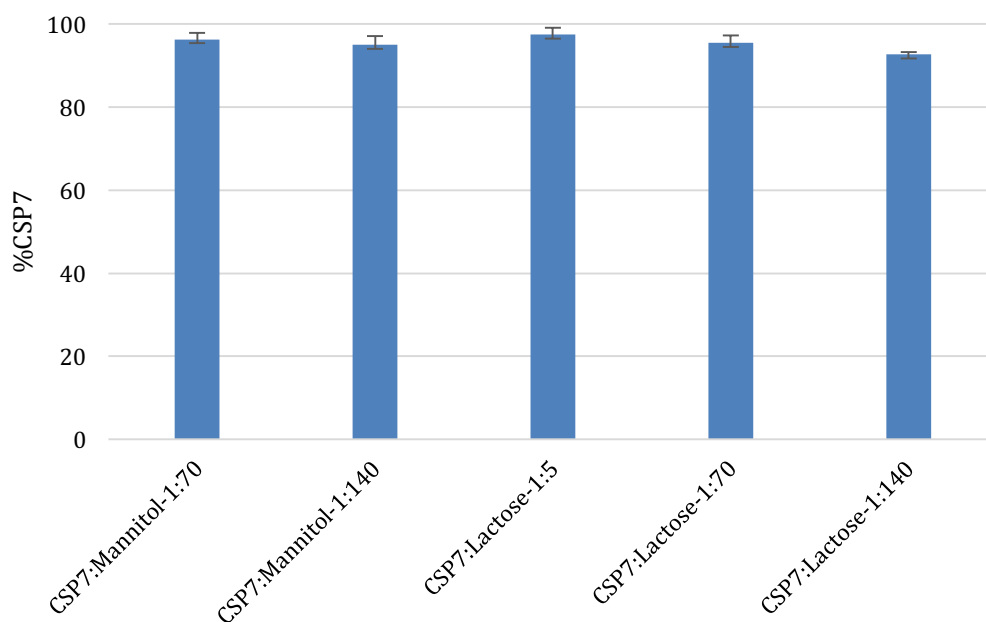


Figure 3.3: Chemical analysis of CSP7-bulking agent after 10-month storage without exposure to humidity at 5°C, no data of CSP7-Mannitol (1:5) presented due to its aggregation ($n=3$)

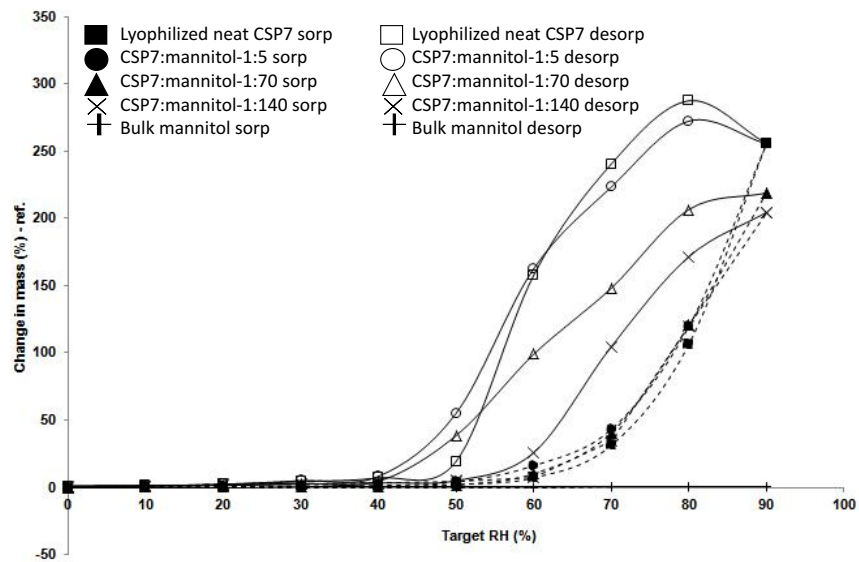
3.3.6 Determination of water sorption isotherm

To evaluate ability of different formulations of CSP7 to absorb moisture, water absorption/desorption isotherms were determined as described under Materials and Methods. Figure 3.4A and 3.4B display the water sorption/desorption isotherms of the lyophilized CSP7 formulations containing mannitol and lactose, respectively. In general, amorphous solids absorb more water than their crystalline counterpart (50). The crystalline

material adsorbs water molecules only at the surface, while amorphous organic solids have glassy state that allows water to diffuse through them as well as onto the surface. This theory coincides with our water sorption/desorption isotherms. The almost unchanged weight of bulk materials indicated that the bulk mannitol and lactose monohydrate were non-hygroscopic and in their crystalline state, which adsorbed minimal water vapor onto only their surface. On the other hand, the significant weight changes of the lyophilized formulations determined that they were hygroscopic solids. Figure 3.4A shows the sorption/desorption cycles of the lyophilized neat CSP7 and CSP7 with mannitol or lactose (1:5 molar ratio) formulations. The isotherm patterns showed that the lyophilized neat CSP7 rapidly absorbed considerable quantities of moisture at high %RH (70-90%RH) and that the lowest level of bulking agents (1:5) slightly affected the moisture sorption of CSP7. Lyophilized CSP7-excipient formulations at all three molar ratios showed that the higher CSP7-excipient molar ratio, the less water was absorbed (Figure 3.4B and 3.4C). We hypothesize that the higher the level of bulking agent, the more interactions can occur between peptide and bulking agents occur. At 1:70 and 1:140, the water sorption of both mannitol- and lactose-based formulations was lower than the neat CSP7. Moreover, at the same molar ratio, the lactose-based formulation adsorbed much less water than the mannitol ones. This can be attributed to the greater chemical interaction between CSP7 and lactose than the mannitol. Once the hydrogen bonds between CSP7 and bulking agents are formed there are less functional groups available for water to interact with the peptide and the less water capable of being absorbed. Sorption isotherms of CSP7-lactose formulations

showed that the lactose-based formulations began adsorbing moisture at about 40% RH. This is attributed to the amorphous state of the formulations. The CSP7-lactose 1:5 formulation showed the highest percentage mass change. Rates of moisture sorption of the 1:70 and 1:140 were slower as a function of % RH, which may result from recrystallization of the lactose at higher % RH and the more interaction between CSP7 and lactose.

(A)



(B)

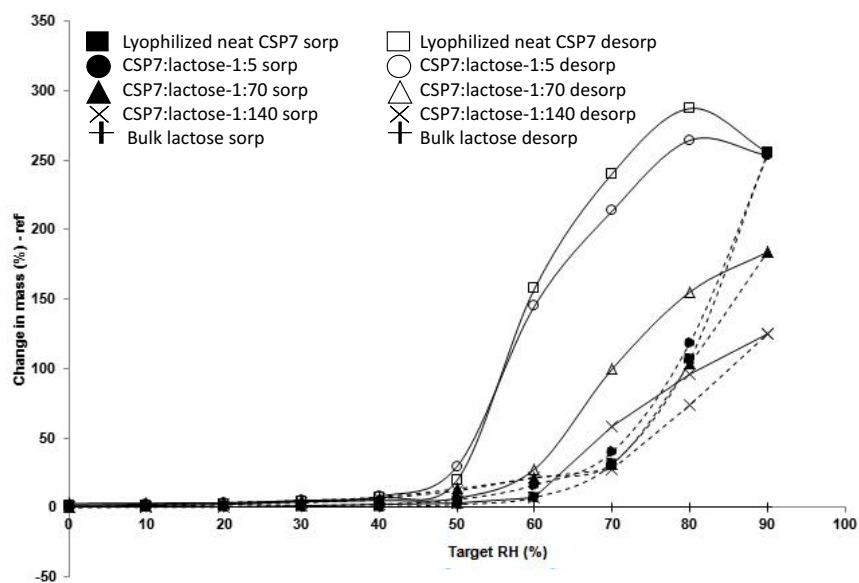


Figure 3.4: Sorption and desorption isotherms of lyophilized neat CSP7 and lyophilized CSP7:mannitol formulations (A), and CSP7:lactose formulations (B)

3.3.7 Effect of bulking agent on moisture-induced lyophilized CSP7 aggregation

Data shown in Figure 3.4 demonstrate that exposure of CSP7 cakes to moisture during storage results in an increase in the moisture content and, potentially, this can affect stability of CSP7 and induce crystallization of the bulking agent. Based on the results shown in Figure 3.4, a 12 hour exposure to 75% RH at 25°C was selected as the condition for further evaluation of the effect of moisture on structure of the cake and CSP7 stability. To investigate the effect of the bulking agents, lactose and mannitol, on aggregation of lyophilized CSP7 formulations, three drug-excipient molar ratios (1:5, 1:70 and 1:140) were prepared and exposed to 75% RH at 25°C. Mannitol and lactose were selected as

bulking agents since they likely exhibit different physical states (crystalline and amorphous) after lyophilization. Exposure of the cakes to 75% RH at 25°C for 12 hours resulted in a significant (up to an order of magnitude) increase in the moisture content (Figure 3.5).

3.3.8 Moisture content after exposure to high humidity environment

Karl Fischer titration (Figure 3.5) measured the moisture content of lyophilized CSP7-bulking agent formulation before (previously discussed in section 3.3.2) and after exposure to 75% RH at room temperature for 12 hours. The results showed that lyophilized neat CSP7 absorbed considerably moisture after exposure to 75% RH. The moisture levels of mannitol- and lactose-based formulations decreased when the amount of bulking agents increased. At the same molar ratio, the lactose-based formulations tended to absorb more moisture than the mannitol-based ones. This was attributed to the addition of amorphous lactose. The amorphous sugars usually absorb water into their bulk structure (51). At the molar ratio of 1:5, mannitol and lactose-based formulations show higher moisture content than the lyophilized neat CSP7, however, there was no statistically significant difference between the formulations with bulking agents and neat CSP7 ($p > .05$). The formulations containing less mannitol exhibited greater moisture content. This can be explained since the 1:5 mannitol-based formulation contained amorphous mannitol, which absorbed more moisture than either the 1:70 and 1:140 formulations which contained a higher degree of recrystallized mannitol.

Such a significant ($p < .05$) increase in the moisture content (up to 36-fold for CSP7-Mannitol 1:70 formulation) upon exposure to 75% RH (Figure 3.5) can reflect formation of crystals in the cakes. It is known that moisture induced crystallization of bulking agents, such as mannitol, or inorganic salts, affects chemical stability of proteins and peptides as well as promote their aggregation (24,27,30,52,53). To test this hypothesis lyophilized cakes exposed to 75% RH were analyzed using PXRD and DSC. Lyophilized cakes of the same formulations, which have not been exposed to 75% RH, were used as controls.

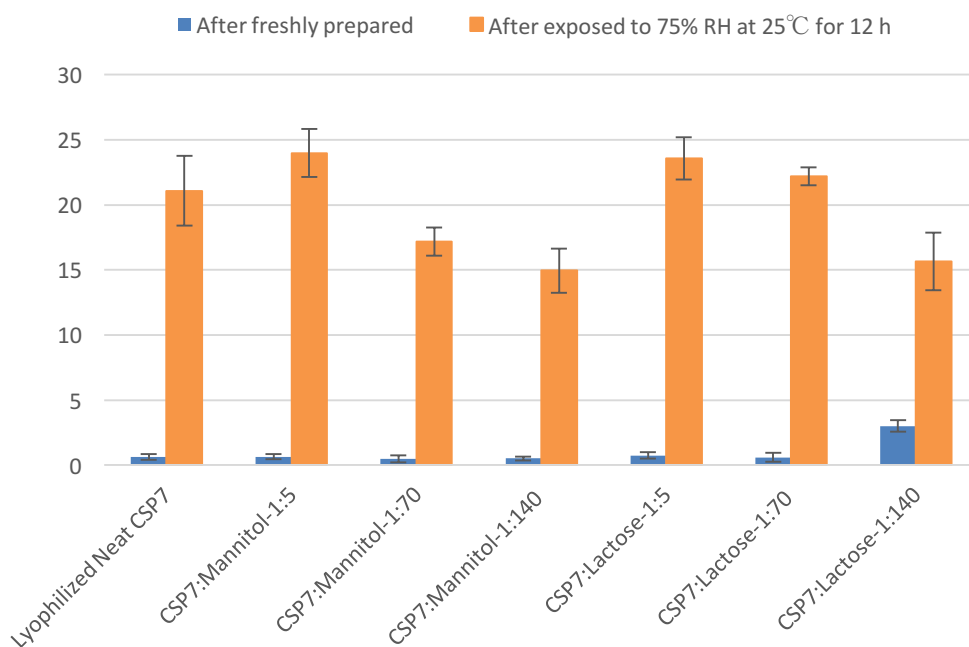


Figure 3.5: Residual moisture content of the lyophilized CSP7, ($n=3$)

3.3.9 Powder X-ray diffraction (PXRD) analysis

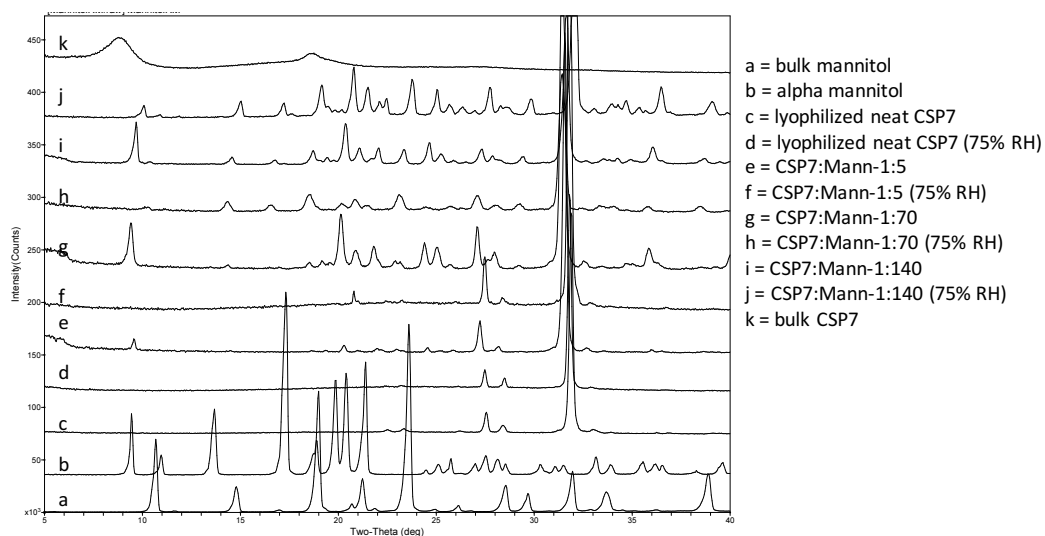
Figure 3.6 shows the X-ray diffractograms of the lyophilized CSP7-stabilizing agent formulations, bulk materials, and lyophilized neat peptide without bulking agent. The sharp peaks at $2\theta = 32^\circ$ and 26° present in all lyophilized samples are phosphate crystal peaks from the DPBS, which is used as solvent buffer in the formulations (54).

The XRD results of neat CSP7 and the mannitol containing formulations are shown in Figure 3.6A. Bulk mannitol as purchased was in β crystalline form and is shown as spectrum “a” while the crystalline mannitol α polymorph is shown as spectrums “b”. The XRD diffractogram of δ mannitol is not shown, however, its predominant peaks at 9.7° , 14.5° , 19.7° , 20.5° and 24.8° , 2θ have been reported (55). The lyophilized neat CSP7 in DPBS before and after exposure to 75% RH were amorphous (spectra “c” and “d”). The lyophilized CSP7-mannitol (1:5) formulation was partially transformed to its amorphous state therefore, very low intensity peaks of δ mannitol were observed (spectrum “e”) (56). The XRD patterns of the 1:70 and 1:140 molar ratio of the mannitol-based formulations (spectrum “g” and “i”) indicate the mixtures of polymorphs of crystalline mannitol. The peaks of δ , α and β mannitol are present. Intensity of the crystalline mannitol peaks (at 9.7° , 14.5° , 19.7° , 20.5° and 24.6° ; Figure 3.6A) increased as the amount of mannitol in the formulation was increased. Based on the XRD data acquired in this study, β mannitol was predominantly transformed to mixtures of δ (and/or α) polymorphs after lyophilization. In addition, the peak at 9.7° , and 18° , 2θ may be the peaks of mannitol

hemihydrate, which is the crystalline fraction within the freeze-dried products, and this hydrate is metastable and prone to lose water at room temperature easily (55,57). As a result, water can interact with the peptide and induce aggregation. After exposure to 75% RH, the major peaks of δ , α (and/or hemihydrate form) mannitol were smaller or no longer so apparent while the intensity of the β polymorph peaks increased (spectrum “f”, “h” and “j”). The results indicate that unstable polymorphic forms of crystalline mannitol are converted to the more stable β form when moisture in the cakes is increased. Formation of crystalline mannitol coincided with an increase in the moisture in the formulation (Figure 3.5) and with aggregation of CSP7 upon reconstitution of the lyophilized cakes.

Figure 3.6B shows the XRD results of CSP7-lactose formulations. The absence of crystalline lactose patterns (peaks 12.5, 20 and 21.5, Figure 3.6B) indicated that amorphous lactose was fully formed at all CSP7-lactose molar ratios following lyophilization (spectra “d”, “f” and “h”). Amorphous lactose in the 1:5 CSP7-lactose formulation remained unchanged after exposure to 75% RH (spectrum “e”); whereas the crystalline lactose developed in the 1:70 and 1:140 formulations after exposure to 75% RH (spectrum “g” and “i”). Thus, similar to mannitol, lactose recrystallization was also induced by water absorbed during 12h exposure to 75% RH. Thus, an increase in the moisture in the cake (Figure 3.5) induces crystallization of bulking agents and inorganic buffer salts, which could significantly affect stability and solubility of the CSP7.

(A)



(B)

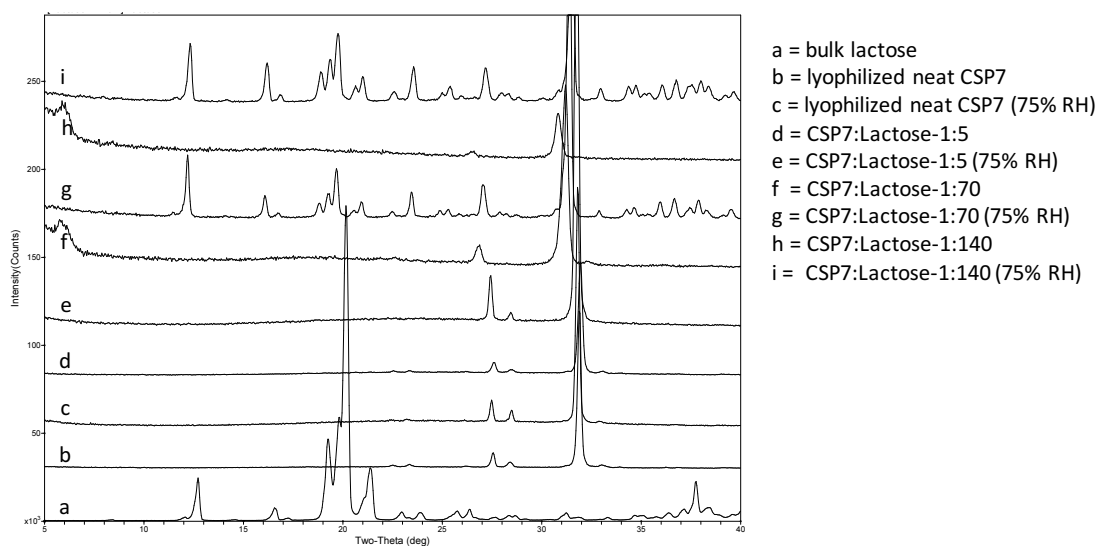


Figure 3.6: PXRD of CSP7:bulking agent; CSP7:mannitol (A), CSP7:lactose (B), before (a, b, d, f, and h) and after exposure to 75% RH (c, e, g and i)

3.3.10 Differential scanning calorimeter (DSC) analysis

DSC is used to detect crystallization of various organic materials including excipients (58). In this study, we focus on the endothermic peaks indicating such events as phase transitions, conformational changes or thermal decomposition of crystal hydrates. Figure 3.7A-D show the effect of exposure to 75% RH on DSC thermograms of the CSP7-mannitol and lactose formulations. The melting peak of peptide was not present indicating the amorphous state. As mentioned earlier, CSP7 formulations were prepared in DPBS buffer, which consists of sodium chloride (NaCl), potassium chloride (KCl), dibasic sodium hydrogen phosphate dihydrate ($\text{Na}_2\text{HPO}_4 \cdot 2\text{H}_2\text{O}$) and monobasic potassium phosphate (KH_2PO_4). There are various studies reporting the effects of buffer salts on crystallinity of the bulking agents, such as delayed lactose crystallization, polymorphic behavior of mannitol, or inhibition of mannitol crystallization (59–62).

DSC data of the CSP7-mannitol formulations before exposure to 75% RH showed that the low extent of crystalline mannitol in the CSP7-mannitol formulation at the lowest molar ratio (1:5) was present as a very small endothermic peak at 135°C. This melting endotherm indicated the endothermic transition of mannitol polymorphism (59). A similar peak was observed such that the melting point of δ mannitol was detected at 139°C or 136°C, when mannitol was prepared in mixtures with inorganic salts 10% w/w of NaCl and KCl, respectively. These melting temperatures are different from the melting point of pure δ mannitol reported as 155°C (59). Even though the δ polymorph is difficult to produce, it frequently occurs in freeze-dried materials (59).

DSC thermograms of the higher CSP7-mannitol molar ratios of 1:70 and 1:140 showed melting endotherms of mannitol at 145°C and 150°C, respectively (Figure 3.7A). These results were comparable to those reported by Telang et al. (2003) (59). Shifting of melting temperatures of the bulk to processed mannitol from 168 °C to 150 °C can be explained by the impact of NaCl on polymorphism of mannitol. The melting point of mannitol when mixed with NaCl was depressed since NaCl had melt miscibility with mannitol (59). The endothermic temperature of CSP7-mannitol (1:70) formulation (145°C) was 5°C lower than that of the reported value of lyophilized mannitol with NaCl. This may be due to the additional effect of salts from DPBS present in the lyophilized sample. For the 1:140 molar ratio formulation, the melting point of the formulation was 150°C since this sample contained a higher amount of β mannitol and less δ form and amorphous mannitol (Figure 3.6). It has also been reported that potassium phosphate salts inhibit crystallization of mannitol during the cooling step of lyophilization (63). However, KH_2PO_4 contained in the DPBS buffer used in our study is much less than the NaCl amount. Thus, the crystalline inhibition effect from this salt may be concealed by the effect of the NaCl.

Following exposure to 75% RH for 12 hours, the DSC thermograms of the CSP7-mannitol (1:5) lyophilized formulation showed the broad endothermic event from 90-130°C. This peak probably corresponds to the melting endotherm of crystalline mannitol shifted in the presence of water. The previous study also reported that in the presence of water, the broad endothermic event at temperature lower than the melting point of mannitol

crystals was attributed to the temperature-depressed melting of anhydrous crystalline mannitol (55). The endothermic peaks at 148°C were determined in the other two mannitol formulations (1:70 and 1:140). The DSC results confirmed the XRD data, indicating that before and after exposure to 75% RH, moisture induced crystallization of mannitol, observed by XRD (Figure 3.6). The small amount of the unstable form of crystalline mannitol in the 1:5 was more difficult to detect by DSC.

The DSC curve of bulk lactose monohydrate shows three distinct endothermic peaks at 146°C, 219°C and 245°C, representing the dehydration of lactose monohydrate, melting, and decomposition temperatures of lactose crystalline lattice, respectively (64). After lyophilization, the dehydration endotherm was absent from all CSP7-lactose formulations. DSC thermograms of the CSP7-lactose 1:70 and 1:140 formulations showed a small melting endotherm at ~195°C (Figure 3.7B), which most likely reflects the DSC-induced lactose recrystallization at elevated temperature. Notably, crystallization of lactose was not detected by XRD without heating the cake (Figure 3.6B).

After exposure to 75% RH, the CSP7-lactose (1:5) formulation showed a relaxation endotherm from the amorphous lactose at 120°C (65). The 1:70 and 1:140 exhibited two distinct endothermic transitions at about 146°C and a broad endothermic event between 160-210°C, which represented the dehydration of lactose monohydrate and the melting lactose (64). These results were in good agreement with the XRD data (Figure 3.6), which indicated that the physical state of the materials (crystallization) depended on the relative amount of lactose in the formulations.

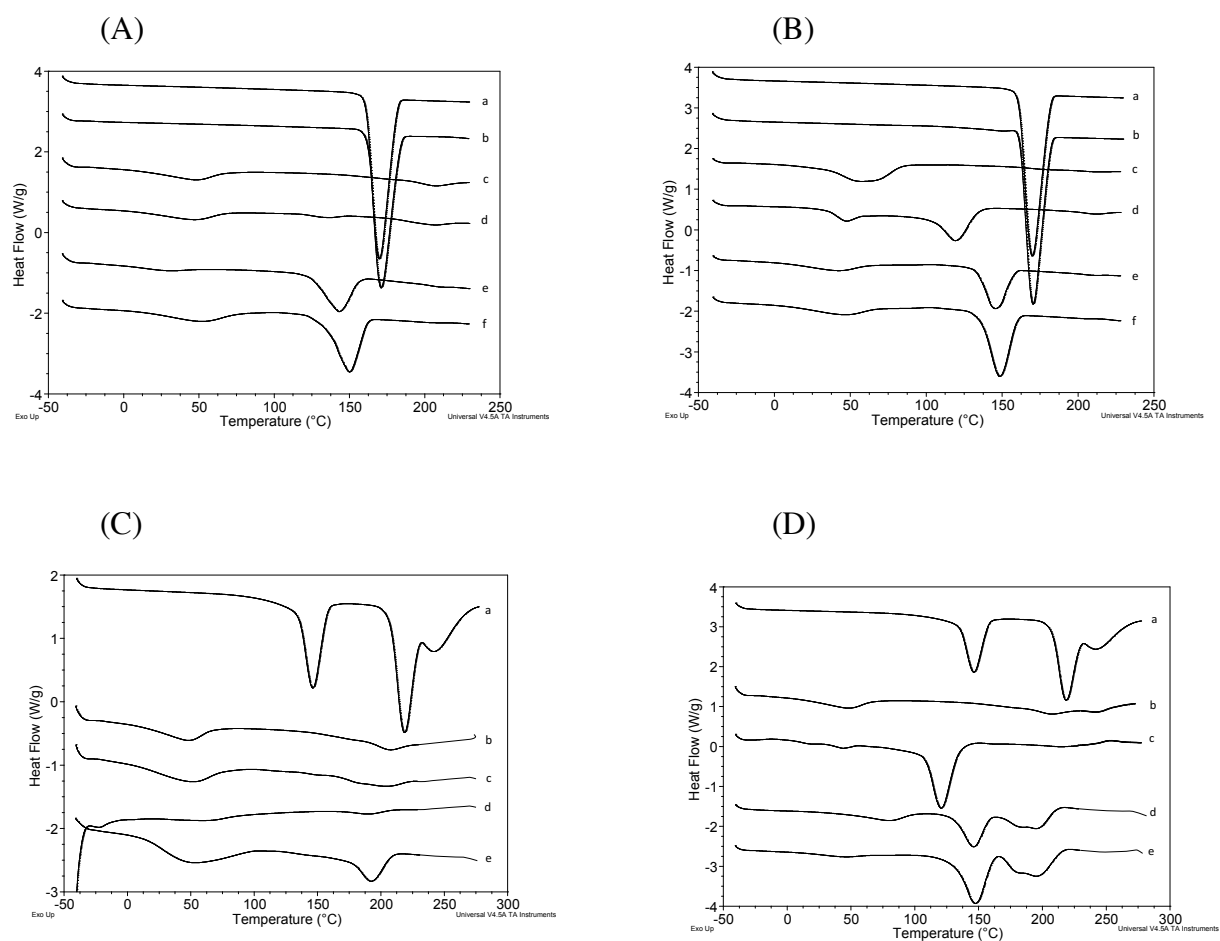


Figure 3.7: DSC thermograms of lyophilized CSP7:bulking agent before (A and C) and after exposure to 75% RH for 12 hours (B and D); mannitol based formulations ((1) and (2)) - bulk mannitol (a), α mannitol (b), lyophilized neat CSP7 (c), 1:5 (d), 1:70 (e), 1:140 (f) and lactose based formulations ((3) and (4)) - bulk lactose monohydrate (a), lyophilized neat CSP7 (b), 1:5 (c), 1:70 (d), and 1:140 (e)

As shown in the PXRD and DSC data, after lyophilization, all CSP7-lactose formulations were amorphous and in the anhydrous form. Therefore, at the same molar ratio, the lactose-based cakes had greater water uptake than CSP7-mannitol cakes. This was described previously (31), where amorphous lyophilized lactose/peptide cakes had greater moisture affinity than those containing mannitol. The stability of protein/peptide products can be affected by crystallization of excipients during freeze-drying (66). Thus, possible mechanisms of CSP7 aggregation as well as properties of aggregates were evaluated next using chemical assay and other analytical methods.

3.3.11 Moisture-induced aggregation of lyophilized CSP7 (mannitol- and lactose-based formulations) is reversible

First, the formation of aggregates induced by moisture in both mannitol- and lactose-based formulations was investigated. After exposure of lyophilized CSP7 formulations to 75% RH for 12 hours followed by reconstitution with SWI, turbid solutions containing aggregates were obtained. The reconstituted solutions of CSP7-mannitol formulations appeared notably more turbid than the lactose-based formulations. The aggregates were isolated by centrifugation and resuspended in DPBS and dissolved by adjusting pH to approximately 8.0 by addition of small amount (less than 1% v/v) of ammonium hydroxide. CSP7 in re-dissolved aggregates was characterized by HPLC, LC/MS and MALDI-TOF MS as described in Materials and Methods. Neither of methods has detected CSP7 multimers proving that the aggregation is reversible and that the soluble aggregates were converted to soluble monomeric species of the peptide. Since degradation

products of the CSP7 were not found, aggregation does not affect chemical stability of CSP7. Previous studies have reported that physical protein/peptide aggregates could be reversible by adjustment of solvent properties such as pH, and/or temperature (67–69). CSP7 consists of four threonines, which contain hydroxyl groups, and are considered to be a strong water-binding residue (70). These water-binding sites on the peptide molecule lead to water adsorption when the peptide is exposed to a high moisture environment (71). The amino acids, which contain weak water-binding sites can also contain sorbed water (70). Reversing CSP7 aggregation by adjusting pH with ammonium hydroxide can indicate stabilization of aggregates by protonated N-terminal amino group. However, an increase in the ionic strength by adding NaCl up to 2 M did not result in dissolving the aggregates (not shown). Therefore, hydrophobic interactions likely significantly contribute to stabilization of CSP7 aggregates. Chemical assay was used next to quantitate CSP7 aggregation in moisture exposed formulations with different molar ratios of mannitol and lactose.

3.3.12 Chemical assay of the aggregates

Two types of clear solutions obtained from the supernatants (1), and the solutions of re-dissolved aggregates (2) were tested by HPLC and LC/MS in order to determine distribution of CSP7 between solution and solid phase after reconstitution of different formulations exposed to 75% RH. Figure 3.8 shows the results of these analyses as the relative percent of each sample as compared to the freshly prepared samples (100%). The total percent recovery of CSP7 from solutions (1) and (2) was nearly 100%, demonstrating

that after reconstitution all CSP7 is distributed between solution and aggregates and confirming that the moisture-induced aggregates of CSP7 are a reversible type. The fraction of aggregates (Figure 3.8) of CSP7 from the mannitol-based formulations (~50%) were substantially greater than that of the lactose-based formulations (~2.4-14.7%). The lyophilized neat CSP7 formulation exhibited the highest aggregation (~58%) since there was no stabilizing agent to protect the peptide from aggregation. It indicates that the peptide itself tends to aggregate. The percentage of aggregates in the mannitol containing formulations was not significantly different. The amount of mannitol in the CSP7-mannitol (1:5) formulation is not sufficient to protect the peptide from aggregation while recrystallization of mannitol in the 1:70 and 1:140 formulations reduced the stabilizing effect of mannitol. Amounts of CSP7 aggregates in lactose-based formulations were ranked from high to low as follows: 1:5, 1:140 and 1:70, respectively. Aggregation of CSP7 in the 1:70 formulation was lowest since this formulation was amorphous. The CSP7-lactose (1:5) formulation was also amorphous. However, the greater extent of aggregation may result from an insufficient stabilizing property of lactose at this low level. Aggregates of peptide in the 1:140 formulation were attributed to the initial high residual moisture content, which can induce peptide aggregation prior to exposure to 75% RH. Two mechanisms can explain this phenomenon, including physical properties of the bulking agents during lyophilization and interactions between bulking agents and CSP7.

The results agreed with a previous study by Herman et al. (1994), which proposed that the effect of water on amorphous drugs does not depend on the amount of water

present, but rather on where it is located. In a lyophilized formulation, mannitol crystallizes either during lyophilization or storage depending on the ratio of mannitol to drug (72). There is not a significant amount of water associated with crystalline mannitol as shown in the sorption/desorption isotherms of bulk mannitol (crystalline) (72). The prior studies also reported similar results; as the crystallinity of mannitol increases, its stabilizing effect is reduced (25,27,73,74). When mannitol recrystallizes with time, water in the lyophilized material redistributes and results in an increase in the free water in the drug microenvironment since mannitol is non-hygroscopic and cannot act as a “sink” for the liberated water (16,66). On the other hand, all lactose formulations remained in their amorphous state after lyophilization. Amorphous lactose may act as an internal desiccant to absorb water into itself therefore, water would not be available to interact with the peptide, resulting in significantly less aggregates formed. Oliyai et al. (31) similarly found that amorphous lactose decreased the number of free water molecules available for chemical reaction with the peptide as compared to the mannitol containing systems. Moreover, lactose also has a much higher T_g than mannitol therefore, it can better retain its glassy state of the formulations with exposure to increased moisture.

An alternative (synergistic) mechanism is interaction between CSP7 and bulking agent. CSP7 containing a high portion of threonine is also able to form intermolecular hydrogen bonds such as crosslinking (75). Mannitol obviously did not affect aggregation since crystallization of mannitol during lyophilization was not able to form hydrogen bonding to the dried protein (32). In contrast, an increase in the molar excess of lactose

almost completely removed aggregation. Interactions of sugars (lactose or trehalose) with dried proteins was investigated (76). The study provided evidence that not only hydrogen bonding occurred between the stabilizing agent-protein, but also that sugar binding is essential for sugar-induced stabilization of protein during lyophilization and rehydration. Moreover, it was conjectured that the hydroxyl groups of bulking agents bond (acting as hydrogen acceptors and donors) with proteins. Therefore, the sugar serves as “water substitutes” to insure conformational stability (77). Finally, lactose, as a reducing sugar, could potentially stabilize peptide in the solution by forming a Schiff base (28,41,78) due to a reaction with N-terminal amino group of CSP7. Since a Schiff base is reversible, its formation should not affect the biological activity of CSP7, and could serve as a reservoir for the peptide in vivo. Based on these results, it appears that lactose stabilized CSP7 against moisture induced aggregation in the solid state to a greater degree than mannitol. In summary, while both pH adjustment and using lactose (1:70 or more) prevented CSP7 aggregation, the stabilizing effect of lactose is valuable for using the formulation at physiological pH.

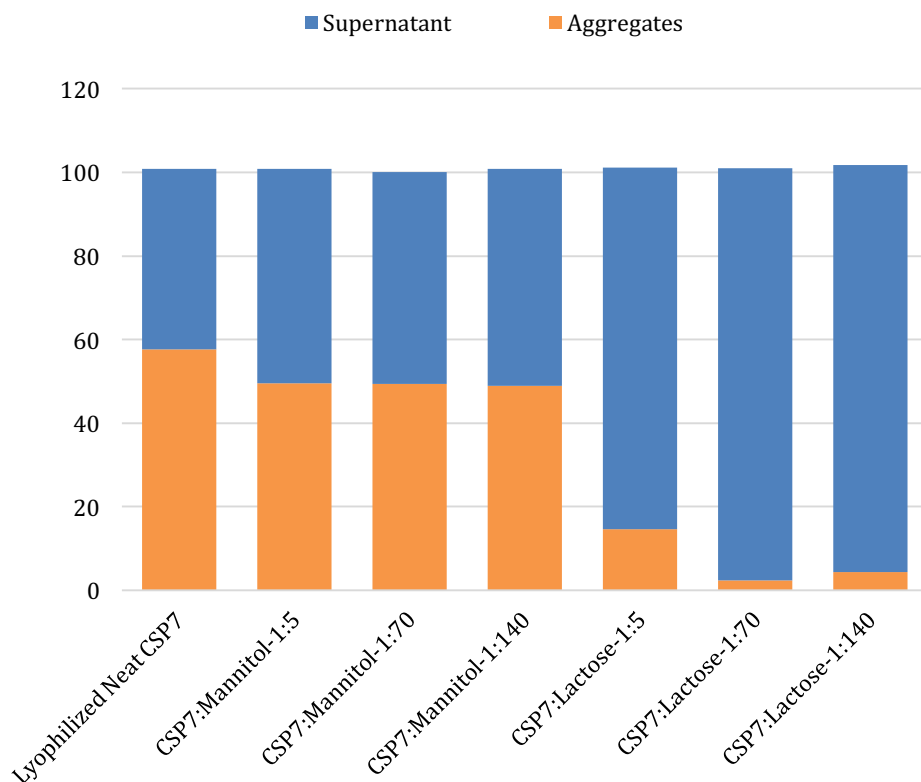


Figure 3.8: Chemical analysis of aggregates CSP7-bulking agent after exposure to 75% RH at room temperature for 12 hours, ($n=2$)

3.3.13 Effect of nebulization on chemical stability of CSP7

Both CSP7 formulations stored without exposure to moisture with mannitol (1:140) and lactose (1:70) easily dissolved in SWI. As compared with the initial bulk solution before lyophilization, the chemical stability of CSP7 was not affected by sterile filtration or lyophilization (recovery nearly 100%). Chemical stability of the CSP7 from mannitol and lactose containing formulations following nebulization by Aeroneb® Pro nebulizer/EZ Breathe® atomizer were 98.9%/98.2% and 98.7%/98.5%, respectively. These results

clearly indicate that efficiency of the vibrating mesh nebulizers; Aeroneb® Pro and the EZ Breathe® was comparable and that nebulization of CSP7 solutions were not significantly different. The nebulization conditions (e.g., shear and temperature from the nebulizers) did not affect the chemical stability of CSP7. Moreover, stability of the peptide was not significantly decreased by the aerosol cloud collection technique (e.g., peptide did not adsorb onto the surface of the collecting tube) and the degradation products and aggregates of the CSP7 were not detected after nebulization.

3.4 CONCLUSION

Lyophilized CSP7 absorbed moisture, which induced its aggregation. Even though the aggregates are reversible by pH adjustment, once they are formed, it lead to a decrease in chemical stability. Amorphous lactose performed remarkably superior to crystallized mannitol in terms of preventing peptide aggregation. Lactose possibly had a significant interaction with amino acids containing in CSP7 exhibiting the stabilizing effect. Long-term stability study indicated the stable formulations and a suitable storage condition for the lyophilized CSP7. While this study determined that 1:70 CSP7:lactose formulation is optimal for long-term shelf storage, possible differences between biological activity of mannitol and lactose formulations will be evaluated in the next step by *in vivo* comparison of moisture free CSP7 formulations. Nebulization using vibrating mesh nebulizers did not affect the potency of the peptide. This optimized formulation is useful in an upcoming *in vivo* study. The mechanisms between lactose and CSP7 in increasing the stability of the lyophilized peptide cake should be further investigated.

REFERENCES

1. Raghu G, Collard HR, Egan JJ, Martinez FJ, Behr J, Brown KK, et al. An official ATS/ERS/JRS/ALAT statement: idiopathic pulmonary fibrosis: evidence-based guidelines for diagnosis and management. *Am J Respir Crit Care Med.* 2011;183(6):788–824.
2. Gribbin J, Hubbard RB, Le Jeune I, Smith CJ, West J, Tata LJ. Incidence and mortality of idiopathic pulmonary fibrosis and sarcoidosis in the UK. *Thorax.* 2006;61(11):980–985.
3. Feghali-Bostwick CA, Yamaguchi Y. Use of endostatin peptides for the treatment of fibrosis. US8507441 B2, 2013.
4. Costabel U, Crestani B, Wells AU. Pharmacological management. In: *Idiopathic Pulmonary Fibrosis.* European Respiratory Society; 2016. p. 196.
5. Salisbury ML, Xia M, Zhou Y, Murray S, Tayob N, Brown KK, et al. Idiopathic Pulmonary Fibrosis. *Chest.* 2016;149(2):491–8.
6. Panos RJ, Mortenson RL, Niccoli SA, King TE. Clinical deterioration in patients with idiopathic pulmonary fibrosis: causes and assessment. *Am J Med.* 1990;88(4):396–404.
7. Richeldi L, du Bois RM, Raghu G, Azuma A, Brown KK, Costabel U, et al. Efficacy and safety of nintedanib in idiopathic pulmonary fibrosis. *N Engl J Med.* 2014;370(22):2071.

8. King, Jr TE, Bradford WZ, Castro-Bernardini S, Fagan EA, Glaspole I, Glassberg MK, et al. A phase 3 trial of pirfenidone in patients with idiopathic pulmonary fibrosis. *N Engl J Med*. 2014;370(22):2083.
9. Raghu G, Rochweg B, Zhang Y, Garcia CAC, Azuma A, Behr J, et al. An official ATS/ERS/JRS/ALAT clinical practice guideline: treatment of idiopathic pulmonary fibrosis. An update of the 2011 clinical practice guideline. *Am J Respir Crit Care Med*. 2015;192(2):e3–e19.
10. Marudamuthu AS, Shetty SK, Bhandary YP, Karandashova S, Thompson M, Sathish V, et al. Plasminogen activator inhibitor-1 suppresses profibrotic responses in fibroblasts from fibrotic lungs. *J Biol Chem*. 2015;290(15):9428–9441.
11. Shetty SK, Bhandary YP, Marudamuthu AS, Abernathy D, Velusamy T, Starcher B, et al. Regulation of airway and alveolar epithelial cell apoptosis by p53-Induced plasminogen activator inhibitor-1 during cigarette smoke exposure injury. *Am J Respir Cell Mol Biol*. 2012;47(4):474–483.
12. Bhandary YP, Shetty SK, Marudamuthu AS, Gyetko MR, Idell S, Gharaee-Kermani M, et al. Regulation of alveolar epithelial cell apoptosis and pulmonary fibrosis by coordinate expression of components of the fibrinolytic system. *Am J Physiol - Lung Cell Mol Physiol*. 2012;302(5):L463–73.
13. Bhandary YP, Shetty SK, Marudamuthu AS, Ji H-L, Neuenschwander PF, Boggaram V, et al. Regulation of lung injury and fibrosis by p53-mediated changes in urokinase and plasminogen activator inhibitor-1. *Am J Pathol*. 2013;183(1):131–143.

14. Marudamuthu AS, Bhandary YP, Shetty SK, Fu J, Sathish V, Prakash YS, et al. Role of the urokinase-fibrinolytic system in epithelial–mesenchymal transition during lung injury. *Am J Pathol.* 2015;185(1):55–68.
15. Bhandary YP, Shetty SK, Marudamuthu AS, Fu J, Pinson BM, Levin J, et al. Role of p53–fibrinolytic system cross-talk in the regulation of quartz-induced lung injury. *Toxicol Appl Pharmacol.* 2015;283(2):92–98.
16. Fakes MG, Dali MV, Haby TA, Morris KR, Varia SA, Serajuddin ATM. Moisture sorption behavior of selected bulking agents used in lyophilized products. *PDA J Pharm Sci Technol.* 2000;54(2):144–9.
17. Costantino HR, Langer R, Klibanov AM. Solid-phase aggregation of proteins under pharmaceutically relevant conditions. *J Pharm Sci.* 1994;83(12):1662–1669.
18. Robbins DC, Cooper SM, Fineberg SE, Mead PM. Antibodies to covalent aggregates of insulin in blood of insulin-using diabetic patients. *Diabetes.* 1987;36(7):838–841.
19. Cleland JL, Powell MF, Shire SJ. The development of stable protein formulations: a close look at protein aggregation, deamidation, and oxidation. *Crit Rev Ther Drug Carrier Syst.* 1992;10(4):307–377.
20. Hsu CC, Ward CA, Pearlman R, Nguyen HM, Yeung DA, Curley JG. Determining the optimum residual moisture in lyophilized protein pharmaceuticals. *Dev Biol Stand.* 1992;74:255.

21. Carpenter JF, Pikal MJ, Chang BS, Randolph TW. Rational design of stable lyophilized protein formulations: some practical advice. *Pharm Res.* 1997;14(8):969–975.
22. Shamblin SL, Hancock BC, Zografi G. Water vapor sorption by peptides, proteins and their formulations. *Eur J Pharm Biopharm.* 1998;45(3):239–47.
23. Costantino HR, Carrasquillo KG, Cordero RA, Mumenthaler M, Hsu CC, Griebenow K. Effect of excipients on the stability and structure of lyophilized recombinant human growth hormone. *J Pharm Sci.* 1998;87(11):1412–20.
24. Izutsu K, Yoshioka S, Terao T. Decreased protein-stabilizing effects of cryoprotectants due to crystallization. *Pharm Res.* 1993;10(8):1232–1237.
25. Izutsu K, Yoshioka S, Terao T. Effect of mannitol crystallinity on the stabilization of enzymes during freeze-drying. *Chem Pharm Bull (Tokyo).* 1994;42(1):5–8.
26. Costantino HR, Langer R, Klibanov AM. Aggregation of a lyophilized pharmaceutical protein, recombinant human albumin: effect of moisture and stabilization by excipients. *Bio/Technology.* 1995;(13):493–6.
27. Li B, O’Meara MH, Lubach JW, Schowen RL, Topp EM, Munson EJ, et al. Effects of sucrose and mannitol on asparagine deamidation rates of model peptides in solution and in the solid state. *J Pharm Sci.* 2005;94(8):1723–1735.
28. Lai MC, Topp EM. Solid-state chemical stability of proteins and peptides. *J Pharm Sci.* 1999;88(5):489–500.

29. Sharma VK, Kalonia DS. Effect of vacuum drying on protein-mannitol interactions: the physical state of mannitol and protein structure in the dried state. *AAPS PharmSciTech*. 2004;5(1):58–69.
30. Izutsu K, Kojima S. Excipient crystallinity and its protein-structure-stabilizing effect during freeze-drying. *J Pharm Pharmacol*. 2002;54(8):1033–9.
31. Oliyai C, Patel JP, Carr L, Borchardt RT. Chemical pathways of peptide degradation. VII. Solid state chemical instability of an aspartyl residue in a model hexapeptide. *Pharm Res*. 1994;11(6):901–908.
32. Kreilgaard L, Frokjaer S, Flink JM, Randolph TW, Carpenter JF. Effects of additives on the stability of *Humicola lanuginosa* lipase during freeze-drying and storage in the dried solid. *J Pharm Sci*. 1999;88(3):281–90.
33. Pilcer G, Amighi K. Formulation strategy and use of excipients in pulmonary drug delivery. *Int J Pharm*. 2010;392(1–2):1–19.
34. Hertel SP, Winter G, Friess W. Protein stability in pulmonary drug delivery via nebulization. *Adv Drug Deliv Rev*. 2015;93:79–94.
39. Hertel S. Pulmonary delivery of pharmaceutical proteins by means of vibrating mesh nebulization. Ludwig-Maximilians-Universität München; 2014.
36. Elhissi AMA, Taylor KMG. Delivery of liposomes generated from proliposomes using air-jet, ultrasonic, and vibrating-mesh nebulisers. *J Drug Deliv Sci Technol*. 2005;15(4):261–5.

37. Hertel S, Pohl T, Friess W, Winter G. Prediction of protein degradation during vibrating mesh nebulization via a high throughput screening method. *Eur J Pharm Biopharm.* 2014;87(2):386–394.
38. Waldrep JC, Dhand R. Advanced nebulizer designs employing vibrating mesh/aperture plate technologies for aerosol generation. *Curr Drug Deliv.* 2008;5(2):114–119.
39. Watts AB, McConville JT, Williams RO. Current Therapies and Technological Advances in Aqueous Aerosol Drug Delivery. *Drug Dev Ind Pharm.* 2008;34(9):913–22.
40. Knoch M, Keller M. The customised electronic nebuliser: a new category of liquid aerosol drug delivery systems. *Expert Opin Drug Deliv.* 2005;2(2):377–90.
41. Wang W. Protein aggregation and its inhibition in biopharmaceutics. *Int J Pharm.* 2005;289(1–2):1–30.
42. Philo JS. Is any measurement method optimal for all aggregate sizes and types? *AAPS J.* 2006 Sep 8;8(3):E564–71.
43. Baheti A, Kumar L, Bansal AK. Excipients used in lyophilization of small molecules. *J Excip Food Chem.* 2010;1(1):41–54.
44. Wang DQ, Hey JM, Nail SI. Effect of collapse on the stability of freeze-dried recombinant factor VIII and α -amylase. *J Pharm Sci.* 2004;93(5):1253–63.

45. Hageman MJ. In *Stability of Protein Pharmaceuticals, Part A: Chemical and Physical Pathways of Protein Degradation*. In: *Water sorption and solid-state stability of proteins*: New York; 1992. p. 273–309.
46. Rey L, May JC (Joan C. *Freeze drying/lyophilization of pharmaceutical and biological products*. 3rd ed. New York: Informa Healthcare; 2010. xiii, 564. (Drugs and the pharmaceutical sciences; vol. 206.).
47. Schoeffel RE, Anderson SD, Altounyan REC. Bronchial hyperreactivity in response to inhalation of ultrasonically nebulised solutions of distilled water and saline. *Br Med J (Clin Res Ed)*. 1981;283(6302):1285–7.
48. Portel L, Tunon de Lara JM, Vernejoux JM, Weiss I, Taytard A. Osmolarity of solutions used in nebulization. *Rev Mal Respir*. 1998;15(2):191.
49. Chan H-K, Chan JGY, Kwok PCL, Young PM, Traini D. Mannitol delivery by vibrating mesh nebulisation for enhancing mucociliary clearance. *J Pharm Sci*. 2011;100(7):2693–702.
50. Brittain HG. *Polymorphism in pharmaceutical solids*. 2nd ed. New York: Informa Healthcare; 2009. xi, 640. (Drugs and the pharmaceutical sciences; vol. 192.).
51. Hancock BC, Shamblin SL. Water vapour sorption by pharmaceutical sugars. *Pharm Sci Technol Today*. 1998;1(8):345–351.
52. Labrude P, Chaillot B, Bonneaux F, Vigneron C. Freeze-drying of haemoglobin in the presence of carbohydrates. *J Pharm Pharmacol*. 1980 Aug;32(8):588.

53. Hellman K, Miller DS, Cammack KA. The effect of freeze-drying on the quaternary structure of L-asparaginase from *Erwinia carotovora*. *Biochim Biophys Acta*. 1983 Dec;749(2):133.
54. Hong Z, Reis RL, Mano JF. Preparation and in vitro characterization of novel bioactive glass ceramic nanoparticles. *J Biomed Mater Res A*. 2009;88(2):304–313.
55. Yu L, Milton N, Groleau EG, Mishra DS, Vansickle RE. Existence of a mannitol hydrate during freeze-drying and practical implications. *J Pharm Sci*. 1999;88(2):196–198.
56. Liao X, Krishnamurthy R, Suryanarayanan R. Influence of processing conditions on the physical state of mannitol—implications in freeze-drying. *Pharm Res*. 2007;24(2):370–6.
57. Nunes C, Suryanarayanan R, Botez CE, Stephens PW. Characterization and crystal structure of D-mannitol hemihydrate. *J Pharm Sci*. 2004;93(11):2800–9.
56. Devi S, Williams DR, Heng JYY. Crystallisation behaviour of D-mannitol as a function of temperature and relative humidity. Available from: <http://www.aidic.it/isic18/webpapers/177Devi.pdf>. Accessed 28 May 2016.
59. Telang C, Suryanarayanan R, Yu L. Crystallization of D-Mannitol in Binary Mixtures with NaCl: Phase Diagram and Polymorphism. *Pharm Res*. 2003;20(12):1939–45.
60. Omar AE, Roos YH. Glass transition and crystallization behaviour of freeze-dried lactose–salt mixtures. *LWT-Food Sci Technol*. 2007;40(3):536–543.

61. Omar AE, Roos YH. Water sorption and time-dependent crystallization behaviour of freeze-dried lactose–salt mixtures. *LWT-Food Sci Technol.* 2007;40(3):520–528.
62. Alqurshi A, Kumar Z, McDonald R, Strang J, Buanz A, Ahmed S, et al. Amorphous formulation and in vitro performance testing of instantly disintegrating buccal tablets for the emergency delivery of naloxone. *Mol Pharm.* 2016;13(5):1688.
63. Cavatur R, Vemuri N, Pyne A, Chrzan Z, Toledo-Velasquez D, Suryanarayanan R. Crystallization behavior of mannitol in frozen aqueous solutions. *Pharm Res.* 2002;19(6):894–900.
64. Araújo AA, Mercuri LP, Carvalho FM, dos Santos Filho M, Matos JR, others. Thermal analysis of the antiretroviral zidovudine (AZT) and evaluation of the compatibility with excipients used in solid dosage forms. *Int J Pharm.* 2003;260(2):303–314.
65. Craig DQ, Barsnes M, Royall PG, Kett VL. An evaluation of the use of modulated temperature DSC as a means of assessing the relaxation behaviour of amorphous lactose. *Pharm Res.* 2000;17(6):696–700.
66. Izutsu K, Yoshioka S, Terao T. Effect of mannitol crystallinity on the stabilization of enzymes during freeze-drying. *Chem Pharm Bull (Tokyo).* 1994;42(1):5–8.

67. Kurochkin IV, Procyk R, Bishop PD, Yee VC, Teller DC, Ingham KC, et al. Domain structure, stability and domain-domain interactions in recombinant factor XIII. *J Mol Biol.* 1995;248(2):414–30.
68. Cholewinski M, Lückel B, Horn H. Degradation pathways, analytical characterization and formulation strategies of a peptide and a protein calcitonine and human growth hormone in comparison. *Pharm Acta Helv.* 1996;71(6):405–19.
69. Picotti P, De Franceschi G, Frare E, Spolaore B, Zambonin M, Chiti F, et al. Amyloid fibril formation and disaggregation of fragment 1-29 of apomyoglobin: insights into the effect of pH on protein fibrillogenesis. *J Mol Biol.* 2007;367(5):1237–45.
70. Costantino HR, Langer R, Klibanov AM. Moisture-induced aggregation of lyophilized insulin. *Pharm Res.* 1994;11(1):21–29.
71. Costantino HR, Curley JG, Hsu CC. Determining the water sorption monolayer of lyophilized pharmaceutical proteins. *J Pharm Sci.* 1997 Dec 1;86(12):1390–3.
72. Herman BD, Sinclair BD, Milton N, Nail SL. The effect of bulking agent on the solid-state stability of freeze-dried methylprednisolone sodium succinate. *Pharm Res.* 1994;11(10):1467–1473.
73. Costantino HR, Andya JD, Nguyen P-A, Dasovich N, Sweeney TD, Shire SJ, et al. Effect of mannitol crystallization on the stability and aerosol performance of a spray-dried pharmaceutical protein, recombinant humanized anti-IgE monoclonal antibody. *J Pharm Sci.* 1998 Nov 1;87(11):1406–11.

74. Andya JD, Maa Y-F, Costantino HR, Nguyen P-A, Dasovich N, Sweeney TD, et al. The effect of formulation excipients on protein stability and aerosol performance of spray-dried powders of a recombinant humanized anti-IgE monoclonal antibody1. *Pharm Res.* 1999;16(3):350–358.

73. AnaSpec Inc. Peptide Solubility Guidelines. Available from: <http://www.anaspec.com/content/pdfs/PeptidesolubilityguidelinesFinal.pdf> Accessed 30 Jul 2016.

76. Carpenter JF, Crowe JH. An infrared spectroscopic study of the interactions of carbohydrates with dried proteins. *Biochemistry (Mosc).* 1989;28(9):3916–22.

77. Arakawa T, Kita Y, Carpenter JF. Protein-solvent interactions in pharmaceutical formulations. *Pharm Res.* 1991;8(3):285.

78. Yaylayan VA, Wnorowski A, Perez Locas C. Why asparagine needs carbohydrates to generate acrylamide. *J Agric Food Chem.* 2003;51(6):1753–1757.

Chapter 4: Optimal Nebulizer for Inhaled Tissue-Type Plasminogen Activator (tPA) and Single-Chain Urokinase Plasminogen Activator (scuPA) for Treatment of Inhalational Smoke-Induced Acute Lung Injury (ISALI)

ABSTRACT

Tissue-type plasminogen activator (tPA) and single-chain urokinase plasminogen activator (scuPA) have attracted interest as enzymes for the treatment of inhalational smoke-induced acute lung injury (ISALI). In this study, the use of commercial human tPA and lyophilization for the preparation of scuPA and subsequent delivery in liquid form using vibrating mesh nebulizers (VMNs) with the appropriate droplet size for pulmonary delivery were demonstrated. Aeroneb® Pro (active) and EZ Breathe® (passive) VMNs were used to nebulize the reconstituted solutions of commercial lyophilized human tPA and lyophilized scuPA formulations. Both the Aeroneb® Pro and EZ Breathe® nebulizers produced atomized protein solutions with droplet sizes smaller than 5 µm, which is appropriate for pulmonary delivery. However, the Aeroneb® Pro nebulizer produced smaller droplets than the EZ Breathe® nebulizer. The enzymatic activity of both tPA and scuPA was maintained at more than 50% after nebulization of the 0.5 mL solutions. The Aeroneb® Pro nebulizer performed slightly better than the EZ Breathe®. Gel electrophoresis did not reveal any degradation products or protein aggregates of the tPA. scuPA maintained nearly 100% of its specific enzyme activity. The loss of the proteins from nebulization is attributed to the residual volume of solutions in the medication cup. Additionally, enzyme activity of tPA and scuPA was not significantly affected by other excipients, sterile filtration, lyophilization process or the reconstitution.

4.1 INTRODUCTION

Tissue-type plasminogen activator (tPA) and urokinase plasminogen activator (uPA) are fibrinolytics, which are proteins that have been used clinically for the treatment of various types of thrombotic disorders with symptoms such as submassive pulmonary embolism (1), pleural effusions (2–4), myocardial infarction (MI) (5), ischemic stroke (6–8), deep vein thrombosis (9,10), and acute respiratory distress syndrome (ARDS) (11–14). Severe burns and smoke exposure develop ARDS in many patients, which is a severe form of acute lung injury (ALI) that has a high mortality rate (30–40%), long-term morbidity (15), and requires protracted hospitalization. Inhalational smoke-induced ALI (ISALI) is one form of ALI, and it is characterized by severe airway obstruction, fibrinous airway casts or debris, and alveolar fibrin deposition (16). Due to its long-term morbidity and high mortality, an efficient and specific treatment for ISALI would have a positive impact on patients. Previous studies have reported that human tPA suppresses activator-induced neutrophil superoxide anion production and has an anti-inflammatory effect on ARDS in an animal model (17,18). tPA is an endogenous serine protease that is found in pleural effusions and cleaves to plasminogen and generates active plasmin; this activity can dissolve thrombosis associated with MI and stroke (19,20). It has also been proven that airway fibrin in a murine model of asthma was dissolved and bronchospasm was relieved by airway administration of tPA (21). The most effective route of tPA delivery for ARDS treatment is direct administration to the airway (19). However, the possibility of direct pulmonary delivery of tPA must be studied further before using this approach (19).

uPA is also found in pleural effusions and potentially useful for ARDS treatment as well. The nebulization of uPA decreased lung fibrosis in rabbits with bleomycin-induced injury (22). Both the upregulation of uPA and the downregulation of plasminogen activator

inhibitor-1 (PAI-1) attenuated the accelerated fibrosis in ALI with accelerated pulmonary fibrosis induced by bleomycin (BLM) (23). An inactive form of uPA, single-chain uPA (scuPA), resists inhibition by PAI-1. A preliminary study reported by the University of Texas Health Science Center at Tyler (UTHSCT) as well as other literature strongly suggests that a recently developed fibrinolysin, scuPA, is advantageous for ISALI, and they hypothesized that scuPA should be more effective and safer than tPA (24,25). It was reported that scuPA exerts relatively low amount, but it has a durable fibrinolytic activity, and it is effective in clearing intrapleural fibrin in rabbits (20,26).

Another potential alternative approach for the local treatment of this respiratory disease is the pulmonary delivery of peptides and proteins directly to the lung. This allows for lower doses and low systemic side effects (27). Nebulization is one of the techniques for airway and pulmonary delivery of protein and peptide drugs in solution or suspension forms. However, after only a few minutes of nebulization, the proteins may denature, which reduces its activity, forms protein aggregates, and increases immunogenic potential (28). These effects may result from excessive stress on the proteins in the droplets and the bulk reservoir. Therefore, testing the nebulization process is a significant step in the development of pulmonary protein delivery.

Although a large number of biologic products are successfully used for various treatments, Pulmozyme® is the only biopharmaceutical product for pulmonary delivery available in the market (28). Moreover, there are no inhaled products of plasminogen activators on the market. Some of the major challenges are the sufficiency and reproducibility of the aerosol deposition, its distribution in the airway due to the complexity of lung geometry, the clearance mechanism, and the uncontrollable breathing of the patient (28). Additionally, generation of the aerosol plume should prevent the activity loss of

biopharmaceutics and not damage their fragile structure (28). User acceptance and patient compliance must also be taken into consideration, as demonstrated by the failure of Exubera® (29–31). Owing to many characteristics (e.g., higher molecular weights, multiple functional groups, 3-dimensional structures of proteins), formulation of these biologics becomes more challenging than small molecules (32). The specific and fragile properties of these proteins cause difficulties in processing, storage, and delivery (33,34). The achievement of protein formulation requires that their enzymatic activity persists during every step of development. Most of these proteins are not stable in liquid form (35) and are more stable as solids (36). Hence, lyophilization is always a preferred type of processing that can prolong the stability of the protein to provide sufficient a shelf-life for commercial products (37–39).

The objective of this study was to evaluate the optimal nebulizer for further use in vivo studies of tPA and scuPA. In addition, for the scuPA, optimal formulation and optimal lyophilization conditions were also determined. The results of these studies support the further development of a protein formulation for the inhibition of epithelial apoptosis and pulmonary fibrosis of the lung.

4.2 MATERIALS AND METHODS

4.2.1 Materials

Human recombinant tPA (Cathflo® Activase® was purchased from Genentech, Inc., South San Francisco, CA). scuPA (purity 73% activity) was a generous present from UTHSCT (Tyler, TX). D-mannitol was purchased from Thermo Fisher Scientific Inc.

(Bridgewater, NJ), and Dulbecco's phosphate buffered saline (DPBS) was purchased from Lonza (Walkerville, MD). BSA was purchased from Sigma-Aldrich (St. Louis, MO) and human plasmin (PL) was purchase from Haematologic Technologies, Inc. (Essex Junction, VT). Urokinase was obtained from Sekisui Diagnostics (Lexington, MA), and Pefachrome uPA (Bz- β -Ala-Gly-Arg-pNA-AcOH) and Pefachrome tPA were bought from Pentapharm (Switzerland). The tcuPA activity standard (100,000 IU/mg) was purchased from Sekisui Diagnostics (Lexington, MA). NuPAGE® Novex® Bis-Tris Mini Gels (Life Technologies, Carlsbad, CA) and 96-well plates were purchased from Thermo Fisher Scientific Inc. (Bridgewater, NJ). Other chemical reagents and solvents used were of analytical grade.

4.2.2 Solid-state preparation of scuPA

Lyophilization to prepare freeze-dried scuPA. In brief, a bulk solution of scuPA in DPBS containing 500 μ g/mL of scuPA and 1.5% w/v of mannitol were prepared and sterilized by filtration through 0.2 μ m of a surfactant-free cellulose acetate (SFCA) sterile syringe filter (Corning Inc., Corning, NY). The effect of filtration was also examined. A half mL of the filtrate was placed in a borosilicate glass vial and lyophilized it using a VirTis Advantage Lyophilizer (VirTis Company Inc., Gardiner, NY). Lyophilization cycle parameters were previously developed by Coldstream Laboratories, Inc. (40), as shown in (Table 4.1). The lyophilized cakes were stored at 5°C until nebulization.

Step	Temperature	Hold Time	Pressure	Ramp	
	(°C)			(min)	(°C/min)
Loading	5	60	—	—	—
Freezing	-55	120	—	0.50	120
Annealing	-15	120	—	0.50	80
Freezing	-55	240	—	0.50	80
Evacuation	-55	10	100	—	—
Primary drying	-30	TBD	100	0.10	250
Secondary drying	30	240	100	0.08	720

Table 4.1: Lyophilization cycle parameters

4.2.3 Karl Fischer titration

Measurement of residual moisture content in the scuPA cakes was demonstrated by Karl Fischer titration using the Aquatest 2000 moisture analyzer (Photovolt Instruments, Minneapolis, MN). A sealed glass vial containing a lyophilized scuPA cake was accurately weighed. Anhydrous methanol (1 mL) was pre-weighed and added to the sealed sample vial by syringe through the rubber stopper and mixed. An aliquot was withdrawn and transferred to the Karl Fischer vessel. The empty vial, including the stopper and the aluminum seal, were washed, dried, and reweighed. The moisture content of 1 mL anhydrous methanol was subtracted from the samples. Percentage of residual moisture content (%w/w) was calculated based on the weight of the cake. Moisture analysis was performed in duplicate for each sample.

4.2.4 Osmolality measurements

Osmolality of the protein solutions were performed on a 5004 Micro-osmette™ High Sensitivity Osmometer (Precision Systems Inc. Natick, MA) with 50 µL sample volume. The equipment was calibrated using the osmometry standard solutions of 100 and 500 mOsm/kg H₂O (Precision Systems Inc., Natick, MA) before measurement. The

osmolality of the reconstituted scuPA solution in sterile water for injection (SWI), DBPS, and a solution of mannitol in SWI were measured in triplicate.

4.2.5 Droplet size distribution

Reconstituted solutions of tPA and scuPA were atomized using the VMNs (EZ Breathe® and Aeroneb® Pro atomizers). The solutions were added to the nebulizer directed towards a vacuum line, positioned horizontally. The reservoir of the Aeroneb® Pro nebulizer, attached to a T-shaped mouthpiece, and the reservoir and mouthpiece of the EZ Breathe® atomizer were parallel to the ground. The nebulizers were placed 2.5 cm from the center of the laser beam, and the aerosol cloud that was produced crossed the beam at a distance of 2.5 cm from the instrument. The aerosol was drawn through the laser beam using the applied vacuum. The droplet size distribution was measured using a laser diffractometer (HELOS, Sympatec GmbH, Clausthal-Zellerfeld, Germany). The two-tail t-test was used to compare the particle size distribution at 50%, $x(50)$.

4.2.6 Nebulization of tPA and scuPA solutions

A commercial human recombinant tPA, Cathflo® Activase®, and lyophilized scuPA were freshly reconstituted with SWI. The tPA and scuPA solutions were prepared at concentrations of 200 µg/mL and 250 µg/mL, respectively. The solution of 0.5 mL was atomized using VMNs, which are Aeroneb® Pro (Aerogen, Mountain View, CA) and EZ Breathe® Atomizer (Model EZ-100, Nephron Pharmaceuticals Corporation, Orlando, FL). Nebulization was performed until the aerosol cloud was no longer produced. Each atomized sample was collected by condensation technique in the polypropylene tube, as

described in the previous study (41). The samples collected were stored at 4°C until analysis.

4.2.7 Kinetic activity assay

The activity of tPA and scuPA was determined as described in the technical report (42). tPA and uPA were determined from the kinetic changes in the absorbance at 405 nm of the chromogenic tPA and uPA substrates (Pefachrome) in 0.1% BSA in a PBS buffer. Samples were prepared by mixing the aliquots with the buffer and diluted as a series (a total volume of 100 µL) in the 96-well plates. In each well, equal volumes of the chromogenic substrate solutions were added in the same buffer, Pefachrome tPA (0.2 mM) and Pefachrome uPA (0.1 mM), then mixed and incubated them at ambient room temperature. Kinetic readings were obtained at 405 nm every minute for a minimum of 30 min by a Varian Cary Eclipse fluorescence spectrophotometer equipped with a 96-well plate reader accessory (Varian, IL). The data from a fitted linear equation were obtained from the Varian software.

Before adding the scuPA to the plate, scuPA had to be activated using plasmin in the nanomolar ratio of a final scuPA-to-plasmin ratio of approximately 50:1. Then, it was incubated in the tubes at 37°C for 3 hours. Inactivated samples (controls) were prepared using the same technique, but a BSA-PBS buffer without plasmin was used instead. Samples in 96-well plates were analyzed. The ability of proteins to cleave human plasminogen to the active plasmin product were reported as enzymatic activity in arbitrary units (AU). The results were calculated based on standards of known activity, which were Cathflow® Activase® and standard tcuPA. The activity of tPA and scuPA in the pre- and post-nebulized samples was calculated as a relative percent as compared with the initial

solutions (with a coefficient of variation $\leq 10\%$). In addition, protein activity before and after sterile filtration, after lyophilization, and after the reconstitution of the scuPA formulated product were also analyzed.

4.2.8 Sodium dodecyl sulfate-polyacrylamide gel electrophoresis (SDS-PAGE)

analysis

The sample solutions of tPA or scuPA (6.5 μL and 7.5 μL for reduced and non-reduced samples, respectively) were mixed with 2.5 μL of concentrated (“4X”) NuPAGE® lithium dodecyl sulfate (LDS) sample buffer. One μL of NuPAGE® Reducing Agent (“10X”) was added to the reduced samples. All samples were heated at 90°C for 2 min, then 10 μL of each sample was loaded and separated on 4–12% NuPAGE® Novex® Bis-Tris gels. SDS running buffer was prepared by adding 50 mL of 20X NuPAGE® MES SDS running buffer to 950 mL of deionized water. The gel was conducted at 200 V for 35 min in MES SDS running buffer, and protein bands were visualized by SimplyBlue™ SafeStain (Thermo Fisher Scientific, Waltham, MA). The gels were imaged by a Bio-Rad molecular imager (Bio-Rad Laboratories, Inc., Philadelphia, PA). Intensity of the bands was visually observed.

4.2.9 Residual volume of Aeroneb® Pro nebulizer

Geometric analysis and measurement of enzymatic activity of tPA and scuPA were used to determine the proteins in the medication cup. A dried, empty medication reservoir from the Aeroneb® Pro nebulizer and a collecting tube were weighed before filling the DPBS. Various volumes of DPBS (0.5 mL, 1 mL, 2 mL, 3 mL, 5 mL, and 8 mL) were loaded into the reservoir, then weighed and nebulized until the aerosol cloud was no longer

produced. The reservoir with the residual solution and the tube with the collected sample were then re-weighed. Each volume was tested in triplicate. The difference in weight before and after nebulization was calculated as the percentage of residual solution, the percentage of solution collected, and the percentage of solution loss.

$$\text{Initial weight} = (\text{cup} + \text{loading solution}) - \text{empty cup} \quad \text{Equation 1}$$

$$\% \text{ residual solution} = \frac{\{(\text{cup} + \text{residual solution}) - \text{empty cup}\}}{\text{Initial weight}} \times 100 \quad \text{Equation 2}$$

$$\% \text{ solution collected} = \frac{\{(\text{tube} + \text{solution collected}) - \text{empty tube}\}}{\text{Initial weight}} \times 100 \quad \text{Equation 3}$$

$$\% \text{ solution loss} = \% \text{ residual solution} - \% \text{ solution collected} \quad \text{Equation 4}$$

Five mL of the tPA and scuPA solutions of 0.2 mg/mL and 0.25 mg/mL, respectively; were nebulized and tested by enzymatic assay. The activity of proteins in the residual solutions in the medication reservoir and the solutions collected in the tubes were compared with the initial solutions before nebulization (100%). Each sample was tested in duplicate.

4.3 RESULTS AND DISCUSSION

4.3.1 Appearance of lyophilized cakes, residual moisture content, and tonicity of scuPA formulation

The lyophilized scuPA with mannitol formulation produced homogeneous cakes, which maintained their structure when tapped and did not exhibit collapse or melt-back. This supports the use of 1.5% w/v mannitol as the bulking agent is sufficient to provide the

appropriate cake structure. The appearance of the lyophilized products significantly could affect their stability. Proper cake formation results in proper pore formation, and this is associated with water escape and the moisture content of the product (43). Moisture determination indicated that the residual moisture content of the lyophilized scuPA was in the range of 0.6–0.8% w/w, which is in the target range of < 3% w/w (44). Generally, lyophilized biopharmaceuticals are more stable at lower water content, since high-level residual moisture frequently leads to higher molecular mobility and in turn induces chemical instability in the solid state of proteins and peptides (36,45,46).

The osmolality of the reconstituted solution of scuPA was 400 mOsm/kg (hypertonic). The osmolality of DBPS and the mannitol solution in water was 294 mOsm/kg and 90 mOsm/kg, respectively. The total osmolality of these solutions was close to the osmolality of the reconstituted solution. The non-isotonic solutions can cause the release of histamine, which results from the changing of the osmotic load surrounding the mast cells (47). The release of histamine is responsible for bronchoconstriction (48). However, using VMNs for drug delivery markedly improved the treatment time and dose delivered. Thus, VMNs have the potential to enhance patient tolerability and adherence to the nebulized therapeutics of the hypertonic solutions (49).

4.3.2 Droplet size distribution

The main goal of nebulization is to deliver the drug formulation to the lungs. Although several factors affect pulmonary drug delivery, such as the patient's age, the patient's lung function, and the stage of the disease; the particle size of the inhaled formulation is one of the most important features that determines its deposition in the airway. VMNs have higher nebulization efficiency than jet or ultrasonic nebulizers in terms

of aerosol droplet size, which relates to deposition characteristics (50). Even though no baffle was needed, both active and passive VMNs generated very fine aerosol droplets (50). In general, the smaller droplets are more likely to reach the distal parts of the lung (51,52). Droplets larger than 5 μm would likely be deposited in the upper airways, while droplets of the optimum droplet size of 3–5 μm would likely be deposited in the tracheobronchial tree (53). Figure 4.1A and 4.1B show the aerosol droplet size distribution of tPA and scuPA formulations, respectively. The droplet size, $x(50)$, of tPA and scuPA atomized from the EZ Breathe® were 4.68 μm and 4.94 μm , respectively, which is significantly larger ($p < .05$) than those from the Aeroneb® Pro nebulizer (3.68 μm and 3.70 μm , respectively). These differences are possibly due to the different designs of the nebulizer; EZ Breathe® is the passive type, while the Aeroneb® Pro is an active vibrating mesh device. However, both types of VMNs produced aerosol droplet sizes smaller than 5 μm .

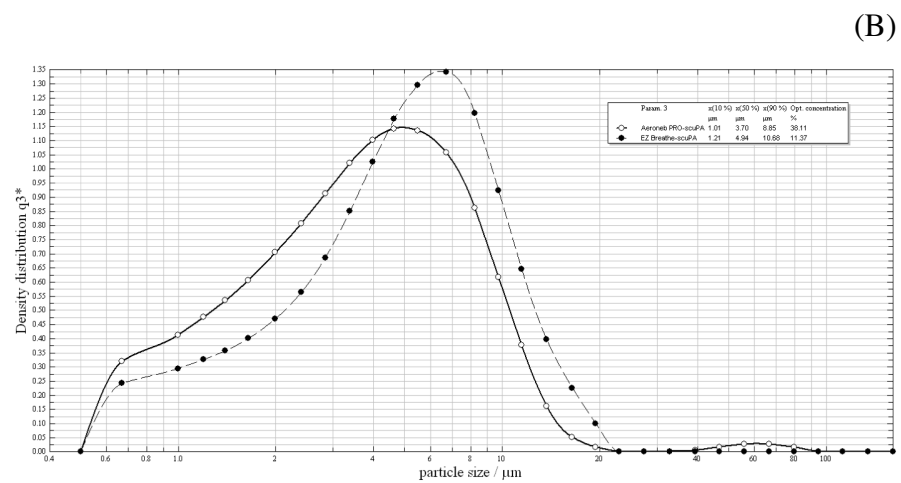
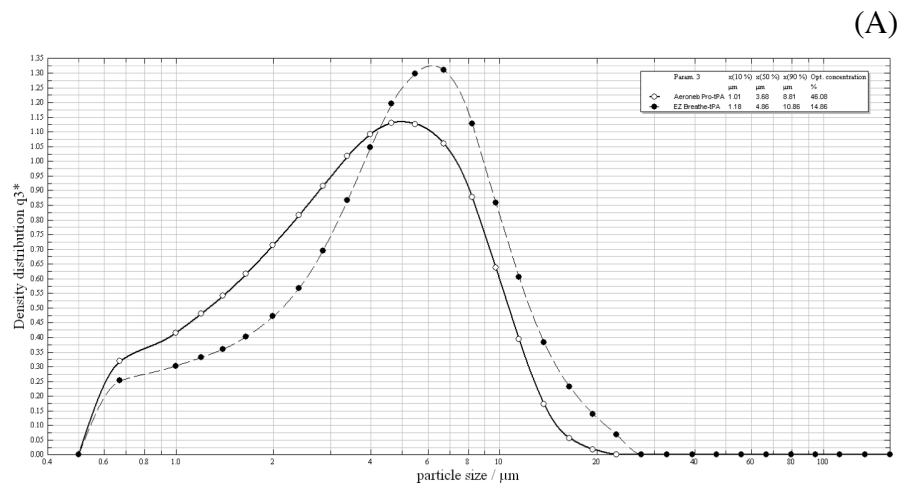


Figure 4.1: Droplet size distribution of tPA solutions (A) and scuPA solutions (B) by Aeroneb® Pro (open circle) and EZ Breathe® (closed circle) nebulizers, respectively ($n=2$)

4.3.3 Nebulization of tPA and scuPA

The various types of nebulizers are categorized according to their mechanism of atomization, such as jet nebulizers, ultrasonic nebulizers, and VMNs (28). Jet nebulizers and ultrasonic nebulizers, by design, suffer from recirculation. The droplets were nebulized at least 10–15 times, which caused an increase in interfacial stress (54,55). VMNs, however, are single-pass devices by design, which prevents the repetition of nebulization stress (56). Moreover, ultrasonic nebulizers generate heat during operation that is not suitable for heat-labile drugs such as proteins or peptides (57), while VMNs do not generate heat (58). VMNs have also been recommended for aerosolized protein and peptide formulations due to factors of protein degradation and inactivation (59–61). Therefore, vibrating mesh nebulization is the expected choice in this study for use with tPA and scuPA, since this method can gently generate the aerosol plume (62,63) with low shear force (64).

The Cathflow® Activase® and scuPA cakes rapidly dissolved in SWI. Figure 4.2 and 4.4 present the biologic activities of tPA and scuPA before and after nebulization. The relative percentages of tPA following nebulization by Aeroneb® Pro and EZ Breathe® nebulizers were 54.9% and 53.7%, respectively; while 57.4% and 56.6% of scuPA were determined, respectively. For both proteins, the Aeroneb® Pro nebulizer exhibited slightly greater activity than the EZ Breathe®. In addition, polyacrylamide gel electrophoresis was used to verify the extent of tPA (Figure 4.3). The band intensity of samples after nebulization were visually lighter than the samples before nebulization (100%, initial). Moreover, degradation products and aggregates of the tPA in the samples were not detected on the gels. The measured activity and band intensity of tPA show strong correlation between enzyme activity and protein loss. In addition, the activity of scuPA was not

significantly affected by the addition of mannitol to the formulation with sterile filtration or the lyophilization process. The band intensity of samples from each device was less intense than the bulk sample, the sample after filtration, and the reconstituted sample before nebulization (data not presented). Loss of both proteins and the corresponding loss of enzyme activity was not significantly decreased due to nebulization. These results show that nebulizing conditions (i.g. solution formation, and the effect of the atomizing process of the nebulizers) did not have an influence on the activity of either protein. However, it was hypothesized that the majority of the loss of enzymes in this in vitro study was attributable to the residual solution that remained in the medication container. Therefore, a study of the residual solution in the nebulizer cup was conducted.

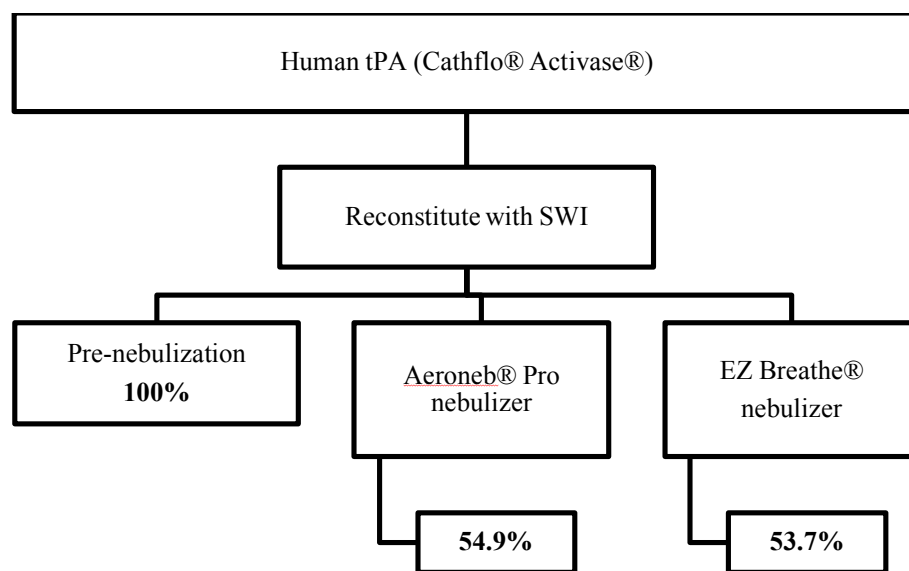


Figure 4.2: Enzymatic activity of tPA after nebulization by Aeroneb® Pro and EZ Breathe® nebulizers

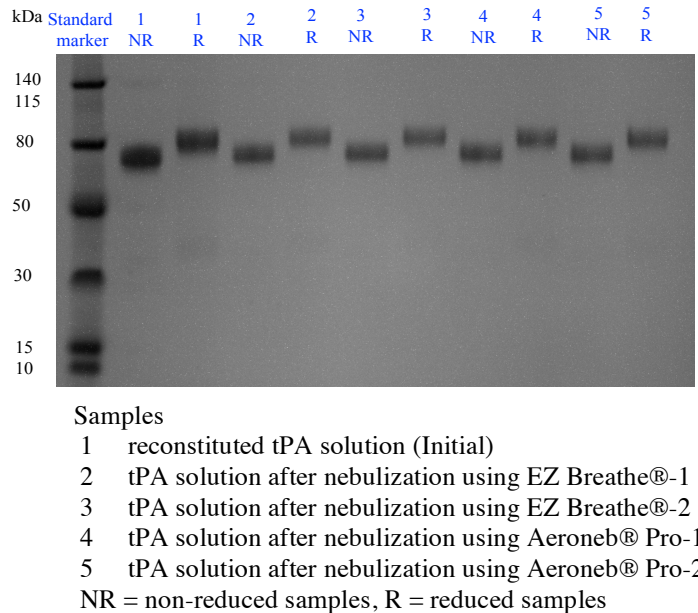


Figure 4.3: SDS-PAGE results of tPA samples before and after nebulization by Aeroneb® Pro and EZ Breathe® nebulizers ($n=2$)

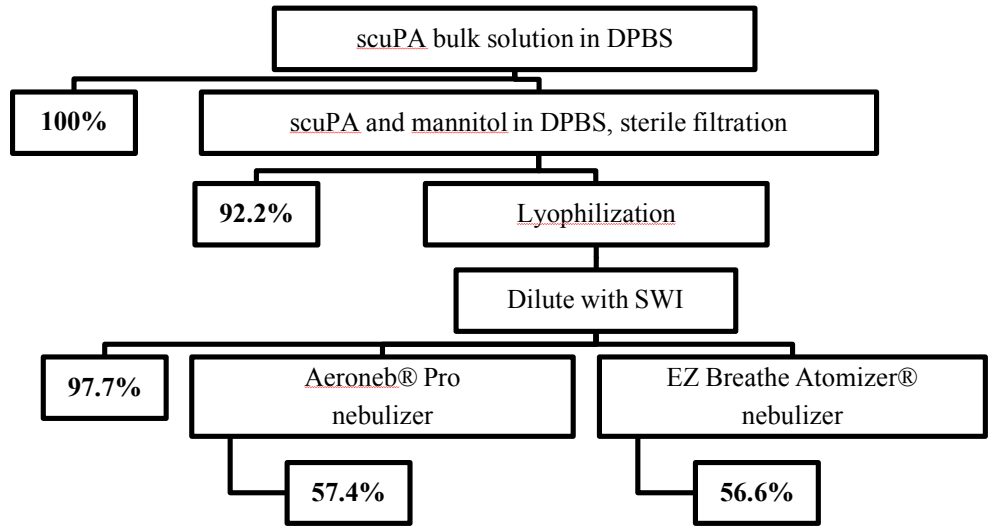


Figure 4.4: Enzymatic activity of scuPA after sterile filtration, lyophilization, and nebulization by Aerone® Pro and EZ Breathe® nebulizers as compared with the bulk solution ($n=2$)

4.3.4 Residual solution remaining in the medication cup

The Aeroneb® Pro nebulizer was used in this study because of its slightly better performance. Figure 4.5A plots the weight difference between the dried empty containers (medication cup and polypropylene tube) and the containers with DPBS (density = 1.01 g/mL) based on gravimetric analysis. The weights of residual DPBS in this study were in the range of 0.17–0.52 mg. These results agree with previous reports, in which the residual volume was between 0.2 mL and 0.4 mL (58,65). Compared with the weight of the loading solution (Equation 2), the percentage of the residual solution that remained in the cup of the 0.5 mL loading volume was the highest (~ 37%), and the residual solution was decreased when the loading volume increased. The residual weight of the 8 mL loading solution was only about 4%.

The enzyme activity of the proteins that remained in the cups and collected in the polypropylene tubes after nebulization of 5 mL of each protein solution was measured and compared to the sample before nebulization (Figure 4.5B). The activity of the residual proteins (tPA and scuPA) in the cup was 6.2% and 8.8%, respectively, and the activity in the collecting tube was 93.9% and 88.4%, respectively. The results by gravimetric method show that a mass of 7.4% remained in the cup, and 90.8% of the solution was collected in the tube following nebulization of the 5 mL DPBS buffer. These mass percentages agree with the enzymatic activity of each fraction of the proteins. Therefore, this supports our premise that the loss of protein activity of tPA and scuPA in the samples collected was not affected by nebulization using the Aeroneb® Pro, but rather it was attributable to the loss of protein retained in the medication reservoir.

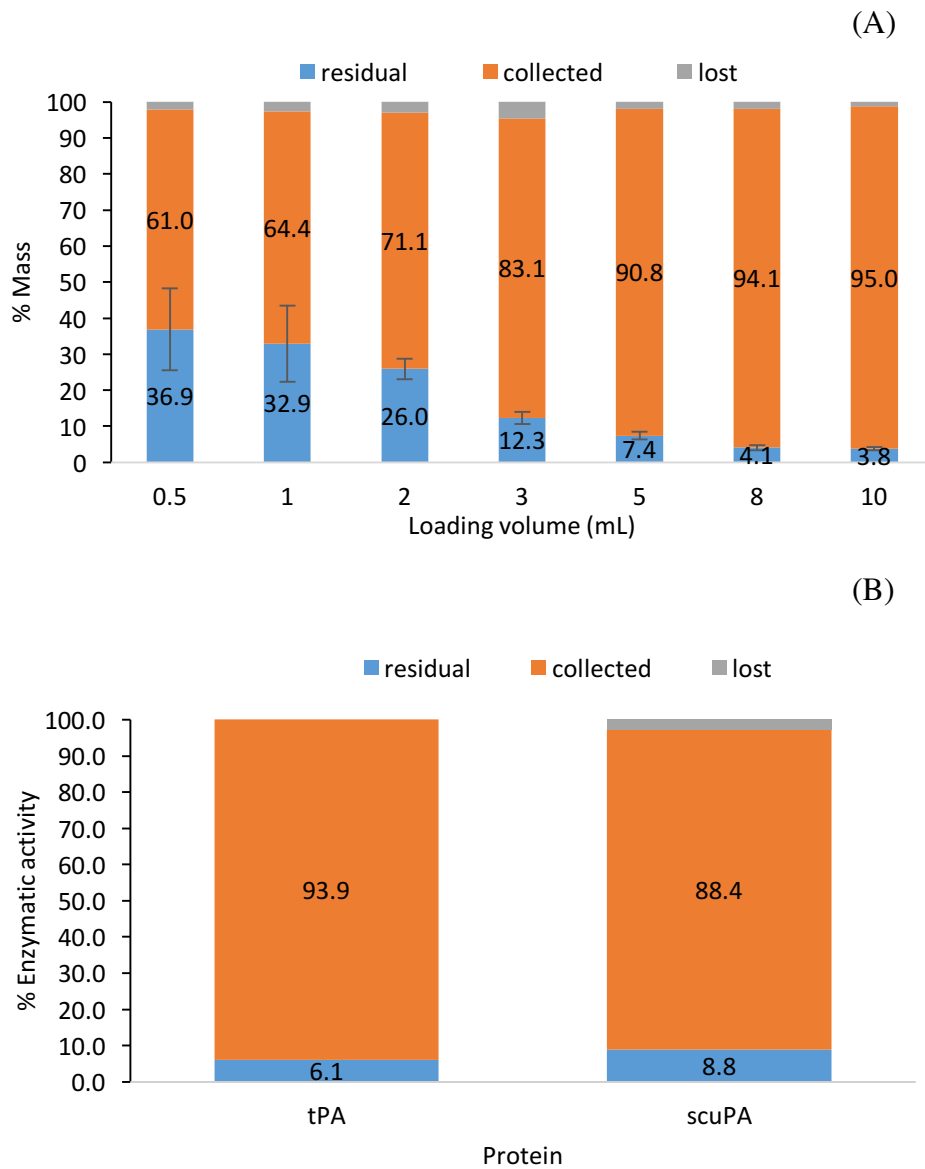


Figure 4.5: (A) Mass (%) of residual DPBS solution in medication reservoir, collected solution in collecting tube, and lost mass ($n=3$), (B) enzymatic activity of tPA and scuPA of the residual solution in the medication reservoir, collected solution in collecting tube, and lost activity ($n=2$).

4.4 CONCLUSION

Reconstituted solutions of lyophilized tPA and optimized scuPA formulation can be delivered to the lungs for the treatment of ISALI by nebulization using VMNs. For inhaled drugs targeted to the lung, a small droplet size and the appropriate adjustment of the nominal dose are both important for obtaining high treatment efficiency and for avoiding the risk of overdose. Therefore, further studies on pulmonary dose delivery using VMNs and mechanical ventilators in animal models can be conducted.

REFERENCES

1. Piazza G, Goldhaber SZ. Management of submassive pulmonary embolism. *Circulation*. 2010;122(11):1124–1129.
2. Idell S. Update on the use of fibrinolytics in pleural disease. *Clin Pulm Med*. 2005;12(3):184–190.
3. Zuckerman DA, Reed MF, Howington JA, Moulton JS. Efficacy of intrapleural tissue-type plasminogen activator in the treatment of loculated parapneumonic effusions. *J Vasc Interv Radiol*. 2009;20(8):1066–1069.
4. Rahman NM, Maskell NA, West A, Teoh R, Arnold A, Mackinlay C, et al. Intrapleural use of tissue plasminogen activator and DNase in pleural infection. *N Engl J Med*. 2011;365(6):518–526.
5. Rogers WJ, Bowlby LJ, Chandra NC, French WJ, Gore JM, Lambrew CT, et al. Treatment of myocardial infarction in the United States (1990 to 1993). Observations from the National Registry of Myocardial Infarction. *Circulation*. 1994;90(4):2103–2114.
6. Albers GW, Amarenco P, Easton JD, Sacco RL, Teal P. Antithrombotic and thrombolytic therapy for ischemic stroke: American College of Chest Physicians evidence-based clinical practice guidelines. *CHEST J*. 2008;133(6_suppl):630S–669S.
7. Saver JL, Fonarow GC, Smith EE, Reeves MJ, Grau-Sepulveda MV, Pan W, et al. Time to treatment with intravenous tissue plasminogen activator and outcome from acute ischemic stroke. *Jama*. 2013;309(23):2480–2488.

8. Xian Y, Smith EE, Zhao X, Peterson ED, Olson DM, Hernandez AF, et al. Strategies used by hospitals to improve speed of tissue-type plasminogen activator treatment in acute ischemic stroke. *Stroke*. 2014;45(5):1387–1395.
9. Marder VJ. Thrombolytic therapy for deep vein thrombosis: potential application of plasmin. *Thromb Res*. 2009;123:S56–S61.
10. Leary SE, Harrod VL, de Alarcon PA, Reiss UM. Low-dose systemic thrombolytic therapy for deep vein thrombosis in pediatric patients. *J Pediatr Hematol Oncol*. 2010;32(2):97.
11. Stringer KA. Tissue plasminogen activator inhibits reactive oxygen species production by macrophages. *Pharmacother J Hum Pharmacol Drug Ther*. 2000;20(4):375–379.
12. Nieuwenhuizen L, De Groot PG, Grutters JC, Biesma DH. A review of pulmonary coagulopathy in acute lung injury, acute respiratory distress syndrome and pneumonia. *Eur J Haematol*. 2009;82(6):413–425.
13. Cornet AD, Hofstra JJ, Vlaar AP, Tuinman PR, Levi M, Girbes AR, et al. Activated protein C attenuates pulmonary coagulopathy in patients with acute respiratory distress syndrome. *J Thromb Haemost*. 2013;11(5):894–901.
14. Gralinski LE, Bankhead A, Jeng S, Menachery VD, Proll S, Belisle SE, et al. Mechanisms of severe acute respiratory syndrome coronavirus-induced acute lung injury. *MBio*. 2013;4(4):e00271–13.

15. Ware LB, Matthay MA. The Acute Respiratory Distress Syndrome. *N Engl J Med*. 2000 May 4;342(18):1334–49.
16. Williams III RO, Idell S. Compositions and methods for administration of an enzyme to a subject's airway. WO2015066664 A2, 2015.
17. Stringer KA, Dunn JS, Gustafson DL. Administration of exogenous tissue plasminogen activator reduces oedema in mice lacking the tissue plasminogen activator gene. *Clin Exp Pharmacol Physiol*. 2004;31(5–6):327–330.
18. Stringer KA, Tobias M, Dunn JS, Campos J, Van Rheen Z, Mosharraf M, et al. Accelerated Dosing Frequency of a Pulmonary Formulation of Tissue Plasminogen Activator is Well-Tolerated in Mice. *Clin Exp Pharmacol Physiol*. 2008;35(12):1454–60.
19. Dunn JS, Nayar R, Campos J, Hybertson BM, Zhou Y, Manning MC, et al. Feasibility of tissue plasminogen activator formulated for pulmonary delivery. *Pharm Res*. 2005;22(10):1700–1707.
20. Idell S, Azghani A, Chen S, Koenig K, Mazar A, Kodandapani L, et al. Intrapleural low-molecular-weight urokinase or tissue plasminogen activator versus single-chain urokinase in tetracycline-induced pleural loculation in rabbits. *Exp Lung Res*. 2007;33(8–9):419–440.
21. Wagers SS, Norton RJ, Rinaldi LM, Bates JH, Sobel BE, Irvin CG. Extravascular fibrin, plasminogen activator, plasminogen activator inhibitors, and airway hyperresponsiveness. *J Clin Invest*. 2004;114(1):104–111.

22. Gunther A, Lubke N, Ermert M, Schermuly RT, Weissmann N, Breithecker A, et al. Prevention of bleomycin-induced lung fibrosis by aerosolization of heparin or urokinase in rabbits. *Am J Respir Crit Care Med.* 2003;168(11):1358–1365.
23. Shetty S, Bdeir K, Cines DB, Idell S. Induction of plasminogen activator inhibitor-1 by urokinase in lung epithelial cells. *J Biol Chem.* 2003;278(20):18124–18131.
24. Hardaway RM, Williams CH, Marvasti M, Farias M, Tseng A, Pinon I, et al. Prevention of adult respiratory distress syndrome with plasminogen activator in pigs. *Crit Care Med.* 1990;18(12):1413–1418.
25. Hardaway RM, Harke H, Williams CH. Fibrinolytic agents: a new approach to the treatment of adult respiratory distress syndrome. *Adv Ther.* 1993;11(2):43–51.
26. Idell S, Allen T, Chen S, Koenig K, Mazar A, Azghani A. Intrapleural activation, processing, efficacy, and duration of protection of single-chain urokinase in evolving tetracycline-induced pleural injury in rabbits. *Am J Physiol-Lung Cell Mol Physiol.* 2007;292(1):L25–L32.
27. Bayat M, Cook AM. Intrapulmonary administration of medications. *J Neurosci Nurs J Am Assoc Neurosci Nurses.* 2004;36(4):231.
28. Hertel SP, Winter G, Friess W. Protein stability in pulmonary drug delivery via nebulization. *Adv Drug Deliv Rev.* 2015;93:79–94.
29. Heinemann L. The failure of exubera: are we beating a dead horse? *J Diabetes Sci Technol.* 2008;2(3):518.

30. Siekmeier R, Scheuch G. Inhaled insulin--does it become reality? *J Physiol Pharmacol Off J Pol Physiol Soc.* 2008;59 Suppl 6:81.
31. Weers JG, Bell J, Chan H-K, Cipolla D, Dunbar C, Hickey AJ, et al. Pulmonary formulations: what remains to be done? *J Aerosol Med Pulm Drug Deliv.* 2010;23 Suppl 2:S5.
32. Manning MC, Patel K, Borchardt RT. Stability of protein pharmaceuticals. *Pharm Res.* 1989;6(11):903–918.
33. Hageman MJ. The role of moisture in protein stability. *Drug Dev Ind Pharm.* 1988;14(14):2047–2070.
34. Pearlman R, Nguyen T. Pharmaceutics of protein drugs. *J Pharm Pharmacol.* 1992;44:178.
35. McGoff P, Scher DS. Solution formulation of proteins/peptides. *Protein Formul Deliv.* 2008;133–51.
36. Costantino HR, Langer R, Klibanov AM. Moisture-induced aggregation of lyophilized insulin. *Pharm Res.* 1994;11(1):21–29.
37. Carpenter JF, Chang BS, Garzon-Rodriguez W, Randolph TW. Rational design of stable lyophilized protein formulations: theory and practice. In: *Rational design of stable protein formulations.* Springer; 2002. p. 109–133.
38. Wang W. Lyophilization and development of solid protein pharmaceuticals. *Int J Pharm.* 2000;203(1–2):1–60.

39. Shalaev EY, Wang W, Gatlin LA. Rational choice of excipients for use in lyophilized formulations. In: Protein Formulation and Delivery. Informa Healthcare New York, NY; 2008. p. 197–217.
40. Coldstream Laboratories, Inc. Formulation development report: laboratory scale lyophilization feasibility study for scuPA for Injection, 3.1 mg/vial. 2014.
41. Hertel S. Pulmonary delivery of pharmaceutical proteins by means of vibrating mesh nebulization. Ludwig-Maximilians-Universität München; 2014.
42. ABL, Inc. Determination of urokinase-type plasminogen activator (uPA) activity in SRI project #M097-14 P22204.026 scuPA dosing study samples. 2014.
43. Baheti A, Kumar L, Bansal AK. Excipients used in lyophilization of small molecules. *J Excip Food Chem.* 2010;1(1):41–54.
44. Hsu CC, Ward CA, Pearlman R, Nguyen HM, Yeung DA, Curley JG. Determining the optimum residual moisture in lyophilized protein pharmaceuticals. *Dev Biol Stand.* 1992;74:255.
45. Hageman MJ. In *Stability of Protein Pharmaceuticals, Part A: Chemical and Physical Pathways of Protein Degradation.* In: Water sorption and solid-state stability of proteins: New York; 1992. p. 273–309.
46. Lai MC, Topp EM. Solid-state chemical stability of proteins and peptides. *J Pharm Sci.* 1999;88(5):489–500.

47. Schoeffel RE, Anderson SD, Altounyan REC. Bronchial hyperreactivity in response to inhalation of ultrasonically nebulised solutions of distilled water and saline. *Br Med J (Clin Res Ed)*. 1981;283(6302):1285–7.
48. Portel L, Tunon de Lara JM, Vernejoux JM, Weiss I, Taytard A. Osmolarity of solutions used in nebulization. *Rev Mal Respir*. 1998;15(2):191.
49. Chan H-K, Chan JGY, Kwok PCL, Young PM, Traini D. Mannitol delivery by vibrating mesh nebulisation for enhancing mucociliary clearance. *J Pharm Sci*. 2011;100(7):2693–702.
50. Dhand R. Nebulizers that use a vibrating mesh or plate with multiple apertures to generate aerosol. *Respir Care*. 2002;47(12):1406.
51. Wood GC, Boucher BA. Aerosolized antimicrobial therapy in acutely ill patients. *Pharmacother J Hum Pharmacol Drug Ther*. 2000;20(2):166–181.
52. Coates AL. Guiding aerosol deposition in the lung. *N Engl J Med*. 2008;358(3):304–305.
53. Michalopoulos A, Metaxas I, Falagas ME. Aerosol delivery of antimicrobial agents during mechanical ventilation: current practice and perspectives. *Curr Drug Deliv*. 2011;8(2):208–212.
54. Uchenna Agu R, Ikechukwu Ugwoke M, Armand M, Kinget R, Verbeke N. The lung as a route for systemic delivery of therapeutic proteins and peptides. *Respir Res*. 2001;2:198.

55. Niven RW. Delivery of biotherapeutics by inhalation aerosol. *Crit Rev Ther Drug Carrier Syst.* 1995;12(2–3):151–231.
56. Lass JS, Sant A, Knoch M. New advances in aerosolised drug delivery: vibrating membrane nebuliser technology. *Expert Opin Drug Deliv.* 2006;3(5):693–702.
57. Niven RW, Ip AY, Mittelman S, Prestrelski SJ, Arakawa T. Some factors associated with the ultrasonic nebulization of proteins. *Pharm Res.* 1995;12(1):53–59.
58. Fink JB, Schmidt D, Power J. Comparison of a nebulizer using a novel aerosol generator with a standard ultrasonic nebulizer designed for use during mechanical ventilation. American Thoracic Society 97th International Conference, San Francisco, CA; 2001.
59. Elhissi AMA, Taylor KMG. Delivery of liposomes generated from proliposomes using air-jet, ultrasonic, and vibrating-mesh nebulisers. *J Drug Deliv Sci Technol.* 2005;15(4):261–5.
60. Ghazanfari T, Elhissi AM, Ding Z, Taylor KM. The influence of fluid physicochemical properties on vibrating-mesh nebulization. *Int J Pharm.* 2007;339(1):103–111.
61. Hertel S, Pohl T, Friess W, Winter G. Prediction of protein degradation during vibrating mesh nebulization via a high throughput screening method. *Eur J Pharm Biopharm.* 2014;87(2):386–394.

62. Waldrep JC, Dhand R. Advanced nebulizer designs employing vibrating mesh/aperture plate technologies for aerosol generation. *Curr Drug Deliv.* 2008;5(2):114–119.
63. Watts AB, McConville JT, Williams RO. Current Therapies and Technological Advances in Aqueous Aerosol Drug Delivery. *Drug Dev Ind Pharm.* 2008;34(9):913–22.
64. Knoch M, Keller M. The customised electronic nebuliser: a new category of liquid aerosol drug delivery systems. *Expert Opin Drug Deliv.* 2005;2(2):377–90.
65. Technology Review and Performance Report for the Aeroneb® Professional Nebulizer system. Aerogen, Inc.; 2002.

Appendices

Appendix A.: Proteins in perfluorocarbon suspensions

A.1tPA in perfluorocarbon suspensions for endotracheal tube drug delivery

A.1.1 MATERIALS AND METHODS

A.1.1.1 Materials

Human recombinant tPA (Cathflo® Activase® was purchased from Genentech, Inc., South San Francisco, CA). scuPA (Lot No. 071407A, purity 73% activity), 3.5 mg/mL was kindly obtained from UTHSCT (Tyler, TX). Perfluorocarbons, Perfluorodecalin (PFD) and Perflubron (PFB), were purchased from FluoroMed, L.P. (Round Rock, TX). 10 mm endotracheal (ET) tube.

A.1.1.2 Methods

tPA was suspended in two types of PFCs (PFD and PFB) (0.2 mg/mL). Each suspension was kept in 5°C refrigerator for 24 hours, and then left it at 25°C for 2 hours. The suspensions were placed at 37°C in an incubator for 15 minutes and then injected into the ET tube at 37°C. The passed-tube sample was collected and stored at 37°C for another 30 minutes. Sample was kept at 5°C until analyzed. Enzymatic activity was tested by ELISA kit (Molecular Innovations, Inc., Novi, MI). Each sample was run in duplicate.

A.1.2 RESULTS

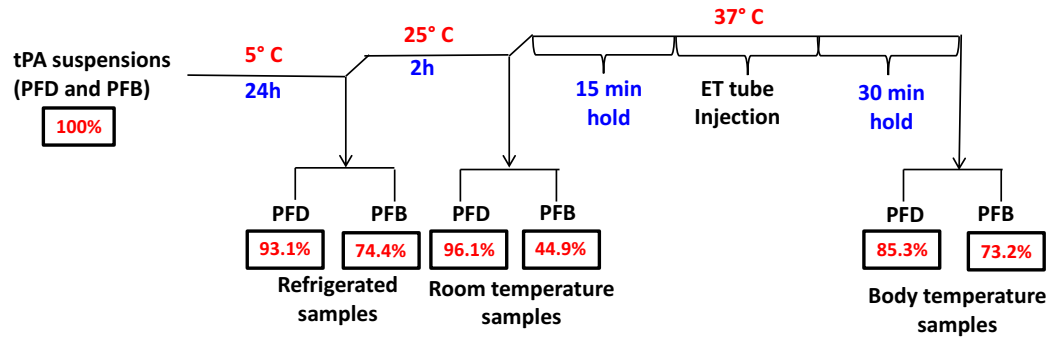


Figure A.1: Enzyme activity of tPA suspensions following the endotracheal tube delivery

A.2 scuPA in perfluorocarbon suspensions

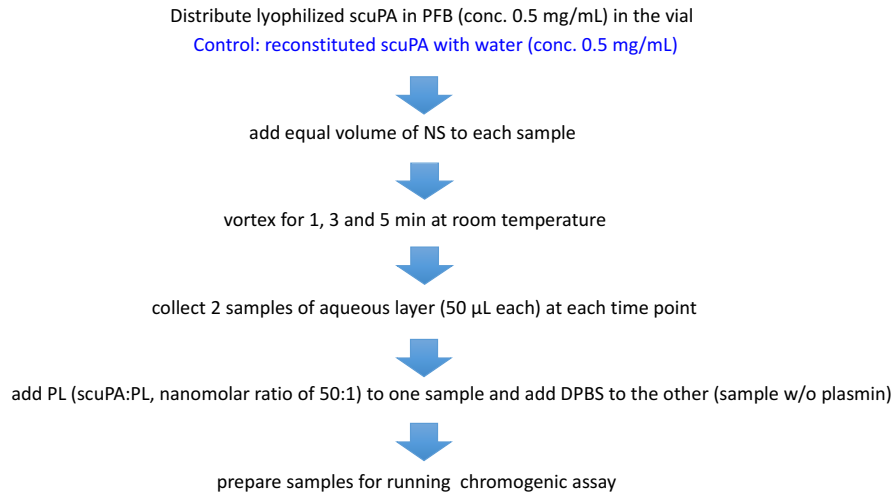
A.2.1 MATERIALS AND METHODS

A.2.1.1 Material

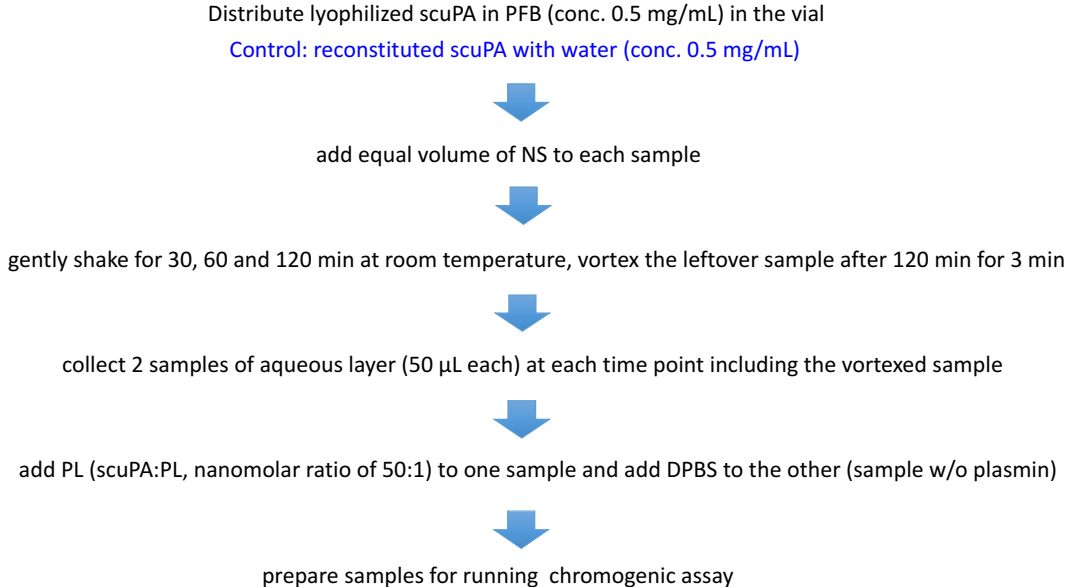
scuPA (Lot No. 071407A, purity 73% activity), 3.5 mg/mL was kindly obtained from UTHSCT (Tyler, TX). PFCs please see A.1.

A.2.1.2 Methods

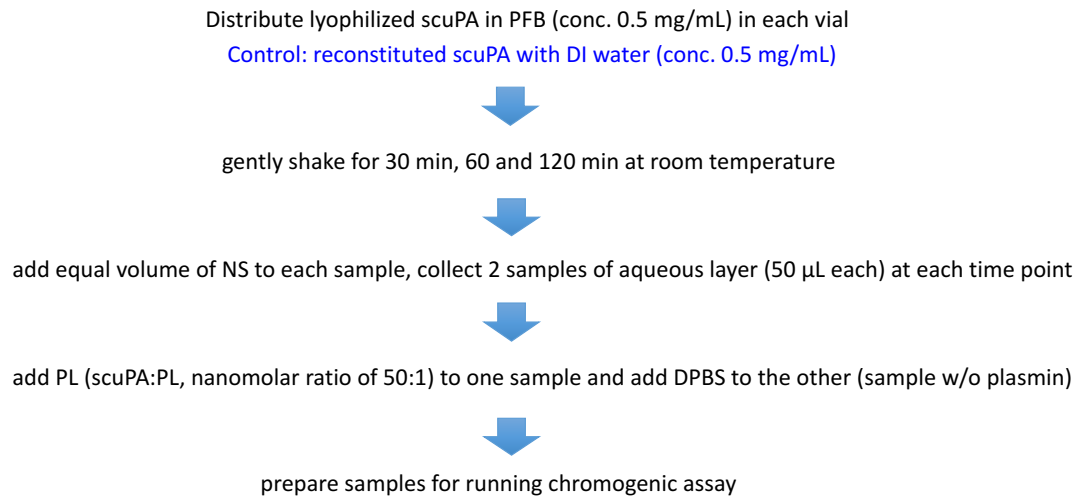
A.2.1.2.1 Vortex mixing of scuPA in PFB suspension



A.2.1.2.2 Gentle mixing of scuPA in PFB suspension



A.2.1.2.3 Stability of scuPA in PFB suspension



A.2.2 RESULTS

A.2.2.1 Effect of vortex mixing and gentle shaking on enzymatic activity

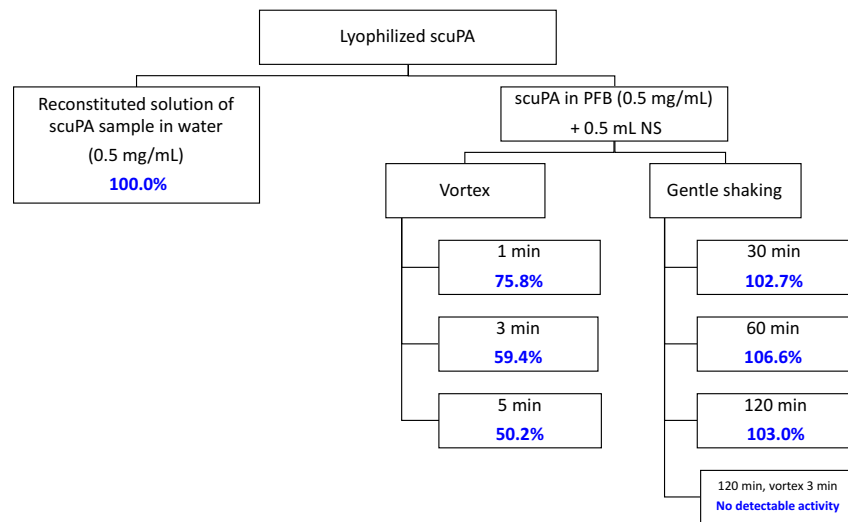


Figure A.2: Activity of scuPA in PFB suspensions following the vortex and gentle mixing

B.1.2.2 Stability of scuPA in PFB suspension

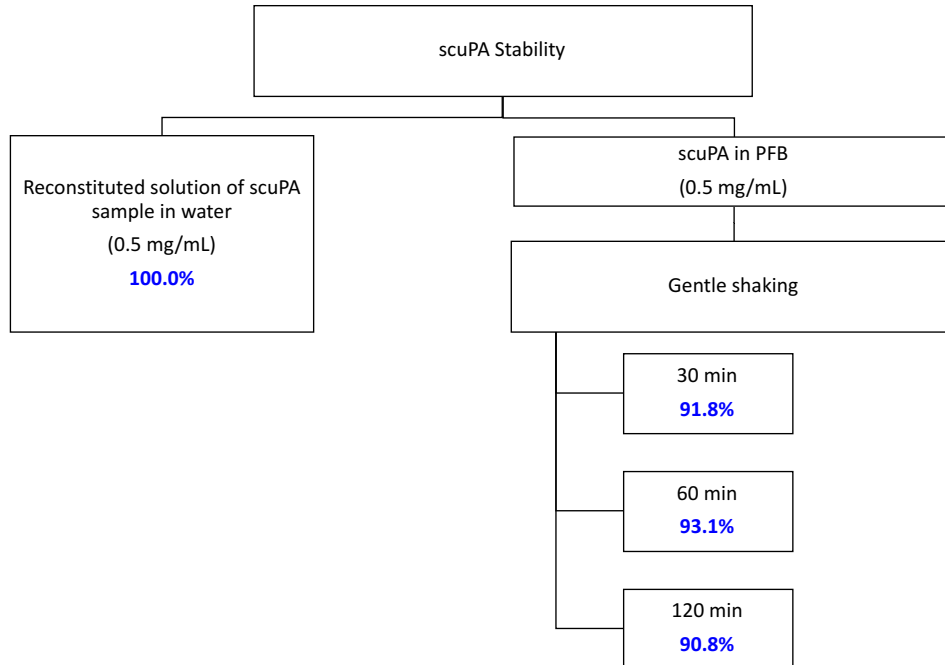


Figure A.3: Activity of scuPA in PFB suspensions following gentle shaking for 30, 60 and 120 minutes

Appendix B.: Delivery of tPA and scuPA into a cold 1 gallon plastic bag with vibrating mesh nebulizer and mechanical ventilator

B.1 METHOD

Setting:



Figure B.1: Ventilation circuit setting

Experimental design:

- Nebulization of 4 mg of the enzyme in 8 ml under
- ventilation into a zip 1 gallon plastic bag .
- Tidal volume 100 ml
- Three work stations (three ventilators) with different settings

Colors (1=blue, 2=green, 3=red) correspond to the symbols at box-plots:

#	Oxygen, %	Humidifier	Repeats	
			tPA	scuPA*
• 1	21	+	2	2
• 2	21	-	2	2
• 3	100	+	2	2

* An additional Exp (n=1 for each Station, scuPA) was run with 10 ml PBS added to the bag prior to nebulization in an attempt to increase yield of scuPA in the bag.



Figure B.2: Experimental design

Ventilator's Settings for Stations



Figure B.3: Mechanical ventilator parameters

Three Samples were Collected from Each Run

1. **“NEU”** – an aliquot prior to the nebulizer
2. **“WASHES”** – an aliquot of 200 ml (4x50 ml) saline, which was used to wash all the ventilator tubes and combined.
3. **“BAG”** – an aliquot from the plastic zipped bag.

Working hypothesis:

Protein: “NEU” = “WASHES” + “BAG”
Activity: “NEU” ≥ “WASHES” + “BAG”



Figure B.4: Samples collection

B.2 RESULTS

Analysis: *Amidolytic Activity & Protein Concentration (BCA)* were measured in the Samples and expressed as Box Plots (separate for tPA and scuPA)

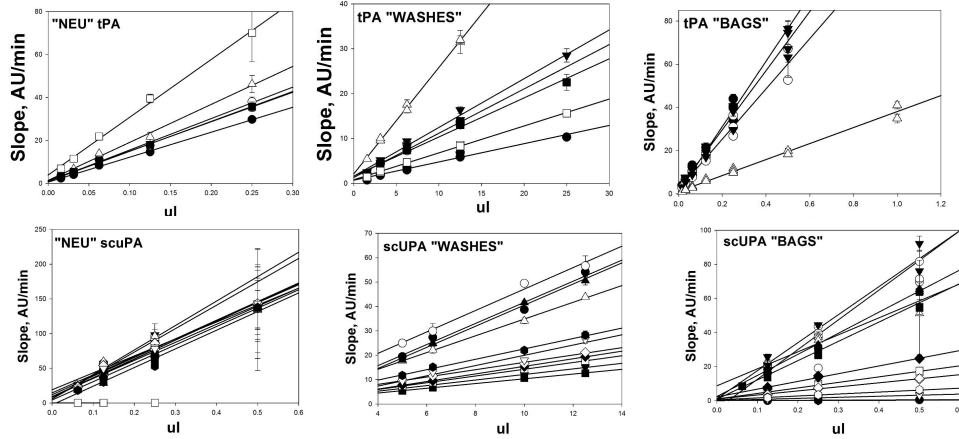


Figure B.5: Enzymatic activity and protein concentration

1. Nebulization results in a decrease in the protein concentration in the bag.

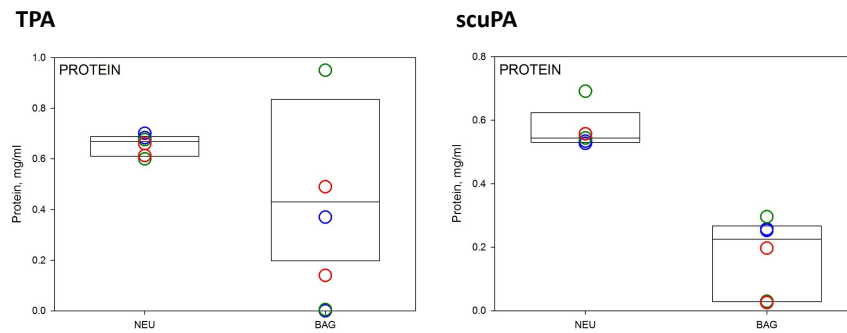


Figure B.6: Nebulization results in a decrease in the protein concentration in the bag

2. Only a fraction of the initial enzymatic activity present in the bags and tube washes

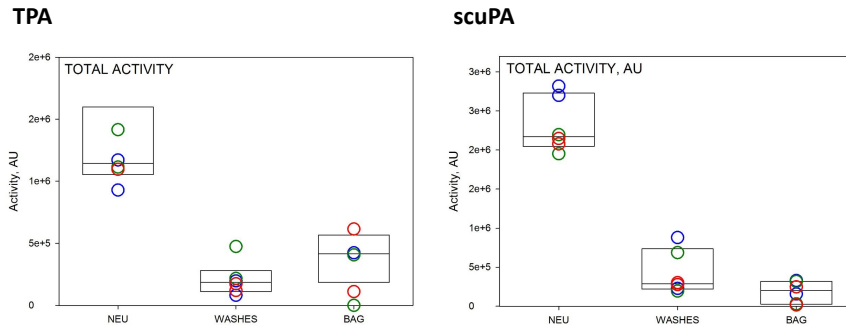


Figure B.7: A fraction of the initial enzymatic presents in the bag and tube washes

3. Only a fraction of the activity was delivered to the bag. Significant activity has “disappeared”

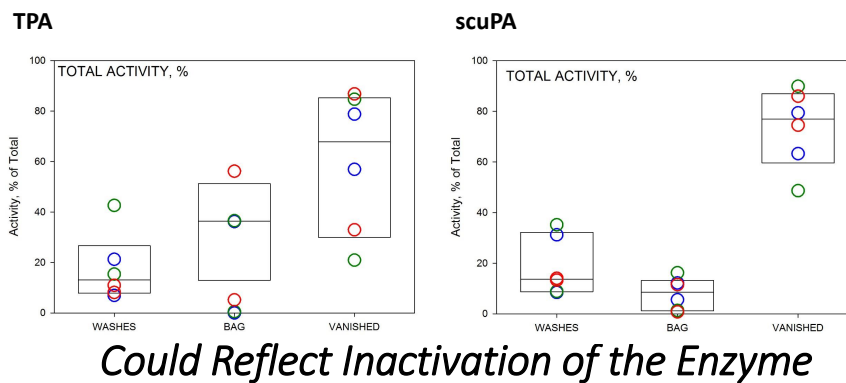


Figure B.8: A fraction of the enzymatic delivered to the bag

4. Nebulization results in a decrease in the "concentration" of the enzymatic activity

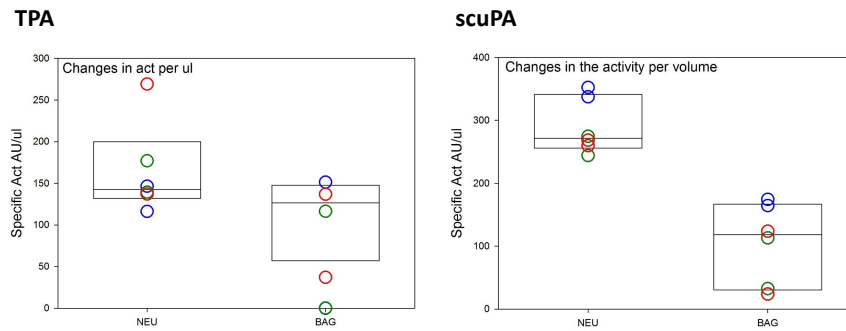


Figure B.9: Enzymatic activity of proteins from nebulization

5. Neither nebulization nor 100% oxygen (red) affect dramatically specific activity of the enzymes

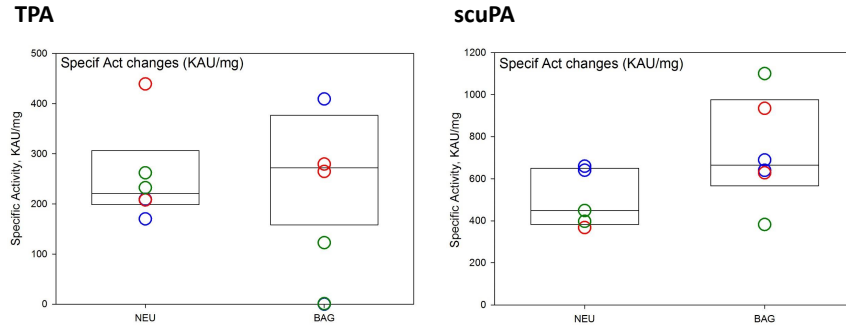


Figure B.10: Effect of nebulization and 100% oxygen on specific activity of the proteins

9. Changes in the Specific Activity due to Nebulization

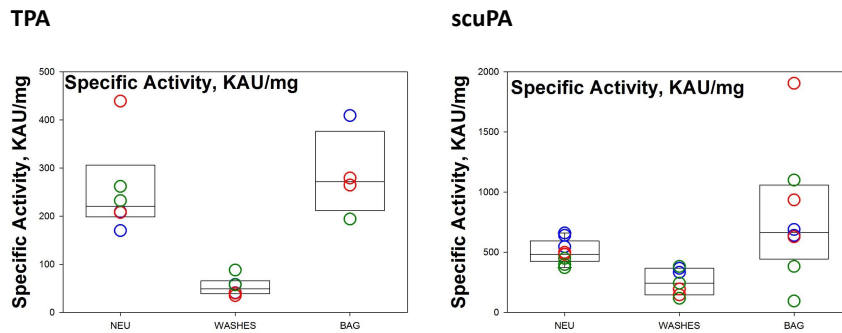


Figure B.13: Changes in specific activity of proteins due to nebulization

Conclusions

- There was no significant decrease in the specific activity of the enzymes due to nebulization
- There was no significant inactivation of the enzymes by 100% oxygen
- There was a decrease in the enzyme concentration in the bag
- Only a small fraction of the activity&protein was detected in the bag
- Significant part of activity and protein was lost during nebulization. If the losses were associated with the enzymes escaping the ventilation circuit, that may be harmful to the personnel.
- An additional experiment(s) may be needed to determine the routes of the loss of the enzymes.
- Washing (200 ml) ventilator tubes after animal nebulization and following assessment of protein+activity could help in estimation of the delivery efficacy.

Figure B.14: Effects of nebulization using vibrating mesh nebulizer and mechanical ventilator on enzymatic activity of tPA and scuPA

References

CHAPTER 1 REFERENCES

1. Shaika RH, Sial AA. Stability of pharmaceutical formulations. *Pak J Pharm Sci.* 1996;9(2):83–86.
2. Guo Y, Shalaev E, Smith S. Solid-state analysis and amorphous dispersions in assessing the physical stability of pharmaceutical formulations. *TrAC Trends Anal Chem.* 2013;49:137.
3. Huynh-Ba K. Handbook of stability testing in pharmaceutical development: regulations, methodologies, and best practices. 1. Aufl. New York: Springer; 2009.
4. Bajaj S, Singla D, Sakhuja N. Stability Testing of Pharmaceutical Products. *J Appl Pharm Sci.* 2012;2(3):129.
5. Wang W. Protein aggregation and its inhibition in biopharmaceutics. *Int J Pharm.* 2005;289(1–2):1–30.
6. Briscoe CJ, Hage DS. Factors affecting the stability of drugs and drug metabolites in biological matrices. *Bioanalysis.* 2009;1(1):205.
7. Asahara K, Yamada H, Yoshida S. Stability of human insulin in solutions containing sodium bisulfite. *Chem Pharm Bull (Tokyo).* 1991;39(10):2662–6.

8. Helm VJ, Müller BW. Stability of the synthetic pentapeptide thymopentin in aqueous solution: Effect of pH and buffer on degradation. *Int J Pharm.* 1991;70(1):29–34.
9. Oliyai C, Patel JP, Carr L, Borchardt RT. Chemical pathways of peptide degradation. VII. Solid state chemical instability of an aspartyl residue in a model hexapeptide. *Pharm Res.* 1994;11(6):901–908.
10. Paborji M, Pochopin NL, Coppola WP, Bogardus JB. Chemical and physical stability of chimeric L6, a mouse-human monoclonal antibody. *Pharm Res.* 1994;11(5):764.
11. Akers MJ, Milton N, Byrn SR, Nail SL. Glycine crystallization during freezing: the effects of salt form, pH, and ionic strength. *Pharm Res.* 1995;12(10):1457–1461.
12. Melveger AJ, Huynh-Ba K. Critical Regulatory Requirements for a Stability Program. In: *Handbook of stability testing in pharmaceutical development: regulations, methodologies, and best practices.* 2nd ed. New York: Springer; 2009. p. 9–19.
13. <1150> Pharmaceutical Stability. In: *US Pharmacopeia 35-NF30* [Internet]. Pharmacopeial Convention, Rockville, MD.; 2012. Available from: www.uspnf.com
14. Volkin DB, Middaugh CR. The effect of temperature on protein structure. In: *Stability of protein pharmaceuticals part A chemical and physical pathways of protein degradation.* New York: Plenum Press; 1992. p. 215–47.

15. Yoshioka S, Stella VJ, NetLibrary, Inc. Stability of drugs and dosage forms. New York: Kluwer Academic; 2002.
16. Munjal M, Stodghill SP, ElSohly MA, Repka MA. Polymeric systems for amorphous Δ^9 -tetrahydrocannabinol produced by a hot-melt method. Part I: Chemical and thermal stability during processing. *J Pharm Sci.* 2006;95(8):1841–1853.
17. Munjal M, ElSohly MA, Repka MA. Chemical stabilization of a Delta9-tetrahydrocannabinol prodrug in polymeric matrix systems produced by a hot-melt method: role of microenvironment pH. *AAPS PharmSciTech.* 2006;7(3):71.
18. Munjal M, Elsohly MA, Repka MA. Polymeric systems for amorphous Delta9-tetrahydrocannabinol produced by a hot-melt method. Part II: Effect of oxidation mechanisms and chemical interactions on stability. *J Pharm Sci.* 2006;95(11):2473.
19. Lai MC, Topp EM. Solid-state chemical stability of proteins and peptides. *J Pharm Sci.* 1999;88(5):489–500.
20. Oliyai C, Patel JP, Carr L, Borchardt RT. Solid state chemical instability of an asparaginylyl residue in a model hexapeptide. *J Pharm Sci Technol.* 1994;48(3):167.
21. Karel M, Yong S. Autoxidation-initiated reactions in foods. In: Water activity: influences on food quality. 1981. p. 511–29.

22. Manning MC, Patel K, Borchardt RT. Stability of protein pharmaceuticals. *Pharm Res.* 1989;6(11):903–918.
23. Costantino HR, Langer R, Klivanov AM. Moisture-induced aggregation of lyophilized insulin. *Pharm Res.* 1994;11(1):21–29.
24. Franks F. Protein destabilization at low temperatures. *Adv Protein Chem.* 1995;46:105.
25. Hertel S, Pohl T, Friess W, Winter G. That’s cool!--Nebulization of thermolabile proteins with a cooled vibrating mesh nebulizer. *Eur J Pharm Biopharm.* 2014 Jul;87(2):357.
26. Ellin RI, Henry Wills J. Oximes Antagonistic to Inhibitors of Cholinesterase: Part I. *J Pharm Sci.* 1964;53(9):995–1007.
27. Deshpande AD, Baheti KG, Chatterjee NR. Degradation of b-lactam antibiotics. *Curr Sci.* 2004;87:1684–1695.
28. Chang BS, Hershenson S. Practical approaches to protein formulation development. In: *Rational design of stable protein formulations: theory and practice.* New York: Kluwer Academic; 2002. p. 1–23.
29. Hertel SP, Winter G, Friess W. Protein stability in pulmonary drug delivery via nebulization. *Adv Drug Deliv Rev.* 2015;93:79–94.

30. Marsac PJ, Rumondor AC, Nivens DE, Kestur US, Stanciu L, Taylor LS. Effect of temperature and moisture on the miscibility of amorphous dispersions of felodipine and poly (vinyl pyrrolidone). *J Pharm Sci.* 2010;99(1):169–185.
31. Flores-Fernández GM, Solá RJ, Griebenow K. The relation between moisture-induced aggregation and structural changes in lyophilized insulin. *J Pharm Pharmacol.* 2009;61(11):1555–61.
32. Jain NK, Roy I. Role of trehalose in moisture-induced aggregation of bovine serum albumin. *Eur J Pharm Biopharm.* 2008;69(3):824–34.
33. Sharma V, Klibanov A. Moisture-Induced Aggregation of Lyophilized DNA and its Prevention. *Pharm Res.* 2007;24(1):168–75.
34. Schwendeman SP, Costantino HR, Gupta RK, Siber GR, Klibanov AM, Langer R. Stabilization of Tetanus and Diphtheria Toxoids Against Moisture-Induced Aggregation. *Proc Natl Acad Sci U S A.* 1995;92(24):11234–8.
35. Jain N, Roy I. Accelerated Stability Studies for Moisture-Induced Aggregation of Tetanus Toxoid. *Pharm Res.* 2011;28(3):626–39.
36. Boccardi G. Oxidative susceptibility testing. Taylor& Francis; 2005.

37. Alsante KM, Ando A, Brown R, Ensing J, Hatajik TD, Kong W, et al. The role of degradant profiling in active pharmaceutical ingredients and drug products. *Adv Drug Deliv Rev.* 2007;59(1):29–37.
38. Camacho W, Karlsson S. Assessment of thermal and thermo-oxidative stability of multi-extruded recycled PP, HDPE and a blend thereof. *Polym Degrad Stab.* 2002;78(2):385–91.
39. Shirwaikar A, Srinivasan K, Alex J, Prabu S, Mahalaxmi R, Kumar R, et al. Stability of proteins in aqueous solution and solid state. *Indian J Pharm Sci.* 2006;68(2):154–63.
40. Lai MC, Topp EM. Solid-state chemical stability of proteins and peptides. *J Pharm Sci.* 1999;88(5):489–500.
41. Crowley MM, Zhang F, Repka MA, Thumma S, Upadhye SB, Kumar Battu S, et al. Pharmaceutical applications of hot-melt extrusion: part I. *Drug Dev Ind Pharm.* 2007;33(9):909–926.
42. Gidalevitz D, Huang Z, Rice SA. Protein Folding at the Air-Water Interface Studied with X-Ray Reflectivity. *Proc Natl Acad Sci U S A.* 1999;96(6):2608–11.
43. Maa Y-F, Hsu CC. Protein denaturation by combined effect of shear and air-liquid interface. *Biotechnol Bioeng.* 1997;54(6):503–12.

44. Bruce CD. Recrystallization of guaifenesin from hot-melt extrudates containing Acryl-EZE or Eudragit L100-55. University of Texas at Austin; 2008.
45. Beyler CL, Hirschler MM. Thermal decomposition of polymers. *SFPE Handb Fire Prot Eng.* 2002;2:110–131.
46. Güres S, Kleinebudde P. Dissolution from solid lipid extrudates containing release modifiers. *Int J Pharm.* 2011;412(1):77–84.
47. DiNunzio JC, Martin, Z.F.C., McGinity JW. Melting extrusion. In: Williams III RO, Watts AB Miller, DA, editors. *Formulating poorly water soluble drugs.* Springer, New York, NY; 2012. p. 311–62.
48. El-Gendy NA. Pharmaceutical plasticizers for drug delivery systems. *Curr Drug Deliv.* 2012 Mar;9(2):148.
49. Ghebremeskel A, Vemavarapu C, Lodaya M. Use of surfactants as plasticizers in preparing solid dispersions of poorly soluble API: stability testing of selected solid dispersions. *Pharm Res.* 2006;23(8):1928–36.
50. Costantino HR, Andya JD, Nguyen P-A, Dasovich N, Sweeney TD, Shire SJ, et al. Effect of mannitol crystallization on the stability and aerosol performance of a spray-dried pharmaceutical protein, recombinant humanized anti-IgE monoclonal antibody. *J Pharm Sci.* 1998;87(11):1406–1411.

51. Cavatur R, Vemuri N, Pyne A, Chrzan Z, Toledo-Velasquez D, Suryanarayanan R. Crystallization behavior of mannitol in frozen aqueous solutions. *Pharm Res.* 2002;19(6):894–900.
52. Al-Hussein A, Gieseler H. The effect of mannitol crystallization in mannitol-sucrose systems on LDH stability during freeze-drying. *J Pharm Sci.* 2012;101(7):2534–44.
53. Carpenter JF, Chang BS, Garzon-Rodriguez W, Randolph TW. Rational design of stable lyophilized protein formulations: theory and practice. In: *Rational design of stable protein formulations.* Springer; 2002. p. 109–133.
54. Yu L. Amorphous pharmaceutical solids: preparation, characterization and stabilization. *Adv Drug Deliv Rev.* 2001;48(1):27–42.
55. Kolter K, Karl M, Gryczke A. Hot-melt extrusion with BASF pharma polymers: extrusion compendium. 2nd ed. 2012.
56. Pikal MJ. Mechanisms of protein stabilization during freeze-drying storage: the relative importance of thermodynamic stabilization and glassy state relaxation dynamics. In: *Freeze-drying/lyophilization of pharmaceutical and biological products.* New York: Marcel Dekker; 1999. p. 198–232.

57. Frokjaer S, Otzen DE. Protein drug stability: a formulation challenge. *Nat Rev Drug Discov.* 2005;4(4):298–306.
58. Yang W, Owens III DE, Williams III RO. Pharmaceutical cryogenic technologies. In: *Formulating poorly water soluble drugs.* New York: Springer; p. 443–500.
59. Carstensen JT, Rhodes CT. *Drug stability: principles and practices.* 3rd ed., and expanded. New York: Marcel Dekker; 2000. (Drugs and the pharmaceutical sciences; vol. 107).
60. Hancock BC, Shamblin SL, Zografi G. Molecular mobility of amorphous pharmaceutical solids below their glass transition temperatures. *Pharm Res.* 1995;12(6):799–806.
61. Shah N, Sandhu H, Choi DS, Kalb O, Page S, Wytttenbach N. Structured development approach for amorphous systems. In: *Formulating poorly water soluble drugs.* New York, NY: AAPS Press; 2012. p. 267–310.
62. Bhardwaj SP, Arora KK, Kwong E, Templeton A, Clas S-D, Suryanarayanan R. Correlation between Molecular Mobility and Physical Stability of Amorphous Itraconazole. *Mol Pharm.* 2013;10(2):694–700.

63. McNally EJ, Hastedt JE. Development of Drug Products: Similarities and Differences Between Protein Biologics and Small Synthetic Molecules. In: Protein Formulation and Delivery. 2nd ed. Informa Healthcare New York, NY; 2007. p. 332.
64. Manning MC, Chou DK, Murphy BM, Payne RW, Katayama DS. Stability of protein pharmaceuticals: an update. *Pharm Res.* 2010;27(4):544–575.
65. Fang W-J, Qi W, Kinzell J, Prestrelski S, Carpenter J. Effects of excipients on the chemical and physical stability of glucagon during freeze-drying and storage in dried formulations. *Pharm Res.* 2012;29(12):3278–91.
66. Pikal M, Rigsbee D. The stability of insulin in crystalline and amorphous solids: observation of greater stability for the amorphous form. *Pharm Res.* 1997;14(10):1379–87.
67. Hovorka SW, Schöneich C. Oxidative degradation of pharmaceuticals: Theory, mechanisms and inhibition. *J Pharm Sci.* 2001;90(3):253–69.
68. Tarelli E, Corran PH. Ammonia cleaves polypeptides at asparagine proline bonds. *J Pept Res.* 2003;62(6):245–251.
69. Chu G, Chelius D, Xiao G, Khor H, Coulibaly S, Bondarenko P. Accumulation of Succinimide in a Recombinant Monoclonal Antibody in Mildly Acidic Buffers Under Elevated Temperatures. *Pharm Res.* 2007;24(6):1145–56.

70. Ueno K, Ueda T, Sakai K, Abe Y, Hamasaki N, Okamoto M, et al. Evidence for a novel racemization process of an asparaginyl residue in mouse lysozyme under physiological conditions. *Cell Mol Life Sci.* 2005;62(2):199–205.
71. Lan X, Liu P, Xia S, Xia W, Jia C, Mukunzi D, et al. Temperature effect on the non-volatile compounds of Maillard reaction products derived from xylose–soybean peptide system: Further insights into thermal degradation and cross-linking. *Food Chem.* 2010;120(4):967–72.
72. Hawe A, Friess W. Development of HSA-free formulations for a hydrophobic cytokine with improved stability. *Eur J Pharm Biopharm.* 2008;68(2):169–82.
73. Carpenter J, Pikal M, Chang B, Randolph T. Rational design of stable lyophilized protein formulations: some practical advice. *Pharm Res.* 1997;14(8):969–75.
74. Pikal MJ, Dellerman KM, Roy ML, Riggin RM. The effects of formulation variables on the stability of freeze-dried human growth hormone. *Pharm Res.* 1991;8(4):427–436.
75. Strickley RG, Visor GC, Lin LH, Gu L. An unexpected pH effect on the stability of moexipril lyophilized powder. *Pharm Res.* 1989;6(11):971.
76. Pearlman R, Nguyen T. Pharmaceutics of protein drugs. *J Pharm Pharmacol.* 1992;44:178.

77. Geller DE. The science of aerosol delivery in cystic fibrosis. *Pediatr Pulmonol.* 2008 Sep 1;43(S9):S5–17.
78. Pilcer G, Amighi K. Formulation strategy and use of excipients in pulmonary drug delivery. *Int J Pharm.* 2010;392(1):1–19.
79. Maillet A, Guilleminault L, Lemarié E, Lerondel S, Azzopardi N, Montharu J, et al. The Airways, a Novel Route for Delivering Monoclonal Antibodies to Treat Lung Tumors. *Pharm Res.* 2011;28(9):2147–56.
80. Fathe K, Ferrati S, Moraga-Espinoza D, Yazdi A, Smyth HDC. Inhaled Biologics: From Preclinical to Product Approval. *Curr Pharm Des.* 2016;22(17):2501.
81. Niven RW, Prestrelski SJ, Treuheit MJ, Ip AY, Arakawa T. Protein nebulization II. Stabilization of G-CSF to air-jet nebulization and the role of protectants. *Int J Pharm.* 1996;127(2):191–201.
82. Uchenna Agu R, Ikechukwu Ugwoke M, Armand M, Kinget R, Verbeke N. The lung as a route for systemic delivery of therapeutic proteins and peptides. *Respir Res.* 2001;2:198.
83. Niven RW. Delivery of biotherapeutics by inhalation aerosol. *Crit Rev Ther Drug Carrier Syst.* 1995;12(2–3):151–231.

84. Niven RW, Ip AY, Mittelman S, Prestrelski SJ, Arakawa T. Some factors associated with the ultrasonic nebulization of proteins. *Pharm Res.* 1995;12(1):53–59.
85. Lass JS, Sant A, Knoch M. New advances in aerosolised drug delivery: vibrating membrane nebuliser technology. *Expert Opin Drug Deliv.* 2006;3(5):693–702.
86. Fink JB, Schmidt D, Power J. Comparison of a nebulizer using a novel aerosol generator with a standard ultrasonic nebulizer designed for use during mechanical ventilation. American Thoracic Society 97th International Conference, San Francisco, CA; 2001.
87. Elhissi AMA, Taylor KMG. Delivery of liposomes generated from proliposomes using air-jet, ultrasonic, and vibrating-mesh nebulisers. *J Drug Deliv Sci Technol.* 2005;15(4):261–5.
88. Hertel S, Pohl T, Friess W, Winter G. Prediction of protein degradation during vibrating mesh nebulization via a high throughput screening method. *Eur J Pharm Biopharm.* 2014;87(2):386–394.
89. Waldrep JC, Dhand R. Advanced nebulizer designs employing vibrating mesh/aperture plate technologies for aerosol generation. *Curr Drug Deliv.* 2008;5(2):114–119.

90. Watts AB, McConville JT, Williams RO. Current Therapies and Technological Advances in Aqueous Aerosol Drug Delivery. *Drug Dev Ind Pharm.* 2008;34(9):913–22.
91. Knoch M, Keller M. The customised electronic nebuliser: a new category of liquid aerosol drug delivery systems. *Expert Opin Drug Deliv.* 2005;2(2):377–90.

CHAPTER 2 REFERENCES

- [1] S.E. Marriner, D.L. Morris, B. Dickson and J.A. Bogan, *Pharmacokinetics of albendazole in man*, *Eur. J. Clin. Pharmacol.* 30 (1986), pp. 705–708.
- [2] M. Lindenberg, S. Kopp and J.B. Dressman, *Classification of orally administered drugs on the World Health Organization Model list of Essential Medicines according to the biopharmaceutics classification system*, *Eur. J. Pharm. Biopharm.* 58 (2004), pp. 265–278.
- [3] H. Jung, L. Medina, L. García, I. Fuentes and R. Moreno-Esparza, *Biopharmaceutics: Absorption Studies of Albendazole and Some Physicochemical Properties of the Drug and Its Metabolite Albendazole Sulphoxide*, *J. Pharm. Pharmacol.* 50 (1998), pp. 43–48.

- [4] K. Daniel-Mwambete, S. Torrado, C. Cuesta-Bandera, F. Ponce-Gordo and J.J. Torrado, *The effect of solubilization on the oral bioavailability of three benzimidazole carbamate drugs*, Int. J. Pharm. 272 (2004), pp. 29–36.
- [5] H. Lange, R. Eggers and J. Bircher, *Increased systemic availability of albendazole when taken with a fatty meal*, Eur. J. Clin. Pharmacol. 34 (1988), pp. 315–317.
- [6] J.L. del Estal, A.I. Alvarez, C. Villaverde, A. Justel and J.G. Prieto, *Increased systemic bioavailability of albendazol when administered with surfactants in rats*, Int. J. Pharm. 102 (1994), pp. 257–260.
- [7] M. Pavan Kumar, Y. Madhusudan Rao and S. Apte, *Improved bioavailability of albendazole following oral administration of nanosuspension in rats*, Curr. Nanosci. 3 (2007), pp. 191–194.
- [8] M. Vogt, K. Kunath and J.B. Dressman, *Dissolution enhancement of fenofibrate by micronization, cogrinding and spray-drying: Comparison with commercial preparations*, Eur. J. Pharm. Biopharm. 68 (2008), pp. 283–288.
- [9] R. Ravichandran, *In Vivo Pharmacokinetic Studies of Albendazole Nanoparticulate Oral Formulations for Improved Bioavailability*, Int. J. Green Nanotechnol. Biomed. 2 (2010), pp. B46–B53.

- [10] G.S. Paulekuhn, J.B. Dressman and C. Saal, *Salt screening and characterization for poorly soluble, weak basic compounds: case study albendazole*, Pharm. - Int. J. Pharm. Sci. 68 (2013), pp. 555–564.
- [11] F.K. Alanazi, M. El-Badry, M.O. Ahmed and I.A. Alsarra, *Improvement of albendazole dissolution by preparing microparticles using spray-drying technique*, Sci. Pharm. 75 (2007), pp. 63.
- [12] L. Martinez-Marcos, D.A. Lamprou, R.T. McBurney and G.W. Halbert, *A novel hot-melt extrusion formulation of albendazole for increasing dissolution properties*, Int. J. Pharm. 499 (2016), pp. 175–185.
- [13] D. Zhou, G.G.Z. Zhang, D. Law, D.J.W. Grant and E.A. Schmitt, *Physical stability of amorphous pharmaceuticals: Importance of configurational thermodynamic quantities and molecular mobility*, J. Pharm. Sci. 91 (2002), pp. 1863–1872.
- [14] D.T. Friesen, R. Shanker, M. Crew, D.T. Smithey, W.J. Curatolo and J.A.S. Nightingale, *Hydroxypropyl methylcellulose acetate succinate-based spray-dried dispersions: an overview*, Mol. Pharm. 5 (2008), pp. 1003–1019.
- [15] K. Pajula, M. Taskinen, V.-P. Lehto, J. Ketolainen and O. Korhonen, *Predicting the Formation and Stability of Amorphous Small Molecule Binary Mixtures from Computationally Determined Flory–Huggins Interaction Parameter and Phase Diagram*, Mol. Pharm. 7 (2010), pp. 795–804.

- [16] Y. Tian, J. Booth, E. Meehan, D.S. Jones, S. Li and G.P. Andrews, *Construction of drug–polymer thermodynamic phase diagrams using Flory–Huggins interaction theory: identifying the relevance of temperature and drug weight fraction to phase separation within solid dispersions*, *Mol. Pharm.* 10 (2012), pp. 236–248.
- [17] R.P. Patel, M.P. Patel and A.M. Suthar, *Spray drying technology: an overview*, *Indian J. Sci. Technol.* 2 (2009), pp. 44–47.
- [18] M.M. Crowley, F. Zhang, M.A. Repka, S. Thumma, S.B. Upadhye, S. Kumar Battu et al., *Pharmaceutical applications of hot-melt extrusion: part I*, *Drug Dev. Ind. Pharm.* 33 (2007), pp. 909–926.
- [19] J.M. Keen, C. Martin, A. Machado, H. Sandhu, J.W. McGinity and J.C. DiNunzio, *Investigation of process temperature and screw speed on properties of a pharmaceutical solid dispersion using corotating and counter-rotating twin-screw extruders*, *J. Pharm. Pharmacol.* 66 (2014), pp. 204–217.
- [20] A. Paudel, Z.A. Worku, J. Meeus, S. Guns and G. Van den Mooter, *Manufacturing of solid dispersions of poorly water soluble drugs by spray drying: Formulation and process considerations*, *Int. J. Pharm.* 453 (2013), pp. 253–284.
- [21] J.R. Hughey, J.C. DiNunzio, R.C. Bennett, C. Brough, D.A. Miller, H. Ma et al., *Dissolution Enhancement of a Drug Exhibiting Thermal and Acidic Decomposition*

Characteristics by Fusion Processing: A Comparative Study of Hot Melt Extrusion and KinetiSol® Dispersing, AAPS PharmSciTech 11 (2010), pp. 760–774.

- [22] D.J. am Ende, *Achieving a Hot Melt Extrusion Design Space for the Production of Solid Solutions*, in *Chemical Engineering in the Pharmaceutical Industry*, John Wiley & Sons, Inc, Hoboken, NJ, USA, pp. 819–836.
- [23] S. Huang, K. O’Donnell, J. Keen, M. Rickard, J. McGinity and R. Williams III, *A New Extrudable Form of Hypromellose: AFFINISOL™ HPMC HME*, AAPS PharmSciTech 17 (2016), pp. 106–119.
- [24] *US Pharmacopeia 36-NF31*, 2013.
- [25] A. Pobudkowska and U. Domańska, *Study of pH-dependent drugs solubility in water*, Chem. Ind. Chem. Eng. Q. 20 (2014), pp. 115–126.
- [26] FDA, *Stability Testing: Drug substance stress testing*, Int. Conf. Harmon. Tech. Requir. Regist. Pharm. Hum. Use Rockv. MD USA (2003), .
- [27] A. Forster, J. Hempenstall, I. Tucker and T. Rades, *Selection of excipients for melt extrusion with two poorly water-soluble drugs by solubility parameter calculation and thermal analysis*, Int. J. Pharm. 226 (2001), pp. 147–161.
- [28] P.J. Flory, *Thermodynamics of High Polymer Solutions*, J. Chem. Phys. 10 (1942), pp. 51–61.

- [29] M.L. Huggins, *Thermodynamic Properties of Solutions of Long-Chain Compounds*, Vol. 43, 1., Annals of the New York Academy of Sciences New York Academy of Sciences, New York, 1942.
- [30] P.J. Marsac, S.L. Shamblin and L.S. Taylor, *Theoretical and Practical Approaches for Prediction of Drug–Polymer Miscibility and Solubility*, Pharm. Res. 23 (2006), pp. 2417–2426.
- [31] P.J. Marsac, T. Li and L.S. Taylor, *Estimation of drug–polymer miscibility and solubility in amorphous solid dispersions using experimentally determined interaction parameters*, Pharm. Res. 26 (2009), pp. 139–151.
- [32] M. Rubinstein and R.H. Colby, *Polymer Physics*, Oxford University Press, Oxford, 2007.
- [33] M. Gordon and J.S. Taylor, *Ideal copolymers and the second-order transitions of synthetic rubbers. i. non-crystalline copolymers*, J. Appl. Chem. 2 (1952), pp. 493–500.
- [34] *Albendazole Tablets*, in *US Pharmacopeia 36-NF 31*, US Pharmacopeia, US Pharmacopeial Convention, Rockville, MD., 2013, .
- [35] P. Venkatesan, *Albendazole.*, J. Antimicrob. Chemother. 41 (1998), pp. 145–147.

- [36] T. Nogrady and D.F. Weaver, *Medicinal Chemistry: A Molecular and Biochemical Approach*, 3rd ed. Oxford University Press, New York, N.Y, 2005.
- [37] M. Blessy, R.D. Patel, P.N. Prajapati and Y.K. Agrawal, *Development of forced degradation and stability indicating studies of drugs—A review*, *J. Pharm. Anal.* 4 (2014), pp. 159–165.
- [38] N. Shah, H. Sandhu, D.S. Choi, H. Chokshi and A.W. Malick, *Amorphous Solid Dispersions: Theory and Practice*, Springer, 2014.
- [39] D.Q. Craig, P.G. Royall, V.L. Kett and M.L. Hopton, *The relevance of the amorphous state to pharmaceutical dosage forms: glassy drugs and freeze dried systems*, *Int. J. Pharm.* 179 (1999), pp. 179–207.
- [40] S. Yoshioka and Y. Aso, *Correlations between molecular mobility and chemical stability during storage of amorphous pharmaceuticals*, *J. Pharm. Sci.* 96 (2007), pp. 960–981.
- [41] D.J. Greenhalgh, A.C. Williams, P. Timmins and P. York, *Solubility parameters as predictors of miscibility in solid dispersions*, *J. Pharm. Sci.* 88 (1999), pp. 1182–1190.
- [42] Y. Zhao, P. Inbar, H.P. Chokshi, A.W. Malick and D.S. Choi, *Prediction of the thermal phase diagram of amorphous solid dispersions by Flory–Huggins theory*, *J. Pharm. Sci.* 100 (2011), pp. 3196–3207.

- [43] F. Qian, J. Huang and M.A. Hussain, *Drug–polymer solubility and miscibility: Stability consideration and practical challenges in amorphous solid dispersion development*, *J. Pharm. Sci.* 99 (2010), pp. 2941–2947.
- [44] A. Forster, J. Hempenstall and T. Rades, *Characterization of glass solutions of poorly water-soluble drugs produced by melt extrusion with hydrophilic amorphous polymers*, *J. Pharm. Pharmacol.* 53 (2001), pp. 303–315.
- [45] *Polymer Extrusion (2nd ed.)*. Hanser Publishers, Munchen, 1990.
- [46] S. Govindasamy, O.H. Campanella and C.G. Oates, *High moisture twin-screw extrusion of sago starch: 1. Influence on granule morphology and structure*, *Carbohydr. Polym.* 30 (1996), pp. 275–286.
- [47] C. Anandharamakrishnan, *Computational Fluid Dynamics Applications in Food Processing*, Springer Science & Business Media, 2013.
- [48] K. Masters, *Impact of spray dryer design on powder properties*, *Drying* 91 (1991), pp. 56–73.
- [49] C. Anandharamakrishnan, C.D. Rielly and A.G.F. Stapley, *Effects of process variables on the denaturation of whey proteins during spray drying*, *Dry. Technol.* 25 (2007), pp. 799–807.

- [50] S.-D. Clas, R. Faizer, R.. O'Connor and E.. Vadas, *Quantification of crystallinity in blends of lyophilized and crystalline MK-0591 using x-ray powder diffraction*, Int. J. Pharm. 121 (1995), pp. 73–79.
- [51] M.M. de Villiers, D.E. Wurster, J.G. Van der Watt and A. Ketkar, *X-Ray powder diffraction determination of the relative amount of crystalline acetaminophen in solid dispersions with polyvinylpyrrolidone*, Int. J. Pharm. 163 (1998), pp. 219–224.
- [52] L.A. Utracki, *Polymer Alloys and Blends: Thermodynamics and Rheology*, Hanser, Munich, 1990.
- [53] G. Van den Mooter, M. Wuyts, N. Blaton, R. Busson, P. Grobet, P. Augustijns et al., *Physical stabilisation of amorphous ketoconazole in solid dispersions with polyvinylpyrrolidone K25*, Eur. J. Pharm. Sci. 12 (2001), pp. 261–269.
- [54] P. Harmon, L. Li, P.J. Marsac, C. McKelvey, N. Variankaval and W. Xu, *Amorphous Solid Dispersions: Analytical Challenges and Opportunities*, AAPS Newsmagazine Sept (2009), pp. 14–20.
- [55] A.C. Rumondor and L.S. Taylor, *Effect of polymer hygroscopicity on the phase behavior of amorphous solid dispersions in the presence of moisture*, Mol. Pharm. 7 (2010), pp. 477–490.

- [56] L. Yu, *Amorphous pharmaceutical solids: preparation, characterization and stabilization*, *Adv. Drug Deliv. Rev.* 48 (2001), pp. 27–42.
- [57] D. Turnbull, *On the relationa between crystallization rate and liquid structure*, *J. Phys. Chem.* 66 (1962), pp. 609–613.
- [58] K.T. Savjani, A.K. Gajjar and J.K. Savjani, *Drug solubility: importance and enhancement techniques*, *ISRN Pharm.* 2012 (2012), .
- [59] M. Shozo, O. Midori and N. Tanekazu, *Unusual solubility and dissolution behavior of pharmaceutical hydrochloride salts in chloride-containing media*, *Int. J. Pharm.* 6 (1980), pp. 77–85.
- [60] B.C. Hancock and G. Zografi, *The Relationship Between the Glass Transition Temperature and the Water Content of Amorphous Pharmaceutical Solids*, *Pharm. Res.* 11 (1994), pp. 471–477.
- [61] T. Taupitz, J.B. Dressman and S. Klein, *New formulation approaches to improve solubility and drug release from fixed dose combinations: case examples pioglitazone/glimepiride and ezetimibe/simvastatin*, *Eur. J. Pharm. Biopharm.* 84 (2013), pp. 208–218.

CHAPTER 3 REFERENCES

1. Raghu G, Collard HR, Egan JJ, Martinez FJ, Behr J, Brown KK, et al. An official ATS/ERS/JRS/ALAT statement: idiopathic pulmonary fibrosis: evidence-based guidelines for diagnosis and management. *Am J Respir Crit Care Med*. 2011;183(6):788–824.
2. Gribbin J, Hubbard RB, Le Jeune I, Smith CJ, West J, Tata LJ. Incidence and mortality of idiopathic pulmonary fibrosis and sarcoidosis in the UK. *Thorax*. 2006;61(11):980–985.
3. Feghali-Bostwick CA, Yamaguchi Y. Use of endostatin peptides for the treatment of fibrosis. US8507441 B2, 2013.
4. Costabel U, Crestani B, Wells AU. Pharmacological management. In: *Idiopathic Pulmonary Fibrosis*. European Respiratory Society; 2016. p. 196.
5. Salisbury ML, Xia M, Zhou Y, Murray S, Tayob N, Brown KK, et al. *Idiopathic Pulmonary Fibrosis*. *Chest*. 2016;149(2):491–8.
6. Panos RJ, Mortenson RL, Niccoli SA, King TE. Clinical deterioration in patients with idiopathic pulmonary fibrosis: causes and assessment. *Am J Med*. 1990;88(4):396–404.
7. Richeldi L, du Bois RM, Raghu G, Azuma A, Brown KK, Costabel U, et al. Efficacy and safety of nintedanib in idiopathic pulmonary fibrosis. *N Engl J Med*. 2014;370(22):2071.

8. King, Jr TE, Bradford WZ, Castro-Bernardini S, Fagan EA, Glaspole I, Glassberg MK, et al. A phase 3 trial of pirfenidone in patients with idiopathic pulmonary fibrosis. *N Engl J Med*. 2014;370(22):2083.
9. Raghu G, Rochweg B, Zhang Y, Garcia CAC, Azuma A, Behr J, et al. An official ATS/ERS/JRS/ALAT clinical practice guideline: treatment of idiopathic pulmonary fibrosis. An update of the 2011 clinical practice guideline. *Am J Respir Crit Care Med*. 2015;192(2):e3–e19.
10. Marudamuthu AS, Shetty SK, Bhandary YP, Karandashova S, Thompson M, Sathish V, et al. Plasminogen activator inhibitor-1 suppresses profibrotic responses in fibroblasts from fibrotic lungs. *J Biol Chem*. 2015;290(15):9428–9441.
11. Shetty SK, Bhandary YP, Marudamuthu AS, Abernathy D, Velusamy T, Starcher B, et al. Regulation of airway and alveolar epithelial cell apoptosis by p53-Induced plasminogen activator inhibitor-1 during cigarette smoke exposure injury. *Am J Respir Cell Mol Biol*. 2012;47(4):474–483.
12. Bhandary YP, Shetty SK, Marudamuthu AS, Gyetko MR, Idell S, Gharaee-Kermani M, et al. Regulation of alveolar epithelial cell apoptosis and pulmonary fibrosis by coordinate expression of components of the fibrinolytic system. *Am J Physiol - Lung Cell Mol Physiol*. 2012;302(5):L463–73.
13. Bhandary YP, Shetty SK, Marudamuthu AS, Ji H-L, Neuenschwander PF, Boggaram V, et al. Regulation of lung injury and fibrosis by p53-mediated changes in urokinase and plasminogen activator inhibitor-1. *Am J Pathol*. 2013;183(1):131–143.

14. Marudamuthu AS, Bhandary YP, Shetty SK, Fu J, Sathish V, Prakash YS, et al. Role of the urokinase-fibrinolytic system in epithelial–mesenchymal transition during lung injury. *Am J Pathol.* 2015;185(1):55–68.
15. Bhandary YP, Shetty SK, Marudamuthu AS, Fu J, Pinson BM, Levin J, et al. Role of p53–fibrinolytic system cross-talk in the regulation of quartz-induced lung injury. *Toxicol Appl Pharmacol.* 2015;283(2):92–98.
16. Fakes MG, Dali MV, Haby TA, Morris KR, Varia SA, Serajuddin ATM. Moisture sorption behavior of selected bulking agents used in lyophilized products. *PDA J Pharm Sci Technol.* 2000;54(2):144–9.
17. Costantino HR, Langer R, Klibanov AM. Solid-phase aggregation of proteins under pharmaceutically relevant conditions. *J Pharm Sci.* 1994;83(12):1662–1669.
18. Robbins DC, Cooper SM, Fineberg SE, Mead PM. Antibodies to covalent aggregates of insulin in blood of insulin-using diabetic patients. *Diabetes.* 1987;36(7):838–841.
19. Cleland JL, Powell MF, Shire SJ. The development of stable protein formulations: a close look at protein aggregation, deamidation, and oxidation. *Crit Rev Ther Drug Carrier Syst.* 1992;10(4):307–377.
20. Hsu CC, Ward CA, Pearlman R, Nguyen HM, Yeung DA, Curley JG. Determining the optimum residual moisture in lyophilized protein pharmaceuticals. *Dev Biol Stand.* 1992;74:255.

21. Carpenter JF, Pikal MJ, Chang BS, Randolph TW. Rational design of stable lyophilized protein formulations: some practical advice. *Pharm Res.* 1997;14(8):969–975.
22. Shamblin SL, Hancock BC, Zografi G. Water vapor sorption by peptides, proteins and their formulations. *Eur J Pharm Biopharm.* 1998;45(3):239–47.
23. Costantino HR, Carrasquillo KG, Cordero RA, Mumenthaler M, Hsu CC, Griebenow K. Effect of excipients on the stability and structure of lyophilized recombinant human growth hormone. *J Pharm Sci.* 1998;87(11):1412–20.
24. Izutsu K, Yoshioka S, Terao T. Decreased protein-stabilizing effects of cryoprotectants due to crystallization. *Pharm Res.* 1993;10(8):1232–1237.
25. Izutsu K, Yoshioka S, Terao T. Effect of mannitol crystallinity on the stabilization of enzymes during freeze-drying. *Chem Pharm Bull (Tokyo).* 1994;42(1):5–8.
26. Costantino HR, Langer R, Klibanov AM. Aggregation of a lyophilized pharmaceutical protein, recombinant human albumin: effect of moisture and stabilization by excipients. *Bio/Technology.* 1995;(13):493–6.
27. Li B, O’Meara MH, Lubach JW, Schowen RL, Topp EM, Munson EJ, et al. Effects of sucrose and mannitol on asparagine deamidation rates of model peptides in solution and in the solid state. *J Pharm Sci.* 2005;94(8):1723–1735.
28. Lai MC, Topp EM. Solid-state chemical stability of proteins and peptides. *J Pharm Sci.* 1999;88(5):489–500.

29. Sharma VK, Kalonia DS. Effect of vacuum drying on protein-mannitol interactions: the physical state of mannitol and protein structure in the dried state. *AAPS PharmSciTech*. 2004;5(1):58–69.
30. Izutsu K, Kojima S. Excipient crystallinity and its protein-structure-stabilizing effect during freeze-drying. *J Pharm Pharmacol*. 2002;54(8):1033–9.
31. Oliyai C, Patel JP, Carr L, Borchardt RT. Chemical pathways of peptide degradation. VII. Solid state chemical instability of an aspartyl residue in a model hexapeptide. *Pharm Res*. 1994;11(6):901–908.
32. Kreilgaard L, Frokjaer S, Flink JM, Randolph TW, Carpenter JF. Effects of additives on the stability of *Humicola lanuginosa* lipase during freeze-drying and storage in the dried solid. *J Pharm Sci*. 1999;88(3):281–90.
33. Pilcer G, Amighi K. Formulation strategy and use of excipients in pulmonary drug delivery. *Int J Pharm*. 2010;392(1–2):1–19.
34. Hertel SP, Winter G, Friess W. Protein stability in pulmonary drug delivery via nebulization. *Adv Drug Deliv Rev*. 2015;93:79–94.
39. Hertel S. Pulmonary delivery of pharmaceutical proteins by means of vibrating mesh nebulization. Ludwig-Maximilians-Universität München; 2014.
36. Elhissi AMA, Taylor KMG. Delivery of liposomes generated from proliposomes using air-jet, ultrasonic, and vibrating-mesh nebulisers. *J Drug Deliv Sci Technol*. 2005;15(4):261–5.

37. Hertel S, Pohl T, Friess W, Winter G. Prediction of protein degradation during vibrating mesh nebulization via a high throughput screening method. *Eur J Pharm Biopharm.* 2014;87(2):386–394.
38. Waldrep JC, Dhand R. Advanced nebulizer designs employing vibrating mesh/aperture plate technologies for aerosol generation. *Curr Drug Deliv.* 2008;5(2):114–119.
39. Watts AB, McConville JT, Williams RO. Current Therapies and Technological Advances in Aqueous Aerosol Drug Delivery. *Drug Dev Ind Pharm.* 2008;34(9):913–22.
40. Knoch M, Keller M. The customised electronic nebuliser: a new category of liquid aerosol drug delivery systems. *Expert Opin Drug Deliv.* 2005;2(2):377–90.
41. Wang W. Protein aggregation and its inhibition in biopharmaceutics. *Int J Pharm.* 2005;289(1–2):1–30.
42. Philo JS. Is any measurement method optimal for all aggregate sizes and types? *AAPS J.* 2006 Sep 8;8(3):E564–71.
43. Baheti A, Kumar L, Bansal AK. Excipients used in lyophilization of small molecules. *J Excip Food Chem.* 2010;1(1):41–54.
44. Wang DQ, Hey JM, Nail SI. Effect of collapse on the stability of freeze-dried recombinant factor VIII and α -amylase. *J Pharm Sci.* 2004;93(5):1253–63.

45. Hageman MJ. In *Stability of Protein Pharmaceuticals, Part A: Chemical and Physical Pathways of Protein Degradation*. In: *Water sorption and solid-state stability of proteins*: New York; 1992. p. 273–309.
46. Rey L, May JC (Joan C. *Freeze drying/lyophilization of pharmaceutical and biological products*. 3rd ed. New York: Informa Healthcare; 2010. xiii, 564. (Drugs and the pharmaceutical sciences; vol. 206.).
47. Schoeffel RE, Anderson SD, Altounyan REC. Bronchial hyperreactivity in response to inhalation of ultrasonically nebulised solutions of distilled water and saline. *Br Med J (Clin Res Ed)*. 1981;283(6302):1285–7.
48. Portel L, Tunon de Lara JM, Vernejoux JM, Weiss I, Taytard A. Osmolarity of solutions used in nebulization. *Rev Mal Respir*. 1998;15(2):191.
49. Chan H-K, Chan JGY, Kwok PCL, Young PM, Traini D. Mannitol delivery by vibrating mesh nebulisation for enhancing mucociliary clearance. *J Pharm Sci*. 2011;100(7):2693–702.
50. Brittain HG. *Polymorphism in pharmaceutical solids*. 2nd ed. New York: Informa Healthcare; 2009. xi, 640. (Drugs and the pharmaceutical sciences; vol. 192.).
51. Hancock BC, Shamblin SL. Water vapour sorption by pharmaceutical sugars. *Pharm Sci Technol Today*. 1998;1(8):345–351.
52. Labrude P, Chaillot B, Bonneaux F, Vigneron C. Freeze-drying of haemoglobin in the presence of carbohydrates. *J Pharm Pharmacol*. 1980 Aug;32(8):588.

53. Hellman K, Miller DS, Cammack KA. The effect of freeze-drying on the quaternary structure of L-asparaginase from *Erwinia carotovora*. *Biochim Biophys Acta*. 1983 Dec;749(2):133.
54. Hong Z, Reis RL, Mano JF. Preparation and in vitro characterization of novel bioactive glass ceramic nanoparticles. *J Biomed Mater Res A*. 2009;88(2):304–313.
55. Yu L, Milton N, Groleau EG, Mishra DS, Vansickle RE. Existence of a mannitol hydrate during freeze-drying and practical implications. *J Pharm Sci*. 1999;88(2):196–198.
56. Liao X, Krishnamurthy R, Suryanarayanan R. Influence of processing conditions on the physical state of mannitol—implications in freeze-drying. *Pharm Res*. 2007;24(2):370–6.
57. Nunes C, Suryanarayanan R, Botez CE, Stephens PW. Characterization and crystal structure of D-mannitol hemihydrate. *J Pharm Sci*. 2004;93(11):2800–9.
56. Devi S, Williams DR, Heng JYY. Crystallisation behaviour of D-mannitol as a function of temperature and relative humidity. Available from: <http://www.aidic.it/isic18/webpapers/177Devi.pdf>. Accessed 28 May 2016.
59. Telang C, Suryanarayanan R, Yu L. Crystallization of D-Mannitol in Binary Mixtures with NaCl: Phase Diagram and Polymorphism. *Pharm Res*. 2003;20(12):1939–45.
60. Omar AE, Roos YH. Glass transition and crystallization behaviour of freeze-dried lactose–salt mixtures. *LWT-Food Sci Technol*. 2007;40(3):536–543.

61. Omar AE, Roos YH. Water sorption and time-dependent crystallization behaviour of freeze-dried lactose–salt mixtures. *LWT-Food Sci Technol.* 2007;40(3):520–528.
62. Alqurshi A, Kumar Z, McDonald R, Strang J, Buanz A, Ahmed S, et al. Amorphous formulation and in vitro performance testing of instantly disintegrating buccal tablets for the emergency delivery of naloxone. *Mol Pharm.* 2016;13(5):1688.
63. Cavatur R, Vemuri N, Pyne A, Chrzan Z, Toledo-Velasquez D, Suryanarayanan R. Crystallization behavior of mannitol in frozen aqueous solutions. *Pharm Res.* 2002;19(6):894–900.
64. Araújo AA, Mercuri LP, Carvalho FM, dos Santos Filho M, Matos JR, others. Thermal analysis of the antiretroviral zidovudine (AZT) and evaluation of the compatibility with excipients used in solid dosage forms. *Int J Pharm.* 2003;260(2):303–314.
65. Craig DQ, Barsnes M, Royall PG, Kett VL. An evaluation of the use of modulated temperature DSC as a means of assessing the relaxation behaviour of amorphous lactose. *Pharm Res.* 2000;17(6):696–700.
66. Izutsu K, Yoshioka S, Terao T. Effect of mannitol crystallinity on the stabilization of enzymes during freeze-drying. *Chem Pharm Bull (Tokyo).* 1994;42(1):5–8.

67. Kurochkin IV, Procyk R, Bishop PD, Yee VC, Teller DC, Ingham KC, et al. Domain structure, stability and domain-domain interactions in recombinant factor XIII. *J Mol Biol.* 1995;248(2):414–30.
68. Cholewinski M, Lückel B, Horn H. Degradation pathways, analytical characterization and formulation strategies of a peptide and a protein calcitonine and human growth hormone in comparison. *Pharm Acta Helv.* 1996;71(6):405–19.
69. Picotti P, De Franceschi G, Frare E, Spolaore B, Zambonin M, Chiti F, et al. Amyloid fibril formation and disaggregation of fragment 1-29 of apomyoglobin: insights into the effect of pH on protein fibrillogenesis. *J Mol Biol.* 2007;367(5):1237–45.
70. Costantino HR, Langer R, Klibanov AM. Moisture-induced aggregation of lyophilized insulin. *Pharm Res.* 1994;11(1):21–29.
71. Costantino HR, Curley JG, Hsu CC. Determining the water sorption monolayer of lyophilized pharmaceutical proteins. *J Pharm Sci.* 1997 Dec 1;86(12):1390–3.
72. Herman BD, Sinclair BD, Milton N, Nail SL. The effect of bulking agent on the solid-state stability of freeze-dried methylprednisolone sodium succinate. *Pharm Res.* 1994;11(10):1467–1473.
73. Costantino HR, Andya JD, Nguyen P-A, Dasovich N, Sweeney TD, Shire SJ, et al. Effect of mannitol crystallization on the stability and aerosol performance of a spray-dried pharmaceutical protein, recombinant humanized anti-IgE monoclonal antibody. *J Pharm Sci.* 1998 Nov 1;87(11):1406–11.

74. Andya JD, Maa Y-F, Costantino HR, Nguyen P-A, Dasovich N, Sweeney TD, et al. The effect of formulation excipients on protein stability and aerosol performance of spray-dried powders of a recombinant humanized anti-IgE monoclonal antibody1. *Pharm Res.* 1999;16(3):350–358.

73. AnaSpec Inc. Peptide Solubility Guidelines. Available from: <http://www.anaspec.com/content/pdfs/PeptidesolubilityguidelinesFinal.pdf> Accessed 30 Jul 2016.

76. Carpenter JF, Crowe JH. An infrared spectroscopic study of the interactions of carbohydrates with dried proteins. *Biochemistry (Mosc).* 1989;28(9):3916–22.

77. Arakawa T, Kita Y, Carpenter JF. Protein-solvent interactions in pharmaceutical formulations. *Pharm Res.* 1991;8(3):285.

78. Yaylayan VA, Wnorowski A, Perez Locas C. Why asparagine needs carbohydrates to generate acrylamide. *J Agric Food Chem.* 2003;51(6):1753–1757.

CHAPTER 4 REFERENCES

1. Piazza G, Goldhaber SZ. Management of submassive pulmonary embolism. *Circulation.* 2010;122(11):1124–1129.

2. Idell S. Update on the use of fibrinolytics in pleural disease. *Clin Pulm Med.* 2005;12(3):184–190.

3. Zuckerman DA, Reed MF, Howington JA, Moulton JS. Efficacy of intrapleural tissue-type plasminogen activator in the treatment of loculated parapneumonic effusions. *J Vasc Interv Radiol*. 2009;20(8):1066–1069.
4. Rahman NM, Maskell NA, West A, Teoh R, Arnold A, Mackinlay C, et al. Intrapleural use of tissue plasminogen activator and DNase in pleural infection. *N Engl J Med*. 2011;365(6):518–526.
5. Rogers WJ, Bowlby LJ, Chandra NC, French WJ, Gore JM, Lambrew CT, et al. Treatment of myocardial infarction in the United States (1990 to 1993). Observations from the National Registry of Myocardial Infarction. *Circulation*. 1994;90(4):2103–2114.
6. Albers GW, Amarenco P, Easton JD, Sacco RL, Teal P. Antithrombotic and thrombolytic therapy for ischemic stroke: American College of Chest Physicians evidence-based clinical practice guidelines. *CHEST J*. 2008;133(6_suppl):630S–669S.
7. Saver JL, Fonarow GC, Smith EE, Reeves MJ, Grau-Sepulveda MV, Pan W, et al. Time to treatment with intravenous tissue plasminogen activator and outcome from acute ischemic stroke. *Jama*. 2013;309(23):2480–2488.
8. Xian Y, Smith EE, Zhao X, Peterson ED, Olson DM, Hernandez AF, et al. Strategies used by hospitals to improve speed of tissue-type plasminogen activator treatment in acute ischemic stroke. *Stroke*. 2014;45(5):1387–1395.
9. Marder VJ. Thrombolytic therapy for deep vein thrombosis: potential application of plasmin. *Thromb Res*. 2009;123:S56–S61.

10. Leary SE, Harrod VL, de Alarcon PA, Reiss UM. Low-dose systemic thrombolytic therapy for deep vein thrombosis in pediatric patients. *J Pediatr Hematol Oncol.* 2010;32(2):97.
11. Stringer KA. Tissue plasminogen activator inhibits reactive oxygen species production by macrophages. *Pharmacother J Hum Pharmacol Drug Ther.* 2000;20(4):375–379.
12. Nieuwenhuizen L, De Groot PG, Grutters JC, Biesma DH. A review of pulmonary coagulopathy in acute lung injury, acute respiratory distress syndrome and pneumonia. *Eur J Haematol.* 2009;82(6):413–425.
13. Cornet AD, Hofstra JJ, Vlaar AP, Tuinman PR, Levi M, Girbes AR, et al. Activated protein C attenuates pulmonary coagulopathy in patients with acute respiratory distress syndrome. *J Thromb Haemost.* 2013;11(5):894–901.
14. Gralinski LE, Bankhead A, Jeng S, Menachery VD, Proll S, Belisle SE, et al. Mechanisms of severe acute respiratory syndrome coronavirus-induced acute lung injury. *MBio.* 2013;4(4):e00271–13.
15. Ware LB, Matthay MA. The Acute Respiratory Distress Syndrome. *N Engl J Med.* 2000 May 4;342(18):1334–49.
16. Williams III RO, Idell S. Compositions and methods for administration of an enzyme to a subject's airway. WO2015066664 A2, 2015.

17. Stringer KA, Dunn JS, Gustafson DL. Administration of exogenous tissue plasminogen activator reduces oedema in mice lacking the tissue plasminogen activator gene. *Clin Exp Pharmacol Physiol*. 2004;31(5–6):327–330.
18. Stringer KA, Tobias M, Dunn JS, Campos J, Van Rheen Z, Mosharraf M, et al. Accelerated Dosing Frequency of a Pulmonary Formulation of Tissue Plasminogen Activator is Well-Tolerated in Mice. *Clin Exp Pharmacol Physiol*. 2008;35(12):1454–60.
19. Dunn JS, Nayar R, Campos J, Hybertson BM, Zhou Y, Manning MC, et al. Feasibility of tissue plasminogen activator formulated for pulmonary delivery. *Pharm Res*. 2005;22(10):1700–1707.
20. Idell S, Azghani A, Chen S, Koenig K, Mazar A, Kodandapani L, et al. Intrapleural low-molecular-weight urokinase or tissue plasminogen activator versus single-chain urokinase in tetracycline-induced pleural loculation in rabbits. *Exp Lung Res*. 2007;33(8–9):419–440.
21. Wagers SS, Norton RJ, Rinaldi LM, Bates JH, Sobel BE, Irvin CG. Extravascular fibrin, plasminogen activator, plasminogen activator inhibitors, and airway hyperresponsiveness. *J Clin Invest*. 2004;114(1):104–111.
22. Gunther A, Lubke N, Ermert M, Schermuly RT, Weissmann N, Breithecker A, et al. Prevention of bleomycin-induced lung fibrosis by aerosolization of heparin or urokinase in rabbits. *Am J Respir Crit Care Med*. 2003;168(11):1358–1365.
23. Shetty S, Bdeir K, Cines DB, Idell S. Induction of plasminogen activator inhibitor-1 by urokinase in lung epithelial cells. *J Biol Chem*. 2003;278(20):18124–18131.

24. Hardaway RM, Williams CH, Marvasti M, Farias M, Tseng A, Pinon I, et al. Prevention of adult respiratory distress syndrome with plasminogen activator in pigs. *Crit Care Med*. 1990;18(12):1413–1418.
25. Hardaway RM, Harke H, Williams CH. Fibrinolytic agents: a new approach to the treatment of adult respiratory distress syndrome. *Adv Ther*. 1993;11(2):43–51.
26. Idell S, Allen T, Chen S, Koenig K, Mazar A, Azghani A. Intrapleural activation, processing, efficacy, and duration of protection of single-chain urokinase in evolving tetracycline-induced pleural injury in rabbits. *Am J Physiol-Lung Cell Mol Physiol*. 2007;292(1):L25–L32.
27. Bayat M, Cook AM. Intrapulmonary administration of medications. *J Neurosci Nurs J Am Assoc Neurosci Nurses*. 2004;36(4):231.
28. Hertel SP, Winter G, Friess W. Protein stability in pulmonary drug delivery via nebulization. *Adv Drug Deliv Rev*. 2015;93:79–94.
29. Heinemann L. The failure of exubera: are we beating a dead horse? *J Diabetes Sci Technol*. 2008;2(3):518.
30. Siekmeier R, Scheuch G. Inhaled insulin--does it become reality? *J Physiol Pharmacol Off J Pol Physiol Soc*. 2008;59 Suppl 6:81.
31. Weers JG, Bell J, Chan H-K, Cipolla D, Dunbar C, Hickey AJ, et al. Pulmonary formulations: what remains to be done? *J Aerosol Med Pulm Drug Deliv*. 2010;23 Suppl 2:S5.

32. Manning MC, Patel K, Borchardt RT. Stability of protein pharmaceuticals. *Pharm Res.* 1989;6(11):903–918.
33. Hageman MJ. The role of moisture in protein stability. *Drug Dev Ind Pharm.* 1988;14(14):2047–2070.
34. Pearlman R, Nguyen T. Pharmaceuticals of protein drugs. *J Pharm Pharmacol.* 1992;44:178.
35. McGoff P, Scher DS. Solution formulation of proteins/peptides. *Protein Formul Deliv.* 2008;133–51.
36. Costantino HR, Langer R, Klibanov AM. Moisture-induced aggregation of lyophilized insulin. *Pharm Res.* 1994;11(1):21–29.
37. Carpenter JF, Chang BS, Garzon-Rodriguez W, Randolph TW. Rational design of stable lyophilized protein formulations: theory and practice. In: *Rational design of stable protein formulations.* Springer; 2002. p. 109–133.
38. Wang W. Lyophilization and development of solid protein pharmaceuticals. *Int J Pharm.* 2000;203(1–2):1–60.
39. Shalaev EY, Wang W, Gatlin LA. Rational choice of excipients for use in lyophilized formulations. In: *Protein Formulation and Delivery.* Informa Healthcare New York, NY; 2008. p. 197–217.
40. Coldstream Laboratories, Inc. Formulation development report: laboratory scale lyophilization feasibility study for scuPA for Injection, 3.1 mg/vial. 2014.

41. Hertel S. Pulmonary delivery of pharmaceutical proteins by means of vibrating mesh nebulization. Ludwig-Maximilians-Universität München; 2014.
42. ABL, Inc. Determination of urokinase-type plasminogen activator (uPA) activity in SRI project #M097-14 P22204.026 scuPA dosing study samples. 2014.
43. Baheti A, Kumar L, Bansal AK. Excipients used in lyophilization of small molecules. *J Excip Food Chem.* 2010;1(1):41–54.
44. Hsu CC, Ward CA, Pearlman R, Nguyen HM, Yeung DA, Curley JG. Determining the optimum residual moisture in lyophilized protein pharmaceuticals. *Dev Biol Stand.* 1992;74:255.
45. Hageman MJ. In *Stability of Protein Pharmaceuticals, Part A: Chemical and Physical Pathways of Protein Degradation.* In: *Water sorption and solid-state stability of proteins*; New York; 1992. p. 273–309.
46. Lai MC, Topp EM. Solid-state chemical stability of proteins and peptides. *J Pharm Sci.* 1999;88(5):489–500.
47. Schoeffel RE, Anderson SD, Altounyan REC. Bronchial hyperreactivity in response to inhalation of ultrasonically nebulised solutions of distilled water and saline. *Br Med J (Clin Res Ed).* 1981;283(6302):1285–7.
48. Portel L, Tunon de Lara JM, Vernejoux JM, Weiss I, Taytard A. Osmolarity of solutions used in nebulization. *Rev Mal Respir.* 1998;15(2):191.

49. Chan H-K, Chan JGY, Kwok PCL, Young PM, Traini D. Mannitol delivery by vibrating mesh nebulisation for enhancing mucociliary clearance. *J Pharm Sci.* 2011;100(7):2693–702.
50. Dhand R. Nebulizers that use a vibrating mesh or plate with multiple apertures to generate aerosol. *Respir Care.* 2002;47(12):1406.
51. Wood GC, Boucher BA. Aerosolized antimicrobial therapy in acutely ill patients. *Pharmacother J Hum Pharmacol Drug Ther.* 2000;20(2):166–181.
52. Coates AL. Guiding aerosol deposition in the lung. *N Engl J Med.* 2008;358(3):304–305.
53. Michalopoulos A, Metaxas I, Falagas ME. Aerosol delivery of antimicrobial agents during mechanical ventilation: current practice and perspectives. *Curr Drug Deliv.* 2011;8(2):208–212.
54. Uchenna Agu R, Ikechukwu Ugwoke M, Armand M, Kinget R, Verbeke N. The lung as a route for systemic delivery of therapeutic proteins and peptides. *Respir Res.* 2001;2:198.
55. Niven RW. Delivery of biotherapeutics by inhalation aerosol. *Crit Rev Ther Drug Carrier Syst.* 1995;12(2–3):151–231.
56. Lass JS, Sant A, Knoch M. New advances in aerosolised drug delivery: vibrating membrane nebuliser technology. *Expert Opin Drug Deliv.* 2006;3(5):693–702.
57. Niven RW, Ip AY, Mittelman S, Prestrelski SJ, Arakawa T. Some factors associated with the ultrasonic nebulization of proteins. *Pharm Res.* 1995;12(1):53–59.

58. Fink JB, Schmidt D, Power J. Comparison of a nebulizer using a novel aerosol generator with a standard ultrasonic nebulizer designed for use during mechanical ventilation. American Thoracic Society 97th International Conference, San Francisco, CA; 2001.
59. Elhissi AMA, Taylor KMG. Delivery of liposomes generated from proliposomes using air-jet, ultrasonic, and vibrating-mesh nebulisers. *J Drug Deliv Sci Technol.* 2005;15(4):261–5.
60. Ghazanfari T, Elhissi AM, Ding Z, Taylor KM. The influence of fluid physicochemical properties on vibrating-mesh nebulization. *Int J Pharm.* 2007;339(1):103–111.
61. Hertel S, Pohl T, Friess W, Winter G. Prediction of protein degradation during vibrating mesh nebulization via a high throughput screening method. *Eur J Pharm Biopharm.* 2014;87(2):386–394.
62. Waldrep JC, Dhand R. Advanced nebulizer designs employing vibrating mesh/aperture plate technologies for aerosol generation. *Curr Drug Deliv.* 2008;5(2):114–119.
63. Watts AB, McConville JT, Williams RO. Current Therapies and Technological Advances in Aqueous Aerosol Drug Delivery. *Drug Dev Ind Pharm.* 2008;34(9):913–22.
64. Knoch M, Keller M. The customised electronic nebuliser: a new category of liquid aerosol drug delivery systems. *Expert Opin Drug Deliv.* 2005;2(2):377–90.

65. Technology Review and Performance Report for the Aeroneb® Professional Nebulizer system. Aerogen, Inc.; 2002.

Vita

Soraya Hengsawas received her Bachelor and Master degrees in Pharmacy from Chulalongkorn University in 1999 and 2005, respectively. Since 1999, she has been working as an analytical pharmacist at the Department of Medical Sciences (DMSc), Ministry of Public Health, Thailand. She afterwards enrolled in the Ph.D. program in Pharmaceutics at the College of Pharmacy at the University of Texas at Austin in January, 2012. She was under supervision of Dr. Robert O. Williams. Following graduation, she will return to Bangkok and continue her career at the DMSc as a pharmacist, professional level.

She is a coauthor of the following publications:

Hengsawas Surasarang, S., Keen, J. M., Huang, S., Zhang, F. McGinity J. W. and Williams III, R.O. Hot Melt Extrusion versus Spray Drying: Hot Melt Extrusion Degrades Albendazole, *Drug Dev. Ind. Pharm.* (in press)

Hengsawas Surasarang, S., Florova, G., Komissarov, A. A., Shetty, S., Idell, S., and Williams III, R.O. Optimization of Formulation for Novel Inhaled Anti-Idiopathic Pulmonary Fibrosis Therapeutics. (in preparation)

Carvalho, S. R., Watts, A. B., Peters, J. I., Liu, S., Hengsawas, S., Escotet-Espinoza, M. S., & Williams III, R. O. (2014). Characterization and pharmacokinetic analysis of crystalline versus amorphous rapamycin dry powder via pulmonary administration in rats. *Eur. J. Pharm. Biopharm.*, 88(1), 136-147.

Liu, S., Watts, A. B., Du, J., Bui, A., Hengsawas, S., Peters, J. I., & Williams, R. O. (2015). Formulation of a novel fixed dose combination of salmeterol xinafoate and mometasone furoate for inhaled drug delivery. *Eur. J. Pharm. Biopharm.*, 96, 132-142.

Permanent address: 222/333 Noble Geo Watcharapol, Watcharapol Road, Bangkhen,
Bangkok, 10220, Thailand

This dissertation was typed by the author.